A Comparative Study Between Three Neuronal Models on Ex Vivo, Intracellular, Electrophysiological Datasets

Word Count: 11,399

Candidate Number: 297755

MSc Computer Science: (Conversion)

August 2025

Department of Informatics and Engineering
The University of Sussex

Supervisor: Dr. Benjamin D. Evans

Statement of Originality

This report is submitted as part requirement for the degree of MSc Computer Science (Conversion) at the University of Sussex. Under the guidance of Dr. Benjamin D. Evans, this is the product of my own labour, except where indicated in the text. The report may be freely copied and distributed provided the source is acknowledged. I hereby give permission for a copy of this report to be loaned out to students in future years.

Acknowledgments

I would like to express my gratitude to Dr. Benjamin D. Evans for his invaluable guidance and unending patience throughout this project. I am especially grateful for being allowed to explore and learn in my own time frame, without being given answers, while having the support and encouragement to overcome the challenges I faced.

I would also like to thank all the lecturers, teaching assistants, administrative staff, and fellow students who have contributed to my education, progress, and confidence over the past year.

Abstract

This study aims to use ex vivo, intracellular, electrophysiological datasets to simulate voltage traces, and explore comparisons between the Leaky Integrate-and-Fire, the Adaptive Exponential Integrate-and-Fire, and the Hodgkin Huxley neuronal models.

The following stimulus types will be explored:

1. Short Square: Triple
2. Long Square
3. Ramp

Each model will be tested with each stimulus type as collections of sweeps and as an individual sweep, then compared with each other.

The means of assessment will initially focus on the mean squared error (MSE) scores between the target voltage trace of the ex vivo sample and that of the neuronal models.

A simple calculation of matches for the first and last spikes, the number of spikes produced, and spike time matches with the target trace will also be used as a measure for comparison.

All experiments were subjected to at least two tests to assess the variance in numerical results and visual traces. Where results did not match expectations or were too varied to reach a definitive conclusion, further experiments were run.

Contents

Statement of Originality **i**

Acknowledgments **ii**

Abstract **iii**

1 Introduction **1**

1.1 Leaky Integrate-and-Fire 2

1.2 Hodgkin Huxley 4

1.3 Adaptive Exponential Leaky Integrate-and-Fire 6

2 Data Collection and Computational Tools **9**

2.1 The Allen Institute 9

2.2 Brian2 and Brian2modelfitting 11

3 Methods and Results **14**

3.1 Short Square: Triple 14

3.1.1 Collection of 10 arrays 18

3.1.2 Group of 3 arrays 24

3.1.3 Individual array 34

3.1.4 Evaluation 47

3.2 Long Square 48

3.2.1 Group of 3 arrays 49

3.2.2 Individual array 54

3.2.3 Evaluation 58

3.3 Ramp Stimulus 60

3.3.1 Collection of 3 arrays 60

3.3.2 Individual array 70

3.3.3 Evaluation 74

4 Summary **78**

4.1 Limitations and Future Iterations 79

A Secondary Data Analysis Compliance Form **80**

List of Figures

2.1 Metadata for cell ID: 525011903 10

2.2 Electrophysiology summary for cell ID: 525011903. Image taken from celltypes.brain-map.org 10

2.3 Example of LIF model defined in brian2modelfitting 12

3.1 Input current and output response for sweeps 0-4 of the 'Short Square: Triple' dataset 15

3.2 Input current and output response for sweeps 5-9 of the 'Short Square: Triple' dataset 15

3.3 Close up of input current and output response for sweep 3 of the 'Short Square: Triple' dataset 16

3.4 Close up of input current and output response for sweep 4 of the 'Short Square: Triple' dataset 17

3.5 Input current and output response for sweep 5 of the 'Short Square: Triple' dataset 17

3.6 LIF voltage traces with a wider ISI 18

3.7 LIF voltage traces with a narrower ISI 18

3.8 AdEx voltage traces with a larger ISI 19

3.9 AdEx voltage traces with smaller ISIs 20

3.10 Comparison between output response and HH voltage trace for sweep 6 on 'Short Square: Triple' stimulus 21

3.11 Comparison between target trace and Hodgkin Huxley voltage trace for all sweeps 21

3.12 Close up of sweeps 3, 4, and 5 22

3.13 Hodgkin Huxley voltage traces with a wider ISI from best fit parameters found 22

3.14 Hodgkin Huxley voltage traces with a narrower ISI 23

3.15 Best fit comparisons for 'Short Square: Triple' stimulus 24

3.16 Comparison on all models for sweeps 3, 4, and 5 24

3.17 Initial run on LIF for Group of 3 on SST stimulus 25

3.18 Best fit found for LIF on SST stimulus, Group of 3 25

3.19 Example of best fit parameters result with lowest MSE score 27

3.20 Run 8 27

3.21 Run 2 28

3.22 Run 5 28

3.23 Sweep 5: run 8, 2, and 5 29

3.24 Sweep 5: run 8, 2, and 5, plotted together 29

3.25 Sweep 4: run 8, 2, and 5 30

3.26 Comparison of voltage traces for low and high MSE scores 33

3.27 Comparison of low and high MSE scores for sweeps 3-5 34

3.28 Initial LIF run on individual sweep 5 35

3.29 Example of inaccurate spike times on LIF 35

3.30 Printed results for 20 rounds 38

3.31 Best fit for LIF on sweep 5, individual array 39

3.32 Comparison results for SST on LIF model 40

3.33 Example output trace with no response upon third input 42

3.34 Best fit for the AdEx model on individual sweep 5 43

3.35 Comparison results for SST on AdEx model 44

3.36 Initial run with Hodgkin Huxley on individual sweep 5 45

3.37 HH on individual sweep 5: lowest and highest MSE results compared 46

3.38 Hodgkin Huxley best fit comparison 46

3.39 Comparison between neuronal models on SST stimulus 47

3.40 Initial input current and output response on sliced Long Square stimulus for 8 sweeps 48

3.41 Voltage traces for sweeps 0, 4, and 7 49

3.42 Voltage traces for sweeps 5 to 7 on reduced data 50

3.43 Spikes produced on wider parameters 50

3.44 Differing voltage trace results on 30 rounds of the same parameters . 52

3.45 Example of run with more accurate spike times 53

3.46 Example of run with fast spiking 54

3.47 Initial run for individual sweep 7 54

3.48 Examples of different trace outputs 55

3.49 Examples of different trace outputs for LIF 56

3.50 Run 0 and run 8 58

3.51 Comparison for best results on sweep 7 59

3.52 Separate comparisons for best results on sweep 7 59

3.53 Visualisation for neuronal response on Ramp stimulus 61

3.54 Initial LIF trial on Ramp stimulus 61

3.55 Close up of sweep 2 62

3.56 Best fit for LIF on Ramp stimulus 62

3.57 Close up for LIF on Ramp stimulus 63

3.58 AdEx on Ramp stimulus 64

3.59 Best fit for AdEx on Ramp stimulus 64

3.60 Close up for best collection AdEx parameters on Ramp stimulus . . . 65

3.61 Damped oscillations for the Hodgkin Huxley model on Ramp stimulus input . . . 65

3.62 Traces for all three sweeps are exactly the same . . . 66

3.63 Close up of damped oscillation from Ramp stimulus . . . 67

3.64 Voltage trace for best parameters found for HH . . . 69

3.65 Only sweep 2 spikes . . . 70

3.66 Best result found for LIF on Ramp stimulus, individual sweep 2 . . . 72

3.67 Best result found for AdEx on Ramp stimulus, individual sweep 2 . . . 72

3.68 An example of an earlier initial spike followed by excessive spiking . . . 73

3.69 Best result found for the Hodgkin Huxley model on Ramp stimulus, individual sweep 2 . . . 73

3.70 Comparison for best LIF result on Ramp stimulus between the collection dataset and the individual array . . . 74

3.71 Comparison for best AdEx result on Ramp stimulus between the collection dataset and the individual array . . . 74

3.72 Comparison for best HH result on Ramp stimulus between the collection dataset and the individual array . . . 75

3.73 Comparison for best results on Ramp stimulus from the Collection of 3 arrays . . . 76

3.74 Comparison for best results on Ramp stimulus for Individual sweep 2 76

3.75 Close up for best results for individual sweep 2 on Ramp stimulus . . . 77

List of Tables

3.1 Conversion for sweep numbers for 'Short Square: Triple' stimulus . . 14

3.2 Best MSE comparison for 'Short Square: Triple' stimulus 23

3.3 Test to see variability in best parameters found within 20 rounds . . . 26

3.4 Calculated values for $\frac{\tau_w}{a+b}$ 30

3.5 Test to see variability in best parameters found within 20 rounds . . . 31

3.6 Test to see variability in best parameters found within 30 rounds . . . 32

3.7 Test to see variability in best parameters found within 30 rounds (2nd trial 33

3.8 Variability on same parameters for LIF on sweep 5 of SST stimulus . 36

3.9 Variability on same parameters for LIF on sweep 5 for 20 rounds . . . 36

3.10 Starting parameters for the runs from Table 2.5 37

3.11 Variability on same parameters for LIF on sweep 5 (trial 2 38

3.12 MSE comparison for the LIF model on different types of datasets . . 39

3.13 SST: Best parameters found for AdEx on Individual sweep 5 41

3.14 Best parameters found on 20 rounds 41

3.15 Best parameters tested for 30 rounds 42

3.16 MSE comparison for AdEx on different types of datasets 43

3.17 Ten runs of Hodgkin Huxley on best fit parameters for individual sweep 5 45

3.18 MSE comparison for Hodgkin Huxley on different sizes of data 46

3.19 MSE comparisons for neuronal models on SST stimulus 47

3.20 Conversion for sweep numbers for 'Long Square' stimulus 48

3.21 Best parameters tested for 30 rounds 51

3.22 Correlation between $\frac{\tau_w}{a+b}$ and MSE 52

3.23 Reduced ranges for optimised parameters tested for 30 rounds 53

3.24 Initial parameter ranges for AdEx on individual sweep 7 55

3.25 Parameters tested for LIF 56

3.26 Variability on same parameters for LIF on sweep 5, for 20 rounds . . 57

3.27 Best fit MSE comparison for LS: sweep 7 58

3.28 Conversion for sweep numbers 60

3.29 Results for HH on Ramp stimulus and the differing effects caused on same parameters 68

3.30 LIF run on same parameters for Ramp stimulus 71

3.31 MSE comparisons for neuronal models on Ramp stimulus 75

Chapter 1

Introduction

The human brain, with an estimated 170 billion cells, and the complex interrelationship between the neurons and glial cells it contains continues to fascinate. The quest to understand our cognitive processes, and the essence of consciousness, in some ways becomes more elusive as we gather increasing amounts of data and plot the results using mathematical algorithms. Meanwhile, the contest between disease and cure continues.

Extraordinary efforts are being made to reproduce details of morphology and connectivity in the brains of animals and humans. The most computationally detailed reconstruction available of a human brain to date is the H01 dataset, a collaboration between Harvard University's Lichtman Laboratory and the Connectomics at Google team [1]. This is a 1 mm^3 reconstruction of the human cerebral cortex taken from a woman who had undergone surgery to alleviate symptoms of epilepsy.

Despite the impressive undertaking and the new insights that have been acquired, it is only a one-millionth volume of a whole human brain, of which we currently cannot be certain mirrors neurotypical brains.

Presently, to reach the inner layers of the human brain involves invasive surgery. This limits examination of human tissue to segments of the brain from donors undergoing necessary surgery, or from postmortem tissue specimens.

It is difficult to test electrophysiological activity on the latter. Therefore, experiments on animals remain the standard.

Aside from the ethical debates, this is limited in scope as human brains are much more complex than that of the animal brains that are used for testing. For example they have 'an enlarged forebrain, a more complex layered organization, temporally ex-

tended developmental processes (e.g., the progenitor expansion phase), and increased cellular diversity' [2].

This means that, although a seemingly logicial route, desired results are sometimes not replicated once tests are implemented on human volunteers [3].

Besides this, if we are to limit analysis and experimentation in human brains to those already affected by neurological conditions, it remains difficult to assess when diseases and conditions arise, and what causes might instigate them [4].

An area of research and experimentation that is advancing what might be feasible in terms of predicting and mitigating neurodegenerative diseases and neurological conditions is that of brain organoids [3], [5].

However, these human induced pluripotent stem cells currently have their limitations, as they are not fully-formed brains, and their ongoing development is accompanied by questions of whether consciousness may arise, and the ethical debates that co-exist with such possibilities [6].

Concurrently, the rapid advancements of AI models [7], [8], is at the center of present debates around the Turing test [9], the meaning of intelligence [10], consciousness [11], and our moral obligations towards that which we create [12].

As we reach further heights, whether expanding into interdisciplinary areas of research [13], or delving deeper into increasingly microscopic details [1], it is probable that with the assistance of AI, future breakthroughs will be accelerated.

To consider the wealth of knowledge that has already been accumulated, in 1868 Julius Bernstein, by constructing a differential rheotome [14], plotted the first accurate depiction of an action potential [15]. His findings titled, 'Membrane Theory of Electrical Potentials', were published in 1902.

Since then, the study of action potentials has been integral to our understanding of how neurons communicate with each other.

1.1 Leaky Integrate-and-Fire

There is a baseline of general activity contained within a cell membrane, known as the resting potential, which maintains a continuous leak of ionic currents flowing in and out.

Excitatory neurons, the primary source of communication between cells, are composed of three compartments.

The dendrites receive neurotransmitters from presynaptic cells and these chemical messages are processed in the soma. An action potential is triggered when an integrated sum of input current allows the cell membrane's potential to reach a threshold. If this all-or-nothing event occurs, it is then propagated down the axon towards the dendrites of the postsynaptic cells.

The Leaky Integrate-and-Fire model simulates this and can be described mathematically as:

$\tau \frac{dV}{dt} = -(V - V_{rest}) + R \cdot I$ [16]

where:

τ = membrane time constant

$\frac{dV}{dt}$ = change in voltage over time

V = voltage

V_{rest} = resting potential

R = resistance

I = input current

and if:

$V > V_T$ then $V = V_{reset}$

where:

V_T = threshold

V_{reset} = voltage reset

Which is to say that a threshold value is set, and once this target has been reached, the voltage is reset to a pre-assigned value. Additionally, a refractory period can also be assigned (which we do not make use of in this study.)

1.2 Hodgkin Huxley

At resting potential, there is a greater concentration of potassium ions contained within the intracellular environment, whereas sodium ions are found to be in a higher concentration outside the cell membrane.

The Nernst potential (which is the potential at which an ionic current is at equilibrium), can be calculated using the Boltzmann equation. This will vary according to individual cells, but for potassium is approximately -75 mV. As the concentration of potassium ions is higher inside the cell, the steady state for the cell membrane gravitates towards this value.

There are ion-selective channels which are pores for specific ions. When a sufficient quantity of integrated input current has been received, and the threshold (approximately -55 mV) has been reached, a sudden influx of sodium ions enter the cell through the voltage-gated sodium channel, causing the membrane potential to rise rapidly and cause depolarisation.

At the peak of an action potential, there is a sodium inactivation gate which inhibits further sodium ions entering the cell and the sodium channel closes. Voltage-gated potassium channels open fully, allowing potassium ions to leave the cell, which causes repolarisation.

In 1951, Alan Hodgkin and Andrew Huxley published a series of papers describing their groundbreaking theory of how gating variables in ionic channels affect action potentials [17], [18], [19], [20], [21]. Using voltage clamp experiments on a giant squid axon, they used the biological insight gathered from the electrophysiological data collected and produced four voltage and time-dependent differential equations to model their findings.

Using Kirchhoff's Law (which states that current in must equal current out), the core mathematical equation can be described as:

$Cm\frac{dV}{dt} = -I_{total} + I_{ext}$ [21]

where:

Cm = membrane capacitance

$\frac{dV}{dt}$ = change in voltage over time

I_{total} = total ionic current

I_{ext} = external current (from an injected stimulus or received from a synapse)

If we divide the total ionic current into three separate currents for sodium, potassium, and a general leak current, we have:

$$Cm\frac{dV}{dt} = -(I_{Na} + I_K + I_L) + I_{ext}$$

where:

I_{Na} = total sodium current

I_K = total potassium current

I_L = total leak current

The total for individual ionic currents can be further calculated as follows:

$$I_{ion} = g_{ion}(V - E_{ion})$$

where:

I = current

g = conductance. Note: for g_L it would be $\bar{g}_L$ for maximum conductance.

V = membrane potential

E = reversal potential, or equilibrium potential. Note: for E_L, this is "the potential at which the 'leakage current' due to chloride and other ions is zero." [21]

$_{ion}$ = specific ion (i.e., $_{Na}$, $_K$, etc...)

Hodgkin and Huxley deduced that there must be three activation gates (which they named m) and one inactivation gate (which they named h) in the sodium channel, plus four activation gates (which they named n) in the potassium channel.

All gates must be open for a channel to open, at which point the conductance of a channel is at its maximum.

Thus we can further describe the potassium conductance as:

$$g_K = \bar{g}_K n^4$$

and the sodium conductance as:

$$g_{Na} = \bar{g}_{Na} m^3 h$$

If we combine all this together, we have the first differential equation:

1. $\frac{dV}{dt} = \frac{-(\bar{g}_{Na}m^3h(V-E_{Na})+\bar{g}_K n^4(V-E_K)+\bar{g}_L(V-E_L))+I_{ext}}{Cm}$

We can use the Markov transition rate model to calculate the gating variables using the equation:

$$\frac{dn}{dt} = \alpha_n(1-n) - \beta_n n$$

where:

$\frac{dn}{dt}$ = rate of change of n over time

α_n = voltage-dependent transition rate of gate from closed to open

β_n = voltage-dependent transition rate of gate from open to closed

n = the probability that the gate is open

Thus, for the three gates we have:

2. $\frac{dm}{dt} = \alpha_m(1-m) - \beta_m m$
3. $\frac{dn}{dt} = \alpha_n(1-n) - \beta_n n$
4. $\frac{dh}{dt} = \alpha_h(1-h) - \beta_h h$

And the set of four equations.

Since the publication of their seminal papers, further research has discovered that neurons are far more complex, with '≈40 subunit genes coding for K^+ channels alone' [22].

However, their method of turning quantitative, electrophysiological data into mathematical equations remains a benchmark in neuronal modelling [23].

1.3 Adaptive Exponential Leaky Integrate-and-Fire

Although accurate for predicting firing times when neuronal behaviour is uncomplicated, there are obvious limitations with the Leaky Integrate-and-Fire model.

On the other hand, the details of the Hodgkin Huxley model may not always be needed and instead unfavourably affect computational power, time, and energy.

In 2005, Romain Brette and Wulfram Gerstner introduced the Adaptive Exponential Leaky Integrate-and-Fire model (AdEx) [24], which enhances the LIF model, by adding an exponential term to create a curved increase of voltage upon hitting a soft

threshold, and an adaptation current (which mimics the inhibitory channels in the biological version), yet remains much simpler than the Hodgkin Huxley model.

Mathematically, the core equation can be described as:

$$C\frac{dV}{dt} = -g_L(V - E_L) + g_L\Delta T \exp(\frac{V-V_T}{\Delta T}) - w + I \text{ [25]}$$

where:

C = membrane capacitance

V = membrane potential

t = time

$\frac{dV}{dt}$ = rate of change of membrane potential over time

g_L = leak conductance

E_L = leak reversal potential

Δ_T = slope factor

V_T = soft threshold

w = adaptation variable

I = input current

The second equation for the adaptation current can be described as:

$$T_w\frac{dw}{dt} = a(V - E_L) - w$$

where:

T_w = adaptation time constant

$\frac{dw}{dt}$ = rate of change of adaptation variable over time

a = subthreshold adaptation strength

And in addition, upon spiking:

$$V = V_r \text{ and } w \mathrel{+}= b$$

where:

b = spike-triggered adaptation

Which is to say that once the neuron resets after a spike, an amount b is added to w,

to mimic neuronal fatigue.

These are the three neuronal models that we will focus on in this study.

Chapter 2

Data Collection and Computational Tools

2.1 The Allen Institute

Founded in 2003 by Paul and Jody Allen, The Allen Institute is a research institute dedicated to advancing knowledge and scientific discoveries in the fields of biosicence. Their data and scientific resources are open source, lowering barriers of access to information and allowing for worldwide collaborations and accelerated breakthroughs.

As part of their Allen Brain Map data portal, under their Cell Types Database, electrophysiological response data is available for single cells in humans and mice.

Using the Allen Software Development Kit, information for the 2333 available cells was downloaded before those from human donors were separated from the mice data using 'CellTypesApi', leaving 413 human cells.

This data was turned into a pandas dataframe. In this manner, the metadata for a cell can be checked. The details for specimen ID 525011903 can be seen in Figure 2.1.

From this we can deduce that this cell can be located in the External Pyramdidal Layer (layer 3), in the frontal lobe of the right hemisphere, and has a spiny dendrite. In addition, we know that epilepsy can affect the behavior of this cell.

Figure 2.2 illustrates the electrophysiology summary for this cell and verifies some of the data from the pandas dataframe.

In addition, the graphs for the V-I and f-I curve are shown, as well as plots for the

```python
import pandas as pd
from allensdk.core.cell_types_cache import CellTypesCache
from allensdk.api.queries.cell_types_api import CellTypesApi
from allensdk.ephys.ephys_extractor import EphysSweepFeatureExtractor

ctc = CellTypesCache(manifest_file='cell_types/manifest.json')
cell_specimen_id =    525011903
data_set = ctc.get_ephys_data(cell_specimen_id)

human_cells = ctc.get_cells(species=[CellTypesApi.HUMAN])
human_pd = pd.DataFrame(human_cells)
human_ids = human_pd['id']

print(human_pd[human_pd['id']==cell_specimen_id])
```

[3] ✓ 0.0s

```
...  reporter_status     cell_soma_location       species         id  \
0            None  [273.0, 354.0, 216.0]  Homo Sapiens  525011903

                  name structure_layer_name  structure_area_id  \
0  H16.03.003.01.14.02                    3              12113

  structure_area_abbrev transgenic_line dendrite_type  apical  \
0                  FroL                        spiny  intact

  reconstruction_type disease_state   donor_id structure_hemisphere  \
0                None      epilepsy  524848408               right

   normalized_depth
0               NaN
```

Figure 2.1: Metadata for cell ID: 525011903

Figure 2.2: Electrophysiology summary for cell ID: 525011903. Image taken from celltypes.brain-map.org

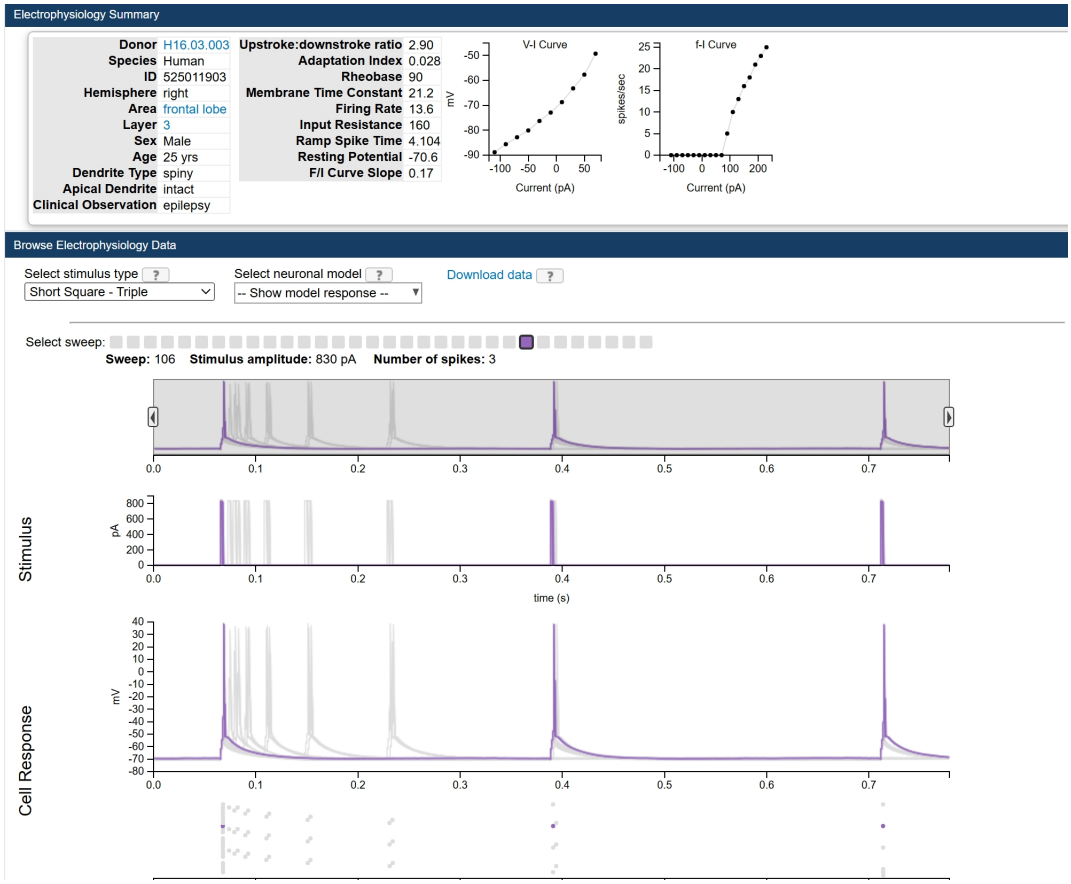

stimulus and cell response for sweep 106. From this we can estimate that the firing rate starts at approximately 80 pA. The steepness of the f-I curve suggests that this neuron is sensitive to input stimuli.

This study will use the data available for cell ID: 525011903, donor: H16.03.003, from the Allen Brain Map, Cell Types Database.

Input current and output response data for the relevant sweeps and desired stimulus types will be extracted and converted into CVS files before being experimented with.

2.2 Brian2 and Brian2modelfitting

In 2008, Dan Goodman and Romain Brette created Brian [26]. This is an open source, clock-driven simulator for spiking neural networks, that uses differential equations and discrete events to define neuronal models, written in the dynamic language of Python.

This was developed with the aim to relieve neuroscientists from the obligation to develop models and write code so that their time could be spent on the application of experimentation instead.

Simple to use, flexible, and regularly updated, it is widely used for the purposes of research.

In this study, we will be using the package brian2modelfitting which is a computational tool provided by Brian2 [27] (an updated version of Brian) for the parameter fitting of neuronal models.

An example of the Leaky Integrate-and-Fire model defined in the brian2modelfitting tool can be seen in Figure 2.3, followed by a brief explanation of the code.

```
def run_model_set_lif(in_c, out_r):

1.      Cm=200*pF
        El=-70*mV

2.      model = '''
a.      dv/dt = (-(v-El)+R*I)/tau : volt
b.      R : ohm (constant)
        tau : second (constant)
        '''

3.      opt = NevergradOptimizer()
        metric = MSEMetric()

4.      fitter = TraceFitter(model=model,
                             input_var='I',
                             output_var='v',
                             input = in_c * amp,
                             output = out_r * mV,
                             dt= 0.02 * ms,
                             n_samples=100,
                             method='exponential_euler',
                             reset='v=-55*mV',
                             threshold='v>-50*mV',
                             param_init={'v': -70*mV})

        np.float = float
5.      res, error = fitter.fit(n_rounds=30,
                                optimizer=opt,
                                metric=metric,
                                R=[100*10**6*ohm, 300*10**6*ohm],
                                tau=[0.01*second, 0.03*second])

6.      traces = fitter.generate_traces()

        return traces
```

Figure 2.3: Example of LIF model defined in brian2modelfitting

1. Constants for the model must be defined:

   here, these are Cm and El.

2. Define the model:

   enclosed by ”’ ”’.

a. use the desired differential equations:

   here, we have implemented the LIF neuronal model (also seen in the introduction.)

b. state the parameters to be optimised:

   here, these are R and τ.

3. Select an optimizing algorithm and a metric:

   here the default for the NevergradOptimizer is ’Differential Evolution’, and MSEMetric refers to Mean Squared Error.

4. Initiate TraceFitter and define parameters.

5. Perform the optimisation and return the results and error:

the ranges for the parameters previously stated must be defined (here, these are R and τ.)

6. Generate traces

Units must always be defined when using Brian. In the model definition, they are stated after the variable followed by a colon (circled in red). Elsewhere by '*' followed by the measure of unit.

Constant variables Cm, E_L, reset, and threshold will be adjusted during the experiments.

Chapter 3

Methods and Results

3.1 Short Square: Triple

The required data was collected for sweeps 100-109 and organised into a collection of 10 arrays. This dataset was sliced to include only the time frame in which the activity of spikes occurred. To ensure that all activity for all sweeps was included, the length of the arrays was taken from the sweep with the longest time frame of recorded activity (here sweep 106.)

For this section, sweeps will be referred to by their index number from the collection dataset. This is to say that sweep 100 from the Allen Institute Cell Types database for cell ID: 525011903 will be referred to as sweep 0, sweep 101 becomes sweep 1, sweep 102 becomes sweep 2, and so forth. Table 3.1 shows the conversions.

Original Sweep Number	becomes	Index of Data Collection (new sweep number)
100	$\Longrightarrow$	0
101	$\Longrightarrow$	1
102	$\Longrightarrow$	2
103	$\Longrightarrow$	3
104	$\Longrightarrow$	4
105	$\Longrightarrow$	5
106	$\Longrightarrow$	6
107	$\Longrightarrow$	7
108	$\Longrightarrow$	8
109	$\Longrightarrow$	9

Table 3.1: Conversion for sweep numbers for 'Short Square: Triple' stimulus

The strength of the input current remains at approximately 800 pA for all sweeps.

An initial analysis of the input current and output response for the neuron shows that there is predominantly a response as soon as the input current is received.

Figure 3.1: Input current and output response for sweeps 0-4 of the 'Short Square: Triple' dataset

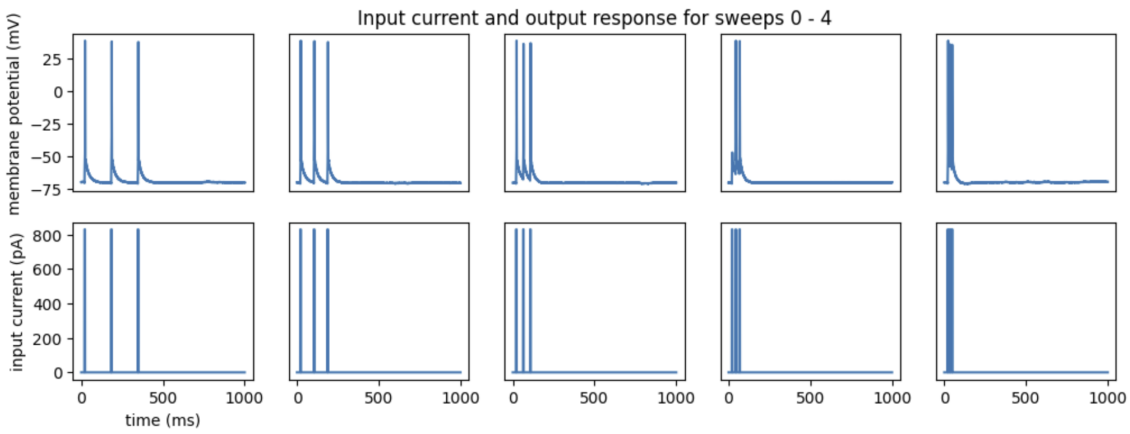

Figure 3.2: Input current and output response for sweeps 5-9 of the 'Short Square: Triple' dataset

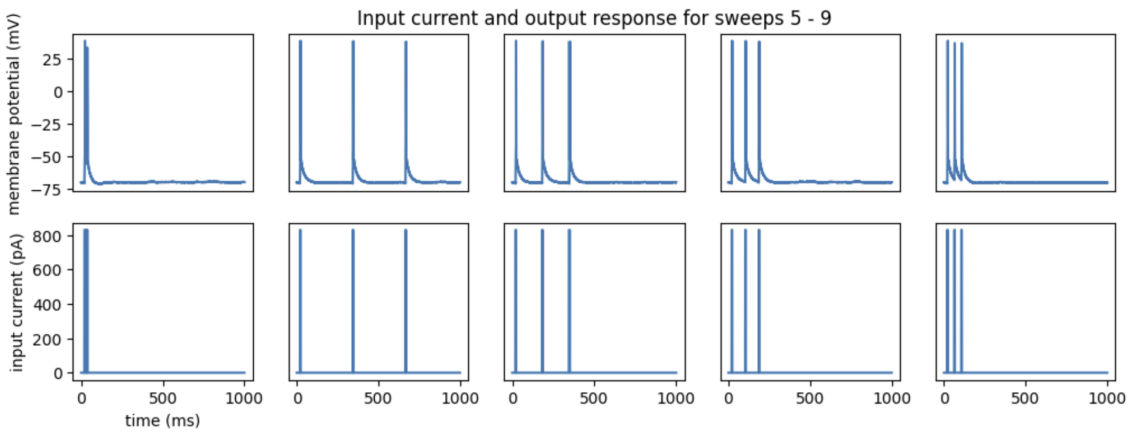

However, we could take a closer look at sweeps 3, 4, and 5.

Figure 3.3: Close up of input current and output response for sweep 3 of the 'Short Square: Triple' dataset

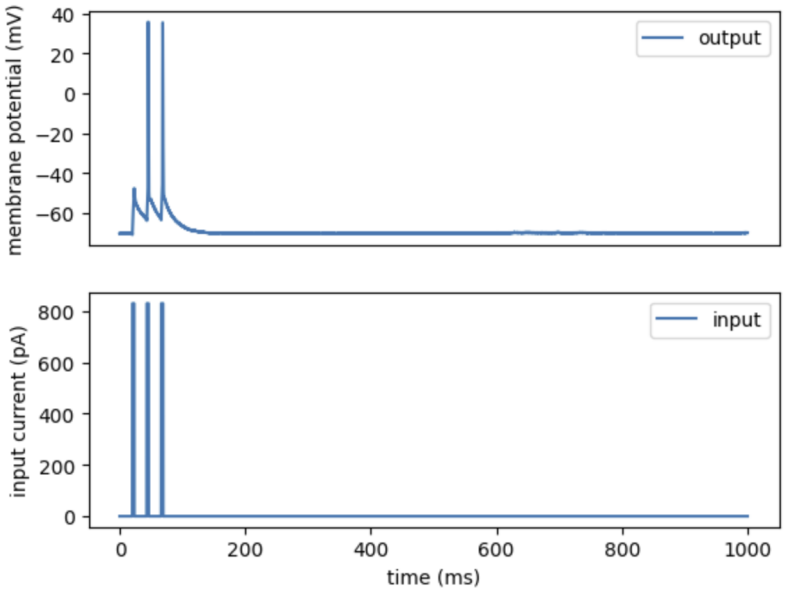

A closer look at sweep 3, illustrated by Figure 3.3, indicates that there is a response for the second and third input current, but not upon the first injected current.

Figure 3.4: Close up of input current and output response for sweep 4 of the 'Short Square: Triple' dataset

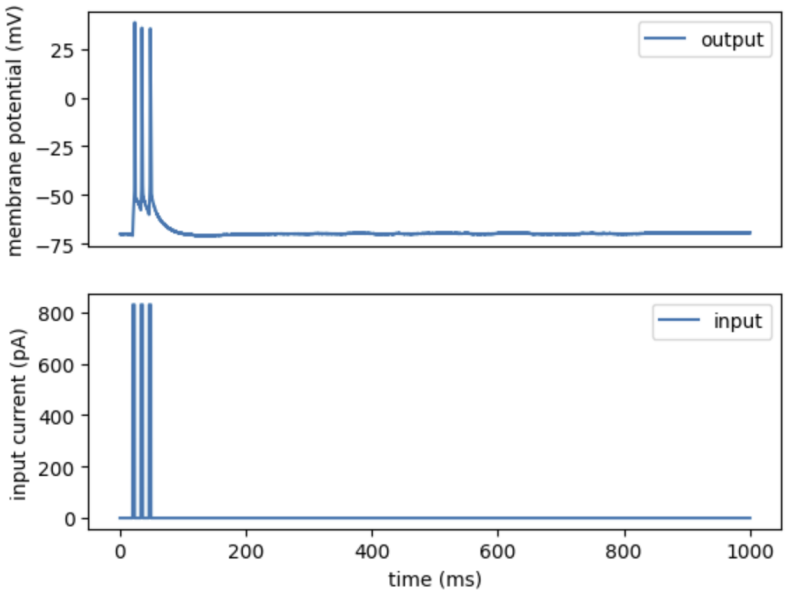

Figure 3.5: Input current and output response for sweep 5 of the 'Short Square: Triple' dataset

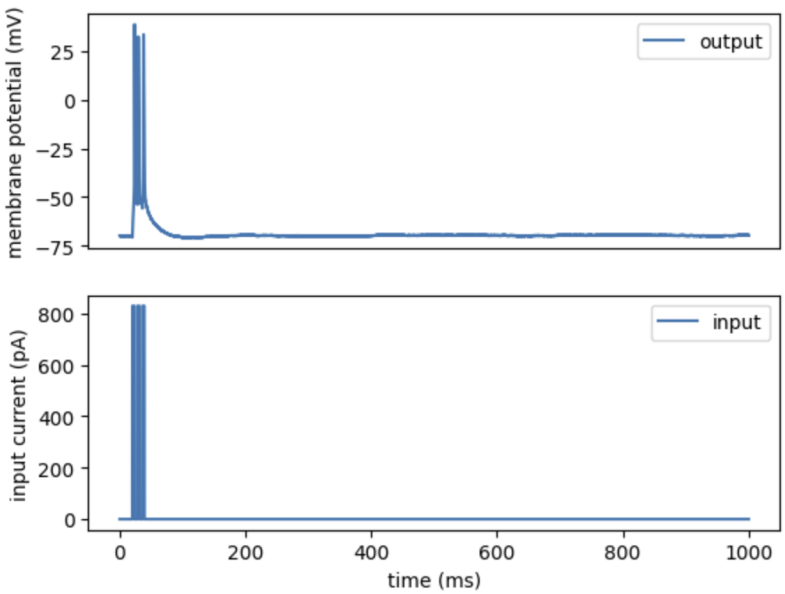

Sweeps 4 (Figure 3.4) and 5 (Figure 3.5) respond to each input current.

3.1.1 Collection of 10 arrays

Leaky Integrate-and-Fire

Initial parameters were set to:

Cm = 200 pF, E_L = -70 mV, reset: v = -70 mV, threshold: $v >$ -50 mV.

The variable for Cm was taken from brian2modelfitting.readthedocs, and the other variables estimated from the target trace.

Best fit parameters were quickly found, with no major adjustments.

Figure 3.6: LIF voltage traces with a wider ISI

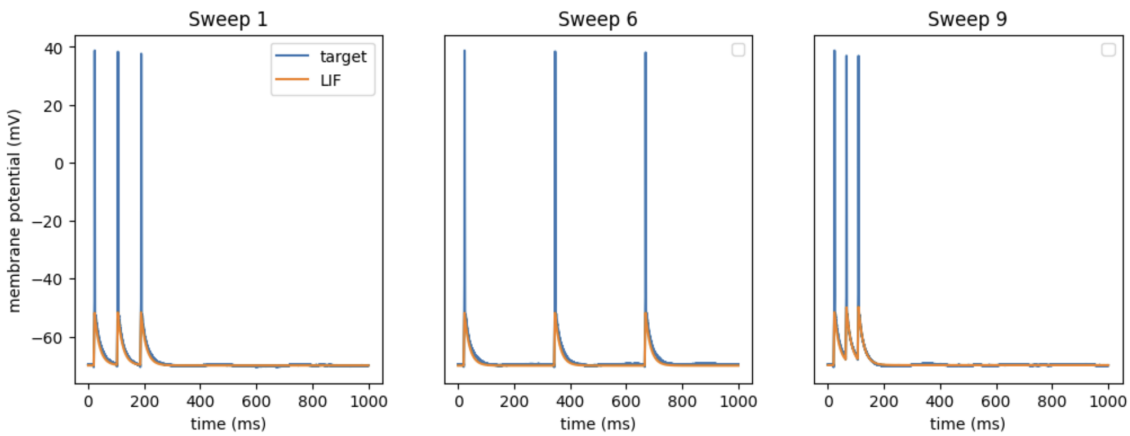

Sweeps 3, 4, and 5, however, were less accurate in their voltage trace outputs.

Figure 3.7: LIF voltage traces with a narrower ISI

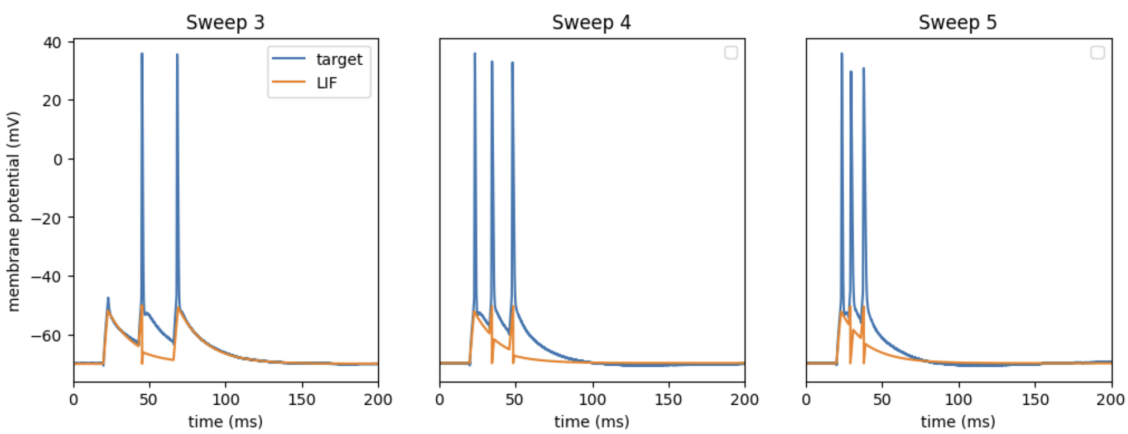

As the majority of the sweeps produced accurate results, this suggested that for sweeps 3, 4, and 5 to be improved upon, they would need to be separated and adjusted further accordingly.

Adaptive Exponential Integrate-and-Fire

Initial parameters were set to:

Cm = 200 pF, G_L = 30 nS, E_L = -70 mV, V_T = -50 mV, Δ_T = 2, vc = 5, and V_r = -70 mV.

Additional parameters were taken from brian2.readthedocs.

As with the Leaky Integrate-and-Fire model, very little adjustments were needed. Best fit parameters were:

Cm = 120 pF, g_L = 5 nS, E_L = -70 mV, V_T = -50 mV, Δ_T = 2, V_r = -70 mV, T_w = 120-160 ms, a = 1-4 nS, and b = 0-0.5 nA.

Figure 3.8: AdEx voltage traces with a larger ISI

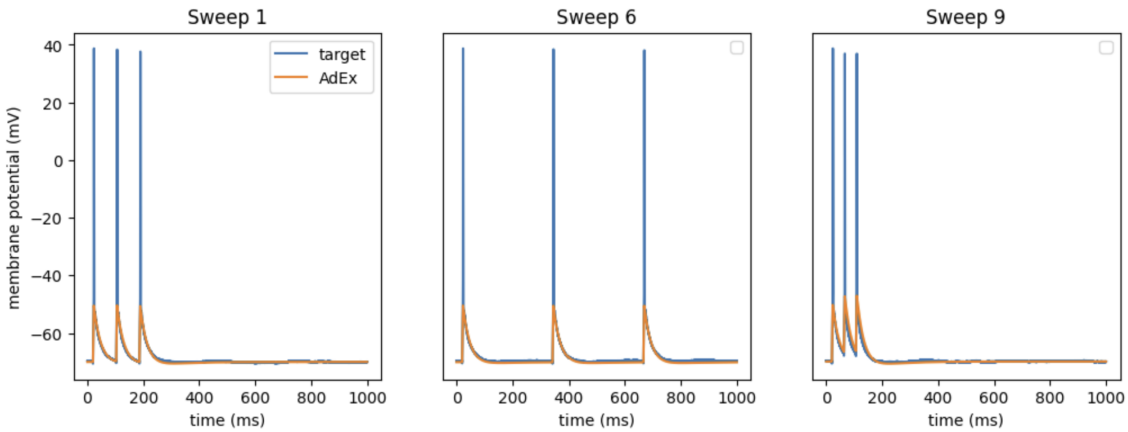

However, sweeps 3, 4, and 5, were less accurate:

Figure 3.9: AdEx voltage traces with smaller ISIs

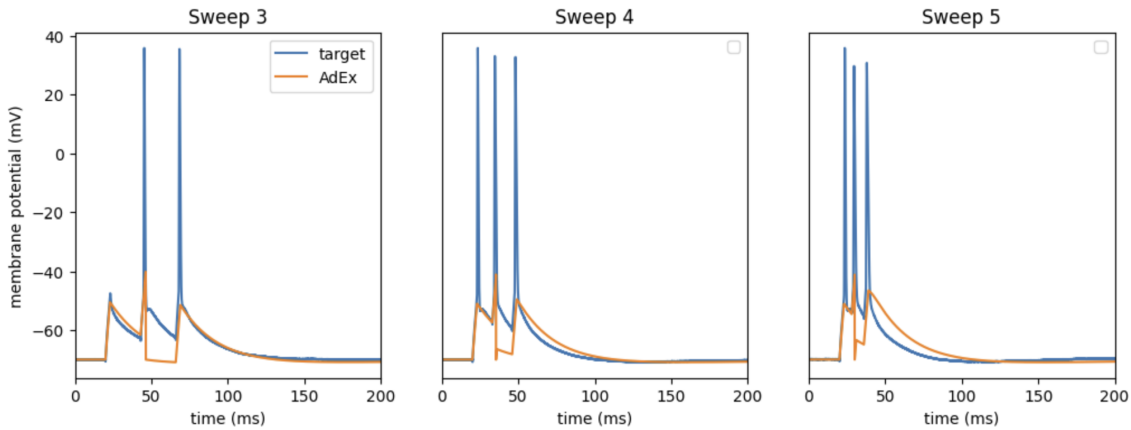

These results were uniform in that the neuronal models found it difficult to match the target voltage trace for sweeps with input current injected within very short time frames of each other.

Hodgkin Huxley

Initial parameters were set at:

Cm = 200 pF, E_L = -65 mV, E_K = -90 mV, E_{Na} = 50 mV, V_T = -63 mV, as seen at brian2modelfitting.readthedocs.

Optimised parameters were set to:

g_L = 1-20 nS

g_{Na} = 0.01-150 μS

g_{Kd} = 1-50 μS

The optimizer was set to 'Differential Evolution' and the method used set to 'exponential euler'. Several other optimizers were tried, but these caused errors, so for this study they were excluded as a possible means for improving accuracy.

These parameters caused hyperpolarisation. See Figure 3.10 for an example:

Figure 3.10: Comparison between output response and HH voltage trace for sweep 6 on 'Short Square: Triple' stimulus

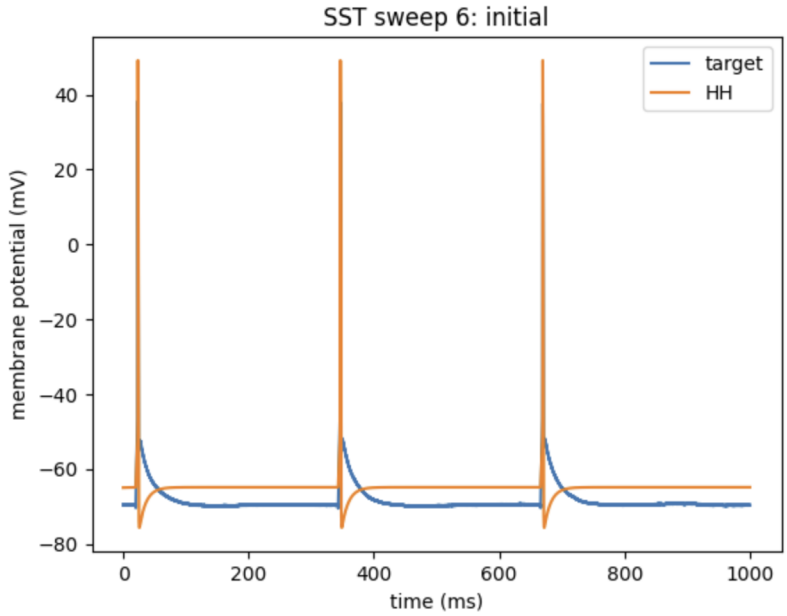

From this we can also deduce that E_L should be set at -70 mV.

Adjustments were made incrementally to explore varying effects.

See Figure 3.11 for an example of the resultant voltage traces of the ten sweeps on the following parameters:

Cm = 120 pF, E_L = -70 mV, E_K = -78 mV, E_{Na} = 40 mV, V_T = -50 mV, g_L = 1-20 nS, g_{Na} = 1-50 μS, and g_{Kd} = 0.01-4 μS.

Figure 3.11: Comparison between target trace and Hodgkin Huxley voltage trace for all sweeps

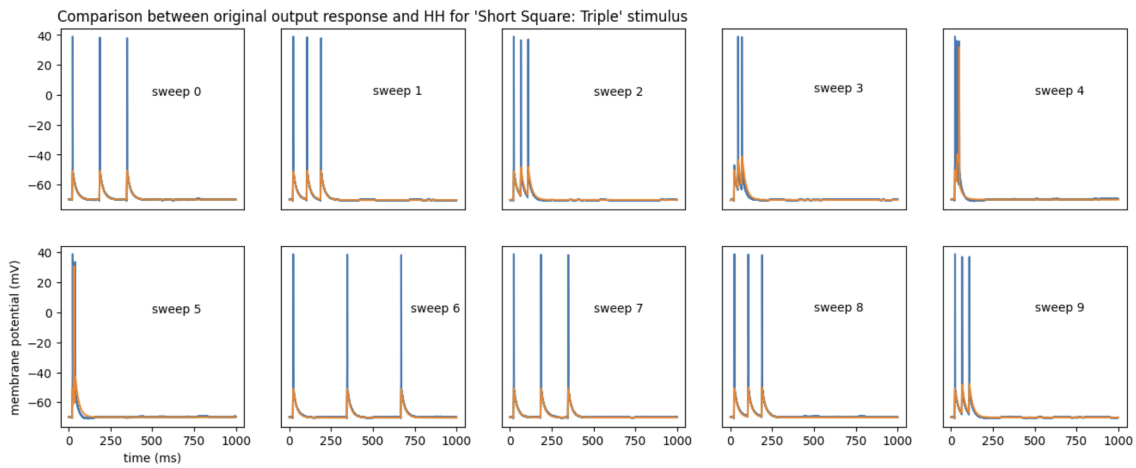

We can see that although the spikes produced by the Hodgkin Huxley model do

not reach the peaks of the target trace, the traces match quite well elsewhere in a uniform pattern, aside from for sweeps 3, 4, and 5.

Figure 3.12: Close up of sweeps 3, 4, and 5

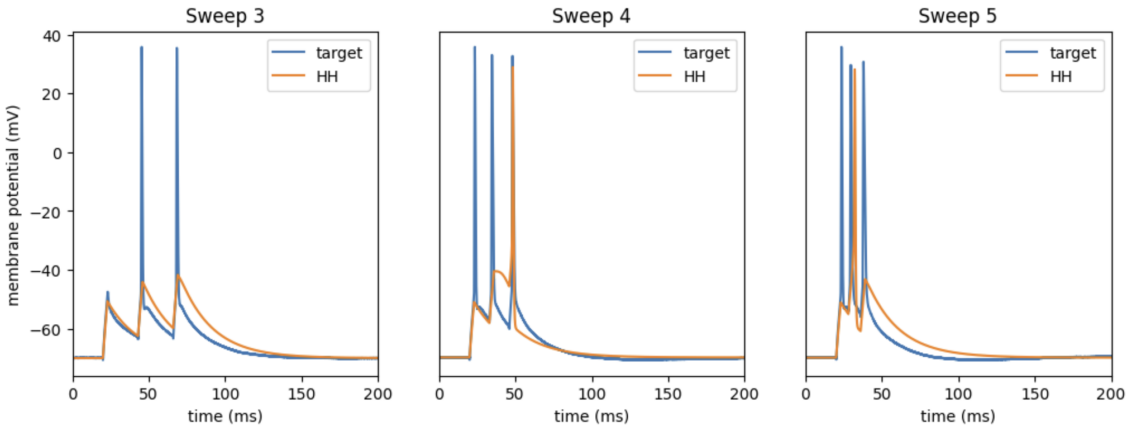

It appears that as the interspike interval (ISI) becomes narrower, the less accurately the models were able to replicate the target trace.

Most sweeps with a wider ISI produced similar traces in relation to the target trace, as seen in Figure 3.13.

Figure 3.13: Hodgkin Huxley voltage traces with a wider ISI from best fit parameters found

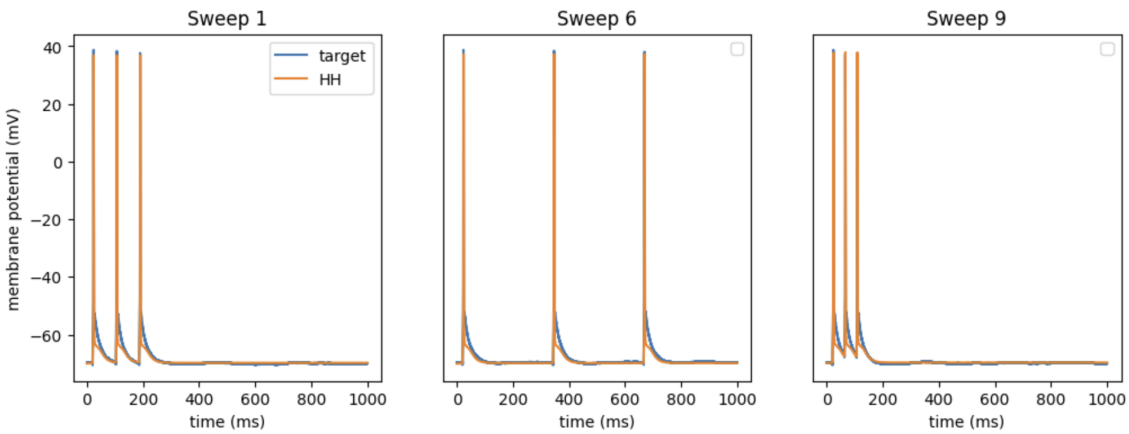

In contrast, when the ISI becomes narrower, the model is less able to produce uniform results. See Figure 3.14.

Figure 3.14: Hodgkin Huxley voltage traces with a narrower ISI

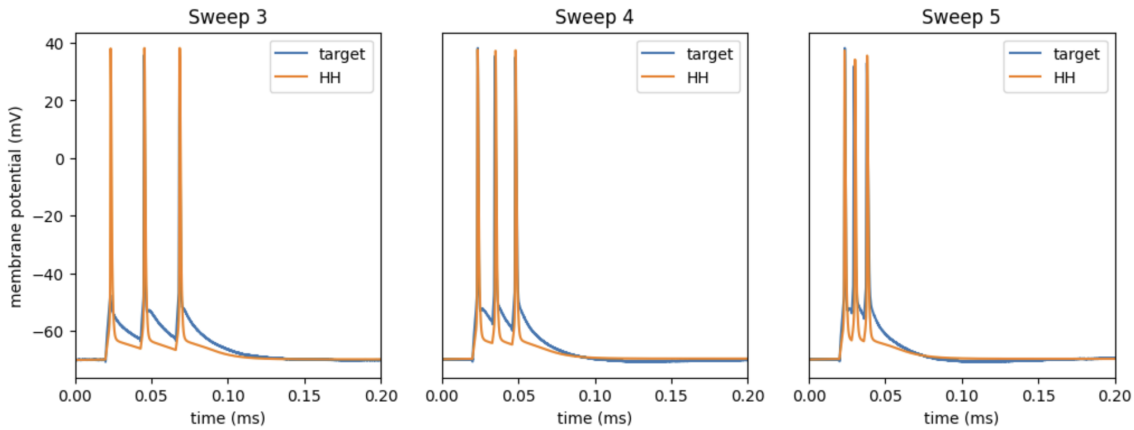

The above are results from the following parameters for the best fit found:

Cm = 200 pF, E_L = -70 mV, E_K = -78 mV, E_{Na} = 40 mV, V_T = -70 mV, g_L = 10-40 nS, g_{Na} = 1-20 μS, g_{Kd} = 0.01-4 μS.

Evaluation

The comparison of mean squared error (MSE) scores for best fit parameters found for the three neuronal models in Table 3.2 suggests that the Hodgkin Huxley model is three times as accurate as both the Leaky Integrate-and-Fire and Adaptive Exponential Integrate-and-Fire models.

Model	Error (mV^2)
LIF	15.71
AdEx	14.05
HH	5.34

Table 3.2: Best MSE comparison for 'Short Square: Triple' stimulus

An interesting note to make is that capacitance for the Hodgkin Huxley model was eventually set to 200 pF, and for the Leaky Integrate-and-Fire and Adaptive Exponential Integrate-and-Fire models, it was set to 120 pF for optimal results.

Figure 3.15 shows the voltage traces that resulted in the closest match with the target trace for all neuronal models:

Figure 3.15: Best fit comparisons for 'Short Square: Triple' stimulus

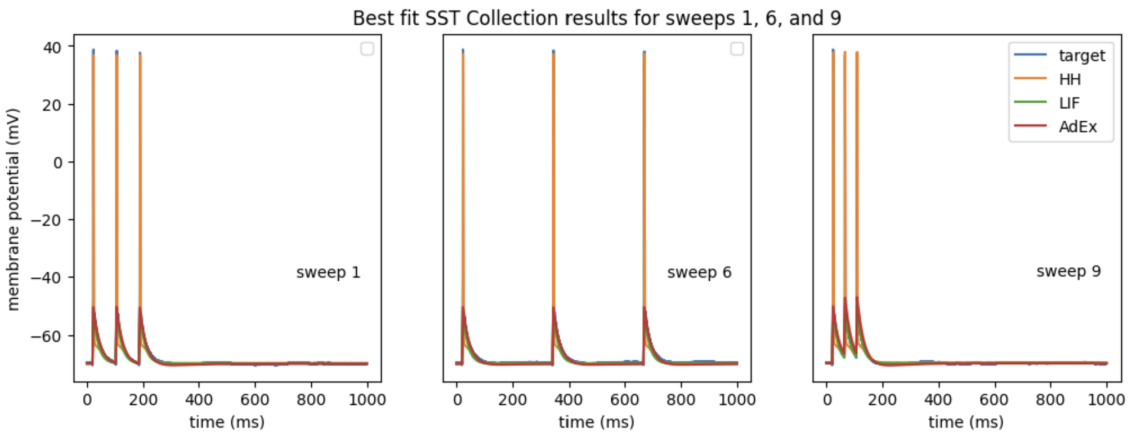

Given that only the Hodgkin Huxley model reaches the peaks of the target trace, it is reasonable that the MSE score is lower.

Figure 3.16 shows the results for sweeps 3, 4, and 5.

Figure 3.16: Comparison on all models for sweeps 3, 4, and 5

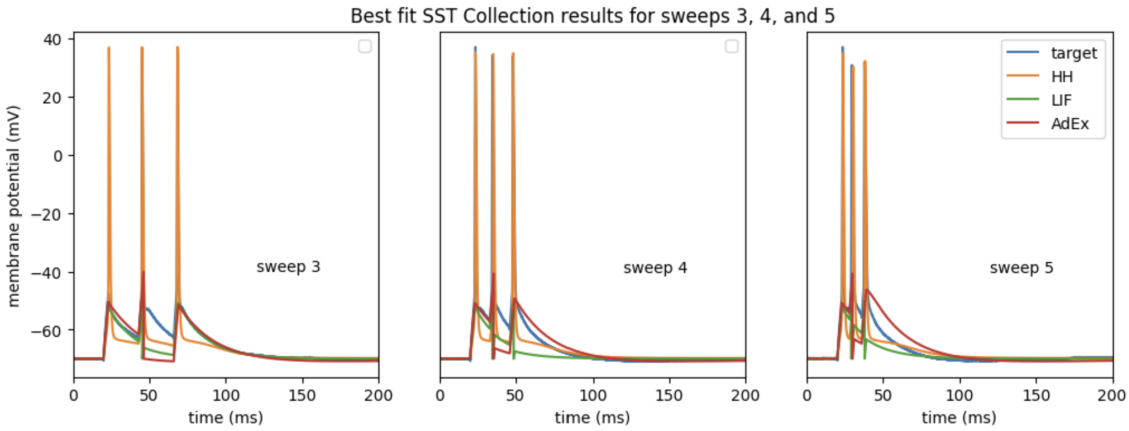

From this we can see that although spike times generally match, there is a tendency to reset too far after the spikes. The exception is the AdEx model for the third spikes in sweeps 4 and 5.

3.1.2 Group of 3 arrays

Given that the majority of the sweeps returned reasonable results with the parameters found, it was possible that further experimentation in this direction would be counterproductive.

Thus, sweeps 3, 4, and 5 were extracted to see if better results could be found for

these sweeps should parameters be adjusted further.

The arrays were sliced again so that only activity for these sweeps was included.

Leaky Integrate-and-Fire

For the initial run, the parameters were set at:

Cm = 120 pF, reset: v = -70 mV, threshold: v > -50 mV.

Figure 3.17: Initial run on LIF for Group of 3 on SST stimulus

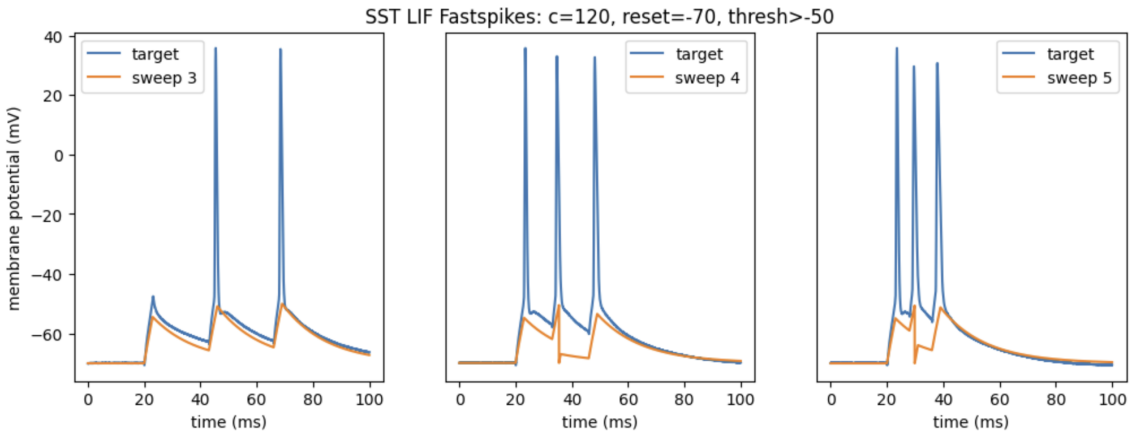

Figure 3.17 shows us that the reset variable should be much higher for sweeps 4 and 5, than for sweep 3.

Adjustments were made and the best parameters found for a balanced result for all sweeps were:

Cm = 120 pF, reset: v = -70 mV, threshold: v > -20 mV.

Figure 3.18: Best fit found for LIF on SST stimulus, Group of 3

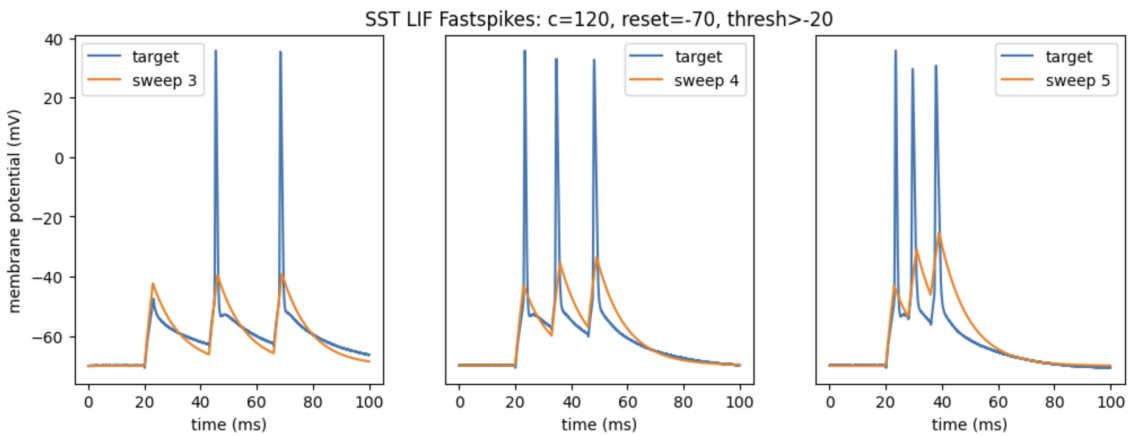

From this point, it appeared that adjusting parameters to improve traces for one sweep would compromise the accuracy in another sweep. This suggested that further improvements would need individual attention.

Adaptive Exponential Integrate-and-Fire

An initial execution of the program on the best parameters previously found (from the Collection of 10 dataset) created the same traces as those found in Figure 3.9.

Parameters were adjusted to the following:

Cm = 120 pF, g_L = 5 nS, V_T = -50 mV, Δ_T = 3, V_r = -53 mV, τ_w = 40-160 ms, a = 1-5 nS, and b = 0-1 nA.

The program was run several times on the neuronal model with the number of rounds set to 20, to see whether there would be any variability in the best parameters found. The results can be seen in Table 3.3.

Run Number	a (nS)	b (pA)	τ_w (ms)	Error (mV^2)
0	1.13	12.90	115.95	119.34
1	1.47	12.54	132.45	119.30
2	1.60	44.52	55.77	130.67
3	1.50	12.98	155.43	119.29
4	1.18	13.04	121.41	119.32
5	1.54	29.63	107.59	127.43
6	1.11	13.50	119.88	119.34
7	1.38	12.87	147.74	119.30
8	2.44	10.13	46.09	119.24
9	1.13	13.77	152.33	119.32

Table 3.3: Test to see variability in best parameters found within 20 rounds

We can see that most runs result in an error close to 119 mV^2. Run numbers 2 and 5, however, result in higher errors, highlighted in red. For these rows, the values for a are higher than average, the values for b are much higher, and the values for τ_w are lower (highlighted in blue.)

If we were to take into account MSE scores alone, we might assume that run 8 would fit into the same category with the rest of the runs, bar 2 and 5. However, we can see that the value for τ_w is lower. It could be assumed that the higher value for a, and/ or the lower than average value for b compensates for this somehow.

We can inspect the voltage traces to ascertain whether these differences in values

relate to differences in the traces.

Most of the runs returned identical traces as illustrated by Figure 3.19.

Figure 3.19: Example of best fit parameters result with lowest MSE score

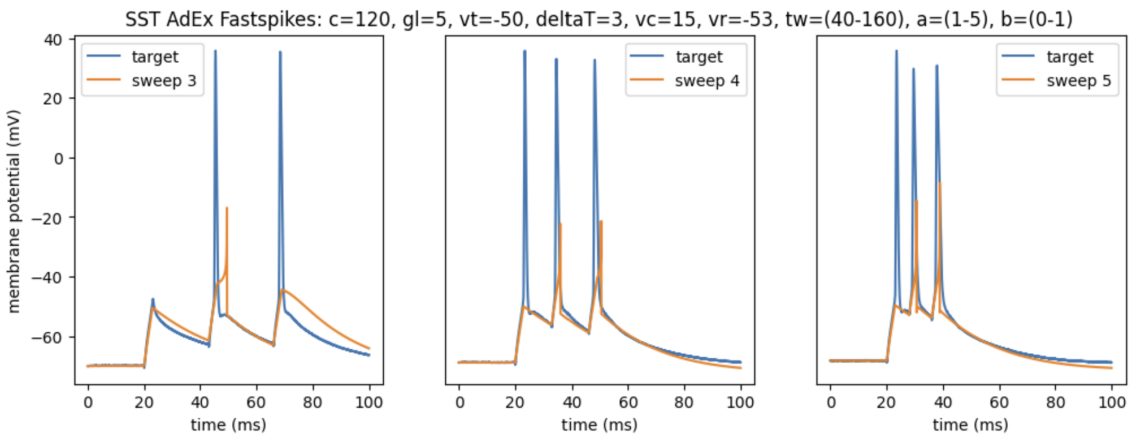

If we have a look at run 8, illustrated by Figure 3.20:

Figure 3.20: Run 8

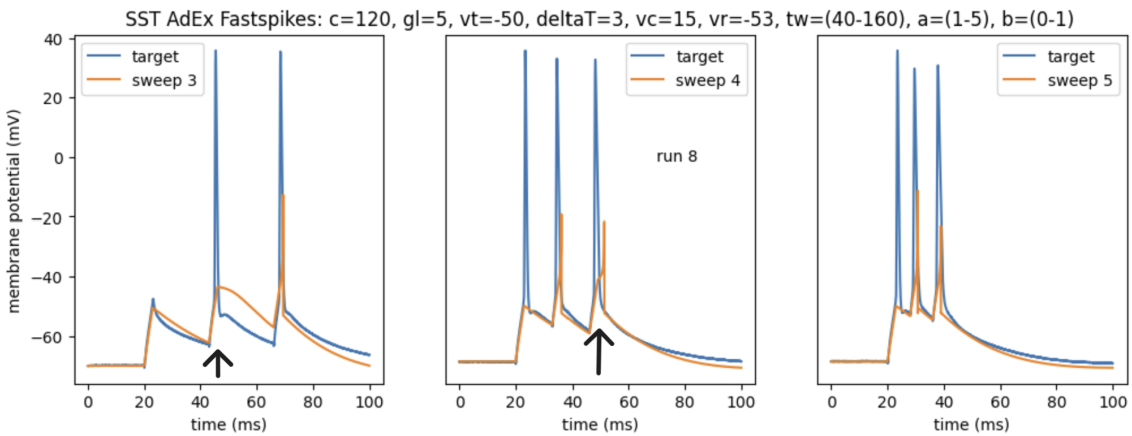

We can see that for sweep 5, the peak of the third spike is lower than that of the second spike, which is in contrast to the other runs with an MSE score of 119 mV^2.

Sweeps 3 and 4 display more obvious contrasts. It seems that these parameters cause a slight divergence after the 40 ms mark. We know that the values for run 8 are markedly different from the other runs with a similar MSE score, and with an especially low value for τ_w. This indicates that we cannot rely on MSE errors alone to judge how similar the results of the traces might be.

If we take a look at run 2 and run 5:

Figure 3.21: Run 2

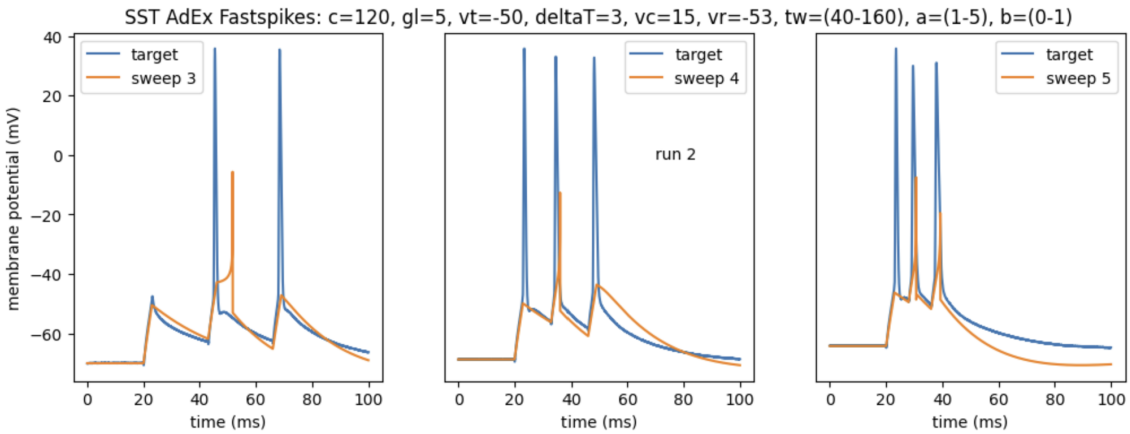

Figure 3.22: Run 5

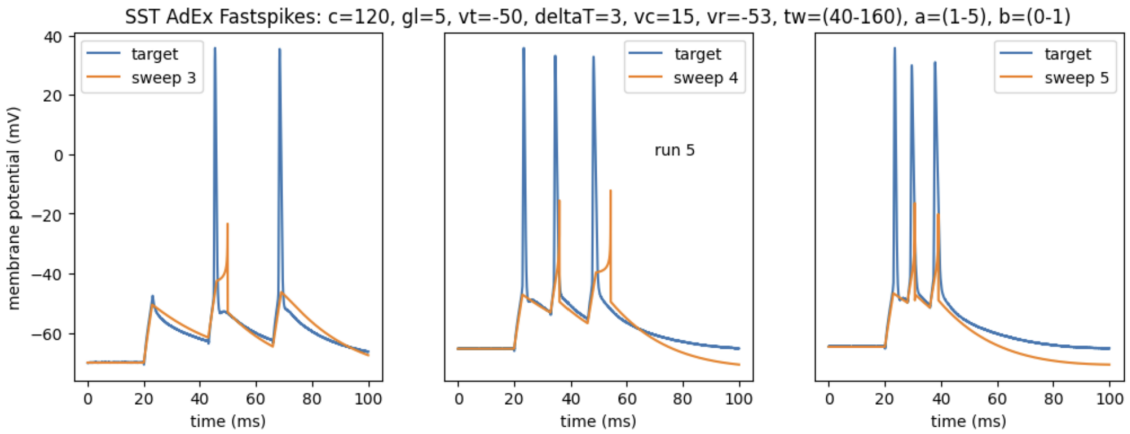

As with run 8, the peak of the third spike is lower than that of the second spike in sweep 5. The peaks themselves differ, however, as do the difference between the two peaks.

Figure 3.23: Sweep 5: run 8, 2, and 5

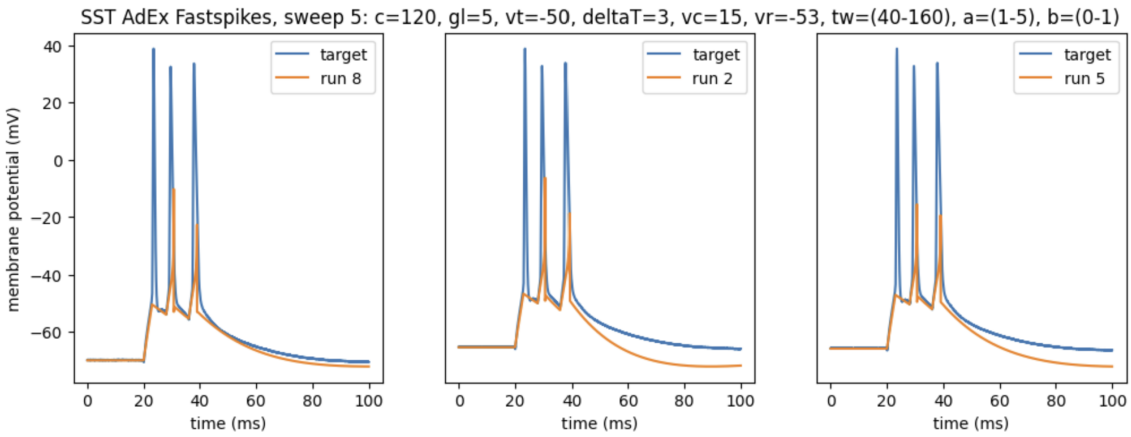

Figure 3.23 shows us that not only is there a difference between the peaks of spikes 2 and 3, but that these parameters also cause hyperpolarisation.

Figure 3.24: Sweep 5: run 8, 2, and 5, plotted together

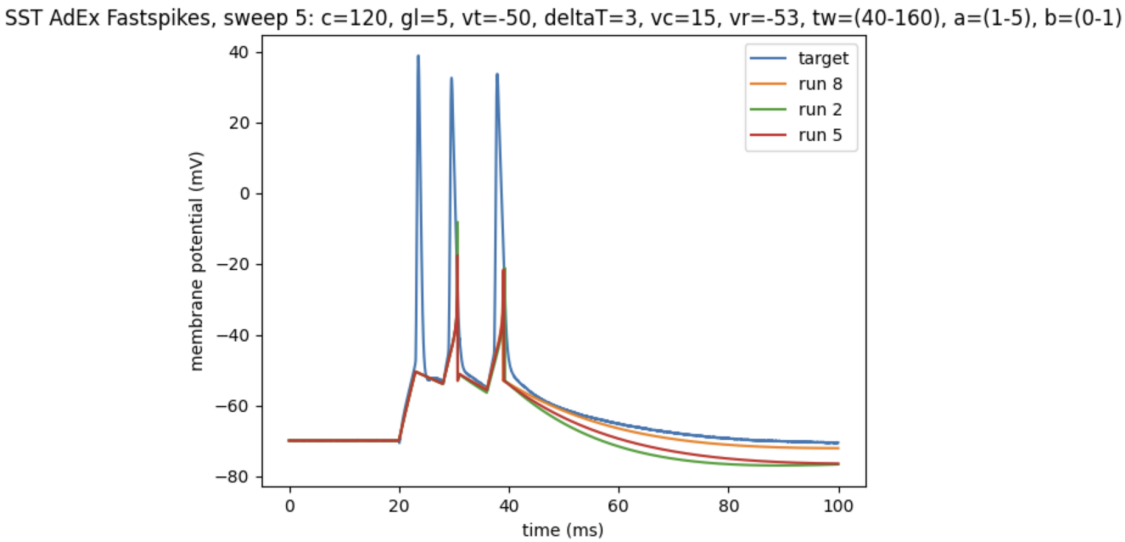

Plotting these together, we can see from Figure 3.24 that the peaks of run 5 are lower than that of run 2. The spikes of run 8 have been concealed so we know that they do not peak past those of run 2. We can also see that lower hyperpolarisation correlates to higher values in a and b. Given that these values are related to adaptation, this seems logical.

We now examine these three runs on sweep 4. See Figure 3.25.

Figure 3.25: Sweep 4: run 8, 2, and 5

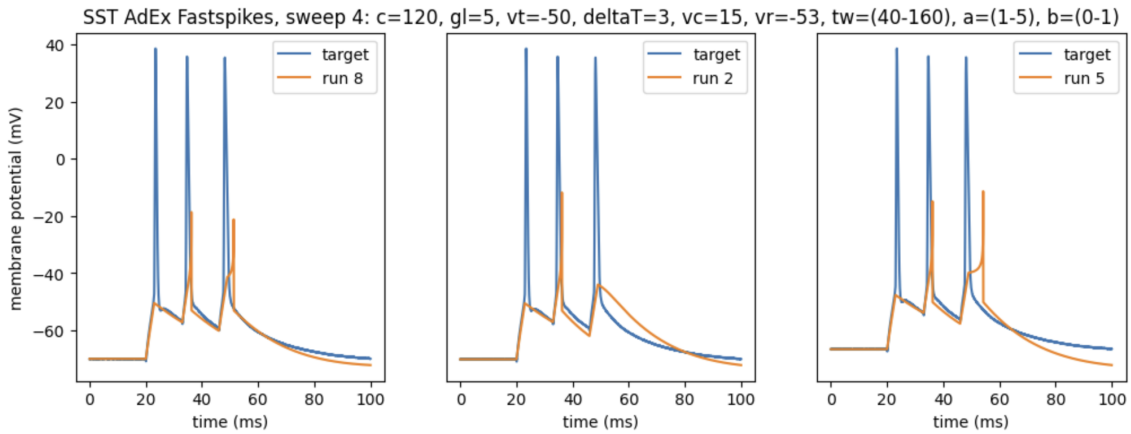

We can see that run 2 does not spike upon the third input current injection.

Run 5 and run 8 have similar trace shapes.

A quick calculation of $\frac{T_w}{a+b}$ shows that the result of this ratio is very close for these two runs. See table 3.4.

Run Number	a (nS)	b (pA)	τ_w (ms)	$\frac{T_w}{a+b}$
0	1.13	12.90	115.95	8.26
1	1.47	12.54	132.45	9.45
2	1.60	44.52	55.77	1.21
3	1.50	12.98	155.43	10.73
4	1.18	13.04	121.41	8.54
5	1.54	29.63	107.59	3.45
6	1.11	13.50	119.88	8.21
7	1.38	12.87	147.74	10.37
8	2.44	10.13	46.09	3.66
9	1.13	13.77	152.33	10.22

Table 3.4: Calculated values for $\frac{\tau_w}{a+b}$

Run 2 has the lowest ratio. This suggests that a lower ratio of $\frac{\tau_w}{a+b}$, as well as high values of a and b and low values of τ_w suppress spikes when input current is injected in short time frames. This matches what we would expect biologically. However, there is currently not enough data to verify this from this experiment.

Hodgkin Huxley

Initial parameters were set to those found from the best fit parameters from the Collection of 10 arrays.

Parameters to be optimised were then widened in range to check whether there would be any variability in the results.

The following parameters were provided to the model and the program executed ten times, with the number of rounds set to 20:

Cm = 120 pF, E_L = -70 mV, E_K = -78 mV, E_{Na} = 40 mV, V_T = -70 mV, g_L = 0-20 nS, g_{Na} = 1-50 μS, g_{Kd} = 0.01-5 μS.

The results can be seen in Table 3.5.

Run Number	g_{Kd} (μS)	g_{Na} (μS)	g_L (nS)	Error (mV^2)
0	0.26	2.05	9.87	62.28
1	0.23	1.51	9.66	53.65
2	0.24	1.39	8.35	51.27
3	0.24	1.45	8.52	50.87
4	0.24	1.77	9.59	56.53
5	0.24	1.47	9.06	51.40
6	0.24	1.40	8.54	50.97
7	0.24	1.55	9.41	55.45
8	0.25	1.91	10.01	60.06
9	0.25	1.95	10.08	60.05

Table 3.5: Test to see variability in best parameters found within 20 rounds

We can see that when g_{Na} reaches 2 μS, this computes the highest g_{Kd}, and a relatively high value for g_L, which creates the highest error, here highlighted in red. g_{Kd} stays within 0.24-0.25 with one instance each of 0.23 and 0.26.

Likewise, the rows for run numbers 8 and 9 have returned comparitively high values in all fields, and higher MSE scores (highlighted in blue.)

Curiously, when the same experiment was applied to the same parameters but with the number of rounds increased to 30, the best fit parameters were more varied. The results can be found in Table 3.7.

Run Number	g_{Kd} (μS)	g_{Na} (μS)	g_L (nS)	Error mV^2
0	0.24	1.44	8.85	50.62
1	0.25	1.48	8.30	52.41
2	0.23	1.21	8.29	47.27
3	0.23	1.65	10.22	54.58
4	0.26	1.61	7.92	56.16
5	0.28	2.88	11.75	79.51
6	0.25	1.89	9.82	60.26
7	0.36	4.18	10.24	108.62
8	0.24	1.60	8.90	53.87
9	0.22	1.29	9.28	49.21

Table 3.6: Test to see variability in best parameters found within 30 rounds

Examining the results, we can immediately see that the highest error by some margin is 108.62 mV^2, which also correlates to high values in all fields. This has been highlighted in red.

The lowest errors correlate to lower values of g_{Kd} and g_{Na}, which have been highlighted in green.

High values for g_L correlate to higher MSE scores, highlighted in blue.

Although the values differ in Tables 3.5 and 3.7, there is a distinct correlation between the values of the rows highlighted in the same colours, compared to the results in the other rows and their MSE scores.

Results often converged before the 30 rounds had concluded. This did not happen as frequently when the number of rounds had been set to 20, although the diminishing difference between values between rounds suggested that best fit parameters had been found, or were close.

To see whether the variability would be repeated, another trial of this experiment (of the same parameters with number of rounds set to 30) was run ten times.

The results can be found in Table 3.8.

Run Number	g_{Kd} (μS)	g_{Na} (μS)	g_L (nS)	Error (mV^2)
0	0.23	1.28	8.58	48.07
1	0.24	1.43	8.70	50.15
2	0.24	1.31	7.98	50.07
3	0.23	1.24	8.30	48.15
4	0.24	1.53	8.57	53.06
5	0.24	1.53	9.21	51.88
6	0.29	2.71	9.31	81.26
7	0.24	1.29	8.21	49.11
8	0.23	1.15	7.57	46.98
9	0.24	1.41	8.46	52.69

Table 3.7: Test to see variability in best parameters found within 30 rounds (2nd trial

The results are much less varied. However, what remains consistent is that high values in all fields (g_{Kd} and g_{Na} highlighted in red, and g_L highlighted in blue) correlate to the highest error (highlighted in purple) and lower values (highlighted in green) correlate to a lower MSE score.

Figure 3.26 shows a comparison for the voltage traces for sweep 3 for the highest MSE and a lower value error compared to the target trace.

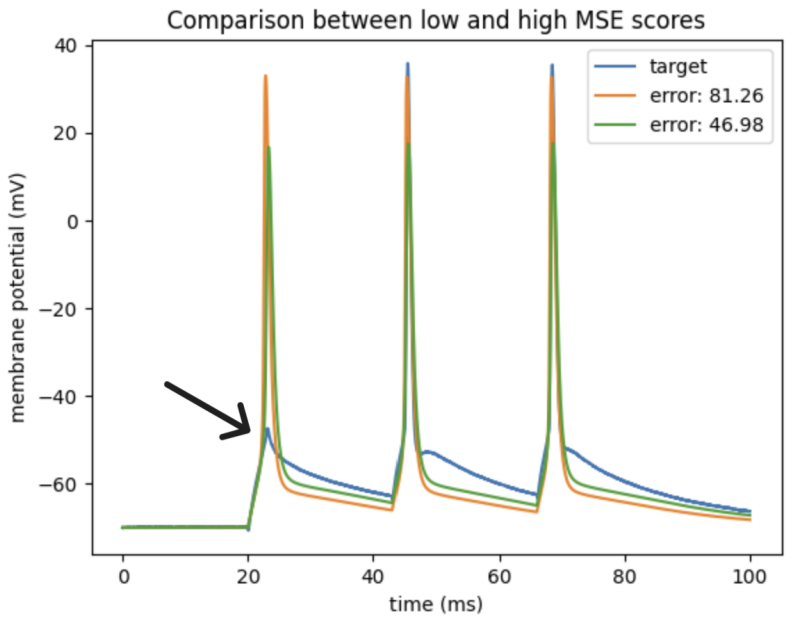

Figure 3.26: Comparison of voltage traces for low and high MSE scores

Despite the higher error, the orange voltage trace almost reaches the peaks of the target trace, whereas the green voltage trace falls short. However, at base, the green trace is closer. For sweep 3, there is a consistent response for the first injected input, in contrast to the target trace. The peak of the first input current of the target trace has been marked by a black arrow for clarity.

As we know that higher MSE scores also returned high values for g_{Na}, this correlates to what we would expect, biologically. In other words, a higher g_{Na} value would allow for higher peaks to be reached.

If we compare traces from low and high MSE scores for all sweeps:

Figure 3.27: Comparison of low and high MSE scores for sweeps 3-5

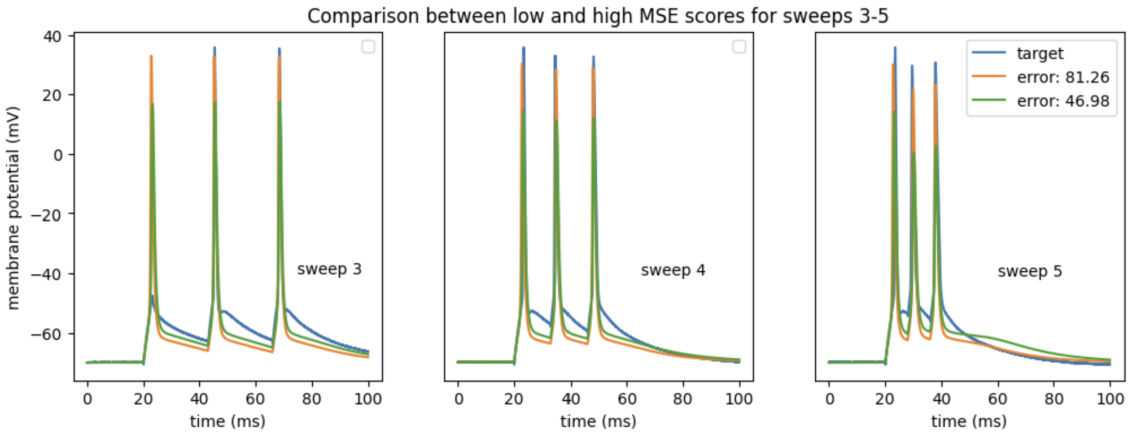

It becomes apparent that as the ISI becomes narrower, the difference between the target trace and the Hodgkin Huxley traces at base become wider, with the higher error producing a lower trace, and therefore further away from the target trace. At the peak, the orange trace is fairly accurate, aside from spiking to reach a peak of 30+ mV for the first input current in sweep 3. As the ISI becomes narrower, the green trace becomes less and less accurate.

3.1.3 Individual array

Leaky Integrate-and-Fire

An initial trial with best parameters found for the Group of 3 arrays produced an arguably worse result as illustrated by Figure 3.28.

Figure 3.28: Initial LIF run on individual sweep 5

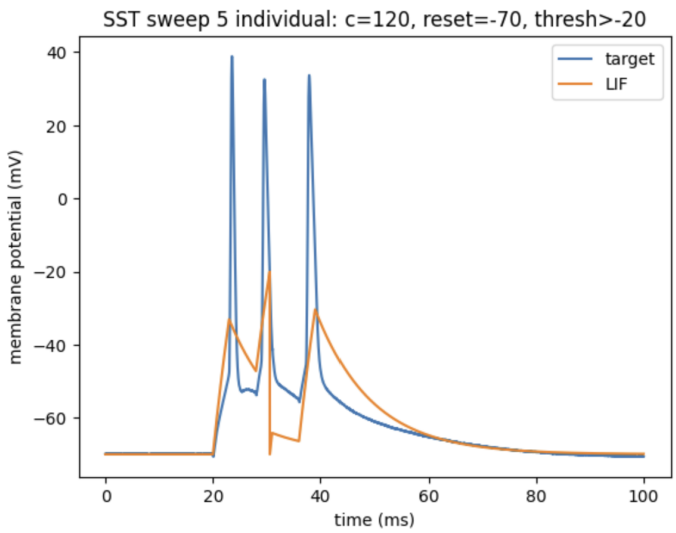

This was run multiple times to see whether results would vary, but results were uniform, with R producing slight variance, but identical voltage traces. Interestingly, the same trace from the 'Group of 3' dataset was not replicated on the same parameters.

The threshold was increased and this improved the model's voltage trace but spike times remained inaccurate, as illustrated by Figure 3.29.

Figure 3.29: Example of inaccurate spike times on LIF

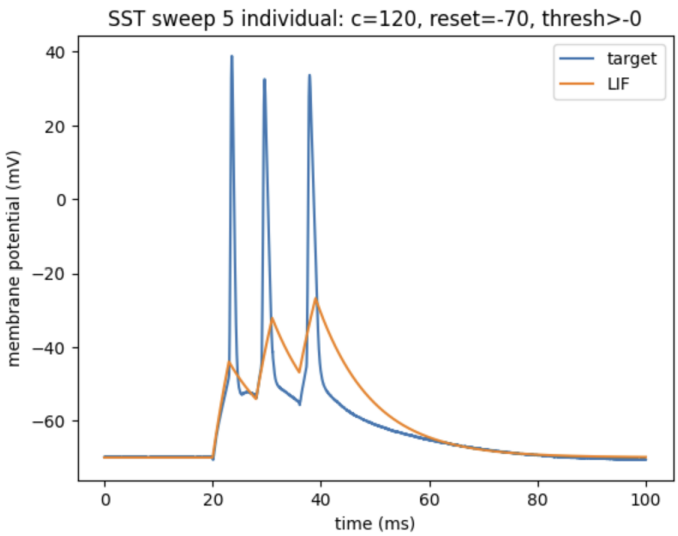

Optimised parameters were widened to see whether the model would be able to find a more accurate fit.

Cm was set to 120 pF, reset for v = -70 mV, threshold for $v > 20$ mV, R between 50-400 MΩ, and τ from 1 - 1000 ms.

Run Number	Resistance (MΩ)	τ (ms)	$\frac{R}{\tau}$	Error (mV^2)
0	100.03	3.95	25.32	101.48
1	114.67	5.91	19.40	108.03
2	120.92	29.14	4.15	205.26
3	113.69	4.84	23.49	104.19
4	103.06	4.42	23.32	102.51
5	111.45	5.26	21.19	105.22
6	107.51	5.43	19.80	106.04
7	111.86	6.41	17.45	110.20
8	116.77	6.66	17.53	111.42
9	100.49	5.11	19.67	106.28

Table 3.8: Variability on same parameters for LIF on sweep 5 of SST stimulus

Observing the values in Table 3.9 shows that the highest values for R and τ, with the smallest ratio between them, result in the highest error, highlighted in red. Likewise, the lowest values for R and τ, with the highest ratio between them, results in the lowest MSE, highlighted in green. Aside from the outlier with an MSE of 205.26 mV^2 (which caused a step response for each input rather than spikes), the traces, with slight variance, were of similar shapes, accuracy aligning with MSE scores.

This also shows us that if there is a wide range for the optimised parameters and the code is run multiple times, it is possible that a variety of results will be produced.

However, extending the number of rounds does not always result in the same best fit parameters found. The same parameters were used and the program run ten times, with the number of rounds set to 20. The results produced can be found in Table 3.10.

Run Number	R (MΩ)	τ (ms)	$\frac{R}{\tau}$	Error (mV^2)
0	101.22	3.31	30.58	100.23
1	100.72	3.27	30.80	100.23
2	100.57	3.29	30.57	100.23
3	100.89	3.31	30.48	100.23
4	101.01	3.35	30.15	100.24
5	100.40	3.28	30.61	100.23
6	100.66	3.29	30.60	100.23
7	148.26	34.45	4.30	214.06
8	100.72	3.28	30.71	100.23
9	131.38	17.08	7.69	160.76

Table 3.9: Variability on same parameters for LIF on sweep 5 for 20 rounds

Values usually converged by the end of the rounds.

Although eight of the runs produced very similar results, there were two that produced high values for R and τ, with a low ratio between their values.

These produced high MSE results and voltage traces that showed steps as responses to injected input, rather than the desired spikes. It appears that more rounds will generally produce less variance, but possibly wider margins of error. Interestingly, this is not due to the starting parameters being higher or there being an insufficient number of rounds for the model to find better fits.

Table 3.11 shows the starting parameters for these runs.

Run Number	Resistance (MΩ)	τ (ms)	Error (mV^2)
0	269.98	137.51	277.16
1	195.74	138.93	281.48
2	214.88	150.45	281.96
3	196.89	105.65	271.02
4	236.42	147.52	279.37
5	290.99	192.89	283.77
6	281.03	133.73	277.42
7	166.04	88.14	266.93
8	239.53	140.57	277.79
9	287.04	141.12	278.34

Table 3.10: Starting parameters for the runs from Table 2.5

If we look at the row for run number 7, highlighted in red in Table 3.11, we can see that it starts with lower values for R and τ. We know that it ends with values of R and τ that are higher than the other runs, so it travels less distance to find the best fit parameters. One might assume that this could be due to a lack of sufficient rounds.

Figure 3.30: Printed results for 20 rounds

```
Round 0: Best parameters R=166.04477899 Mohm, tau=88.13767336 ms (error: 266.92809719 mV^2)
Round 1: Best parameters R=162.91824233 Mohm, tau=63.71330124 ms (error: 251.5656492 mV^2)
Round 2: Best parameters R=120.24951103 Mohm, tau=39.98112578 ms (error: 230.09229996 mV^2)
Round 3: Best parameters R=139.85681996 Mohm, tau=39.98112578 ms (error: 225.25691989 mV^2)
Round 4: Best parameters R=139.85681996 Mohm, tau=39.98112578 ms (error: 225.25691989 mV^2)
Round 5: Best parameters R=139.85681996 Mohm, tau=39.98112578 ms (error: 225.25691989 mV^2)
Round 6: Best parameters R=139.85681996 Mohm, tau=39.98112578 ms (error: 225.25691989 mV^2)
Round 7: Best parameters R=151.99597854 Mohm, tau=34.45395527 ms (error: 214.19398252 mV^2)
Round 8: Best parameters R=151.99597854 Mohm, tau=34.45395527 ms (error: 214.19398252 mV^2)
Round 9: Best parameters R=148.26405207 Mohm, tau=34.45395527 ms (error: 214.06109514 mV^2)
Round 10: Best parameters R=148.26405207 Mohm, tau=34.45395527 ms (error: 214.06109514 mV^2)
Round 11: Best parameters R=148.26405207 Mohm, tau=34.45395527 ms (error: 214.06109514 mV^2)
Round 12: Best parameters R=148.26405207 Mohm, tau=34.45395527 ms (error: 214.06109514 mV^2)
Round 13: Best parameters R=148.26405207 Mohm, tau=34.45395527 ms (error: 214.06109514 mV^2)
Round 14: Best parameters R=148.26405207 Mohm, tau=34.45395527 ms (error: 214.06109514 mV^2)
Round 15: Best parameters R=148.26405207 Mohm, tau=34.45395527 ms (error: 214.06109514 mV^2)
Round 16: Best parameters R=148.26405207 Mohm, tau=34.45395527 ms (error: 214.06109514 mV^2)
Round 17: Best parameters R=148.26405207 Mohm, tau=34.45395527 ms (error: 214.06109514 mV^2)
Round 18: Best parameters R=148.26405207 Mohm, tau=34.45395527 ms (error: 214.06109514 mV^2)
Round 19: Best parameters R=148.26405207 Mohm, tau=34.45395527 ms (error: 214.06109514 mV^2)
```

However, Figure 3.30 shows us that by round 9, the model has found its 'best fit' parameters.

If we now look at Run number 9, highlighted in blue in Table 3.11, the starting parameters do not seem to be noticeably different from the other runs, yet we know that it ends with finding best fit parameters that do not converge to the mean values of the other runs.

This experiment was put through another trial to check whether there would be any variability, with the number of rounds set to 20.

Run Number	Resistance (MΩ)	τ (ms)	Error (mV^2
0	100.57	3.25	100.23
1	100.64	3.29	100.23
2	100.67	3.29	100.23
3	100.70	3.29	100.23
4	101.02	3.30	100.23
5	100.78	3.29	100.23
6	100.81	3.29	100.23
7	100.40	3.29	100.24
8	100.67	3.29	100.23
9	100.65	3.27	100.23

Table 3.11: Variability on same parameters for LIF on sweep 5 (trial 2

There is extremely low variability. As there were only two results that diverged from the mean in the previous trial, this could be because the outliers were avoided during

the ten runs.

However, this was put through another ten runs, with almost identical results. These more recent results were in stark contrast from previous results. As some time had passed between the trials, it could be that the software had been updated in the interim.

We can conclude that best fit parameters have been found.

Figure 3.31 illustrates the resulting voltage trace from these trials.

Figure 3.31: Best fit for LIF on sweep 5, individual array

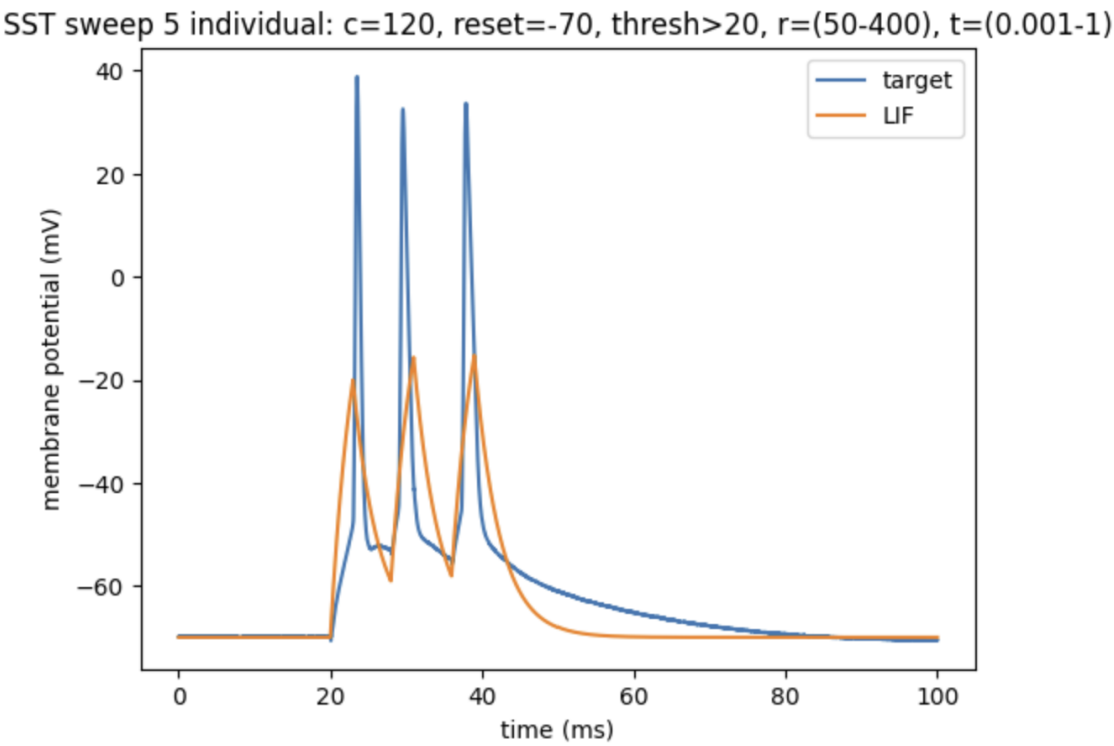

The comparison between the best MSE results found for the LIF model on the Collection of 10 arrays, the Group of 3 arrays, and the Individual array of sweep 5 is given in Table 3.13.

Type of dataset	Error (mV^2)
Collection of 10 sweeps	15.71
Fast spike group of 3	46.98
Individual sweep 5	100.23

Table 3.12: MSE comparison for the LIF model on different types of datasets

This might suggest that accuracy gets worse as data is reduced. However, given that there would be sweeps remaining at resting potential for periods of time in

grouped datasets, and that this in itself would improve accuracy, the contrast seems reasonable.

The results for the first two types of datasets are also mean results for of all sweeps in those collections. It should also be noted that the length of the arrays in the latter two results would be of 5,000, compared to arrays of length 50,000 for the dataset for the 'Collection of 10' arrays.

Figure 3.32: Comparison results for SST on LIF model

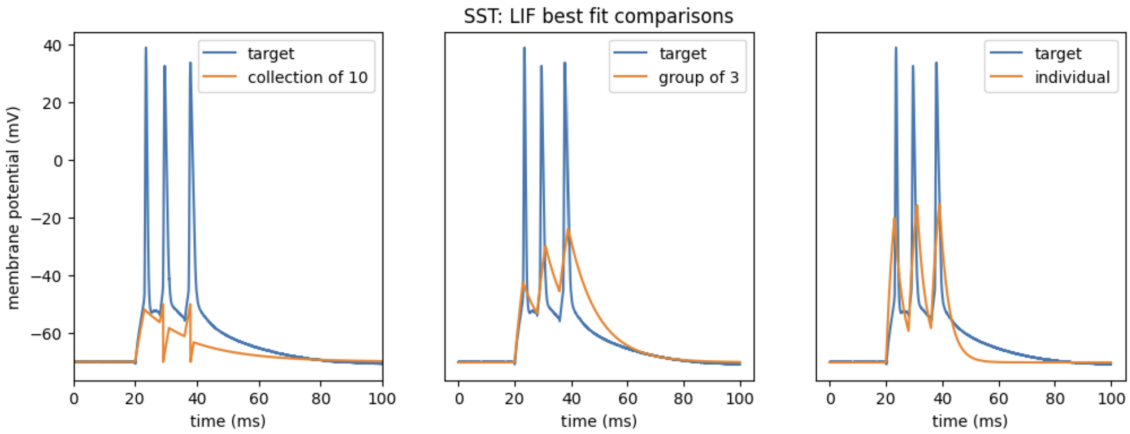

We saw in Figures 3.6 and 3.7 that although the LIF model produced accurate voltage traces for the majority of the sweeps, those with a narrow ISI struggled with accuracy when run together as a collection of 10 sweeps of variable input data.

Extracting the three sweeps with the narrowest ISI allowed for more nuance.

However, separating the sweeps to allow for individual adjustments produces more desirable results still.

Adaptive Exponential Integrate-and-Fire

The initial run for the AdEx model on sweep 5 of the 'Short Square: Triple' stimulus as an individual array produced an identical voltage trace as that for sweep 5 when run as part of the 'Group of 3' arrays.

Parameters a, b, and τ_w were given ranges for the model to optimise, and Cm, g_L, V_T, Δ_T, V_C, and V_r were set in the model equation, and adjusted manually to begin with.

The number of rounds was set to 10. Where results from the voltage trace and best fit parameters found suggested further investigation was desirable, the number of rounds was increased.

There were some attempts to allow the model further optimised parameters, but it was debatable whether the model found better results when there were more parameters to optimise.

Set parameters for the closest solution found were:

Cm = 60 pF, g_L = 20 nS, V_T = -50 mV, ΔT = 3 mV, V_T = 15 mV, V_r = -53 mV,

and the optimised parameters were:

τ_w = 40-160 ms, a = 1-5 nS, and b = 0-1 nA.

This was run five times with the number of rounds set to 10, to see if there would be any variability. The results can be found in Table 3.14.

Run Number	a (nS)	b (pA)	τ_w (ms)	Error (mV^2)
0	1.42	18.88	44.25	201.97
1	1.73	38.16	124.46	207.43
2	4.52	35.37	51.20	203.31
3	2.04	39.84	49.38	201.11
4	1.26	41.14	52.01	203.12

Table 3.13: SST: Best parameters found for AdEx on Individual sweep 5

Although values did not always converge by the end, there was mostly minimal movement by round 10.

However, there was enough variability seen in the voltage traces to suggest that further investigation might produce interesting results. Thus, the code was run on the same parameters a further ten times, with the number of rounds increased to 20.

Run Number	a (nS)	b (pA)	τ_w (ms)	Error (mV^2)
0	1.10	7.17	42.81	191.32
1	1.47	8.48	47.29	193.16
2	1.03	0.20	151.87	184.27
3	1.59	41.21	44.63	200.62
4	1.07	0.66	154.49	184.83
5	1.03	0.16	158.39	184.19
6	1.15	42.17	44.27	201.21
7	1.34	41.44	46.88	201.72
8	1.23	42.08	43.70	200.62
9	1.10	0.43	158.06	184.57

Table 3.14: Best parameters found on 20 rounds

As can be seen in Table 3.15, best fit parameters found were still varied. However,

from these results we can observe that the lowest values for a and b, and the highest values of τ_w correlate with the lowest MSE scores. These rows have been highlighted in green.

Looking at results from both Table 3.14 and Table 3.15, we can see that higher values of a and b correlate to the highest MSE scores. The rows highlighted in red produced similar voltage traces where the third input injection did not produce a response.

An example can be seen in Figure 3.33.

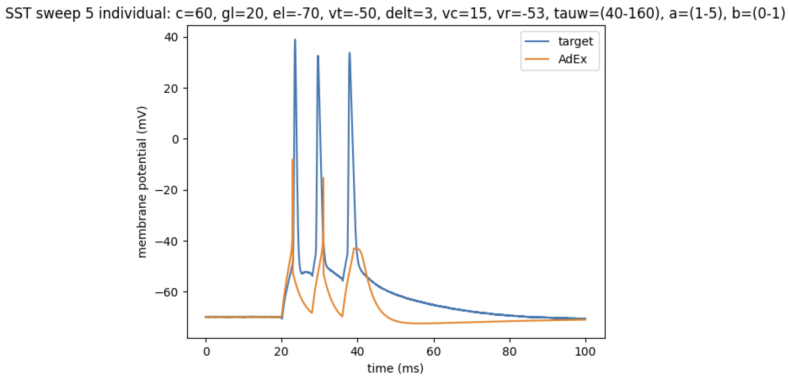

Figure 3.33: Example output trace with no response upon third input

To see if 30 rounds would produce less variability, this was tested ten times and the results can be seen in Table 3.16.

Run Number	a (nS)	b (pA)	τ_w (ms)	Error (mV^2)
0	1.31	41.88	43.98	200.90
1	1.04	0.23	157.02	184.29
2	1.14	41.32	50.80	200.84
3	1.23	41.82	45.42	200.88
4	1.01	0.02	158.75	184.02
5	1.26	42.17	42.73	200.91
6	1.34	42.02	42.60	200.18
7	1.02	0.02	159.47	184.02
8	1.03	0.11	158.67	184.14
9	1.20	1.07	158.48	185.19

Table 3.15: Best parameters tested for 30 rounds

As we can see from the results in Table 3.16, the optimised parameters have become binary. The rows highlighted in red did not respond to the third input current, whereas those highlighted in green produced a spike.

There are an equal number of green and red results. Those with an MSE result of 200 mV^2 converged early. The rows highlighted in green were usually still adjusting their parameters by round 30, although these adjustments were minimal.

This suggests that the best fit for the optimised parameters for this set-up can be found within the ranges produced by the rows highlighted in green. As the rows highlighted in red converge before the end of the 30 rounds, we can deduce that certain combinations of parameters will cause the model to get stuck and be unable to explore further.

The best trace found caused a suppressed doublet, marked by a black arrow in Figure 3.34.

Figure 3.34: Best fit for the AdEx model on individual sweep 5

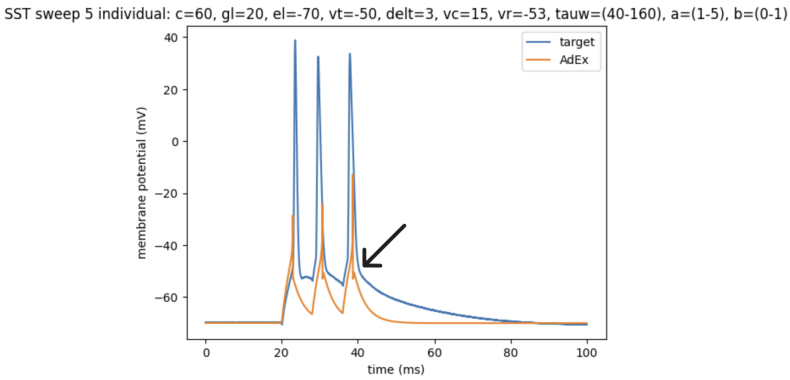

Closer traces were found in previous trials for this experiment, but were unable to be replicated during this trial.

We can now compare the MSE scores for AdEx on the different groups of 'Short Square: Triple' stimulus:

Type of dataset	Error (mV^2)
Collection of 10 sweeps	14.05
Fast spike group of 3	119.45
Individual sweep 5	184.65

Table 3.16: MSE comparison for AdEx on different types of datasets

And the voltage traces are illustrated in Figure 3.35:

Figure 3.35: Comparison results for SST on AdEx model

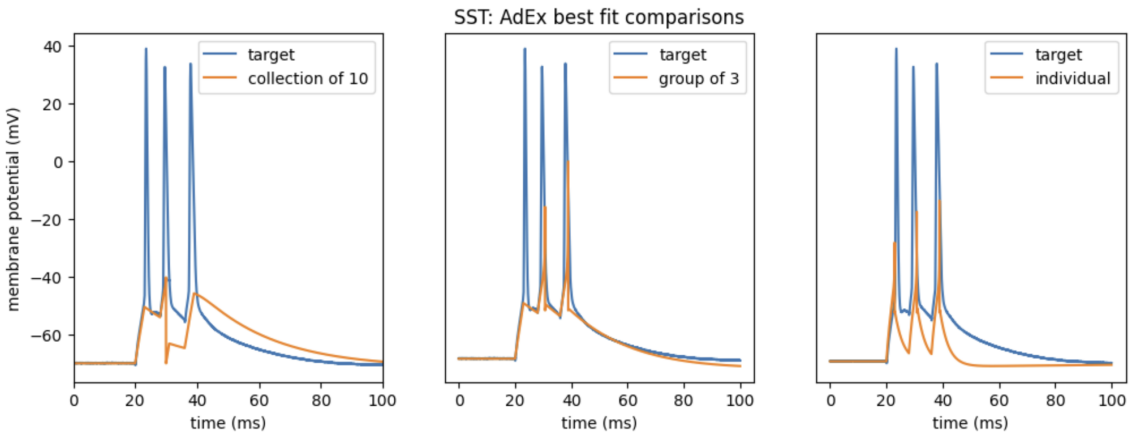

It is apparent that the voltage traces become more accurate as datasets are reduced.

Hodgkin Huxley

An initial run on the following parameters:

Cm = 120 pF, E_L = -70 mV, E_K = -78 mV, E_{Na} = 40 mV, V_T = -50 mV, g_L = 0-10 nS, g_{Na} = 1-20 μS, g_{Kd} = 0.01-0.25 μS,

produced a similar trace to that from the best fit of the 'Group of 3' dataset with an MSE of 45.59 mV^2 as illustrated by Figure 3.36.

Figure 3.36: Initial run with Hodgkin Huxley on individual sweep 5

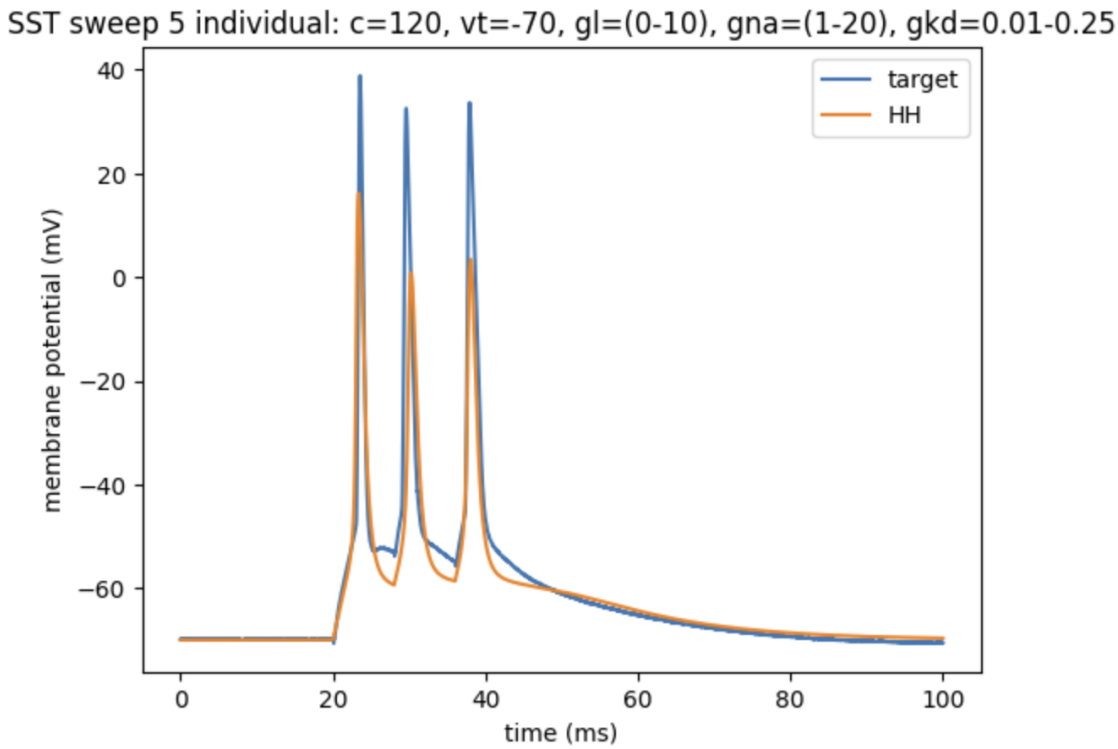

Parameters were adjusted to E_K = -75 mV, E_{Na} = 50 mV, V_T = -70 mV, g_L = 0-15 nS, g_{Na} = 1-30 μS, g_{Kd} = 0.01-0.6 μS

The code was executed ten times. The results produced are given in Table 3.18.

Run Number	g_{Kd} (μS)	g_{Na} (μS)	g_L (nS)	Error (mV^2)
0	0.27	1.86	12.88	68.57
1	0.31	2.14	9.91	85.74
2	0.29	2.06	12.24	80.23
3	0.24	1.58	13.26	52.33
4	0.27	2.03	13.72	74.28
5	0.24	1.71	13.96	54.91
6	0.25	1.88	14.61	60.83
7	0.24	1.53	13.05	55.39
8	0.27	2.16	13.45	71.97
9	0.30	2.75	13.99	90.41

Table 3.17: Ten runs of Hodgkin Huxley on best fit parameters for individual sweep 5

As noted previously, higher MSE results often produced arguably closer voltage traces.

Figure 3.37 shows the voltage traces produced by the lowest and highest MSE results plotted together against the target trace. As some of the traces are concealed and it

is difficult to see where the spikes peak, adjacent to this, the lowest, then highest MSE results have been plotted separately against the target trace.

Figure 3.37: HH on individual sweep 5: lowest and highest MSE results compared

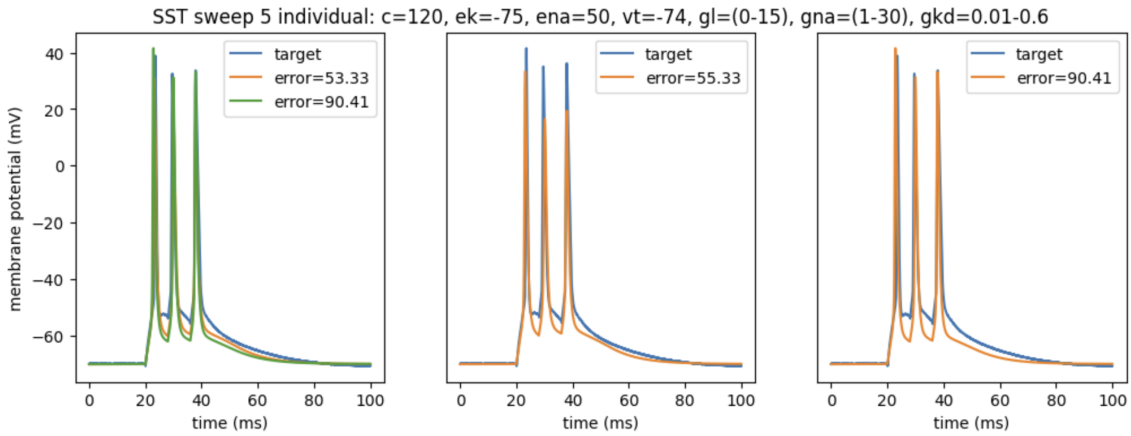

As noted before during the 'Group of 3' assessment, higher MSE results reach a more accurate peak, but are less accurate at the base.

Using the lowest MSE scores, we can compare results for the different data structures. See Table 3.19.

Type of dataset	Error (mV^2)
Collection of 10 sweeps	5.34
Fast spike group of 3	47.10
Individual sweep 5	55.33

Table 3.18: MSE comparison for Hodgkin Huxley on different sizes of data

However, since we are aware that lower MSE results do not necessarily produce more accurate traces, we should also examine the voltage trace outputs.

Figure 3.38: Hodgkin Huxley best fit comparison

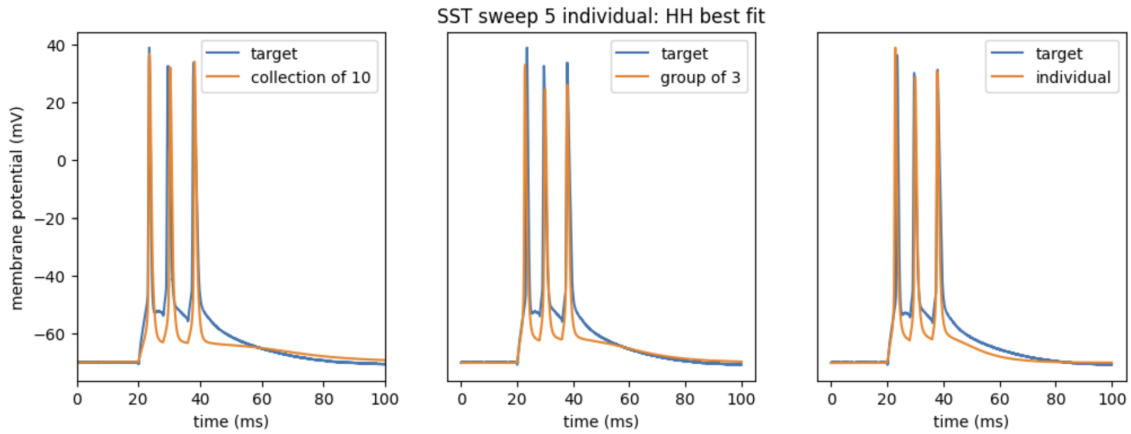

In contrast to the LIF and AdEx models, there is not much difference between the traces for the different datasets for the Hodgkin Huxley model.

3.1.4 Evaluation

We can now compare the models for each type of dataset for the best fit parameters found so far.

Model	Type of dataset	Error (mV^2)
HH	Collection of 10 sweeps	5.34
LIF	Collection of 10 sweeps	15.71
AdEx	Collection of 10 sweeps	14.06
HH	Group of 3 sweeps	47.10
LIF	Group of 3 sweeps	46.98
AdEx	Group of 3 sweeps	119.45
HH	Individual sweep 5	55.33
LIF	Individual sweep 5	100.23
AdEx	Individual sweep 5	184.65

Table 3.19: MSE comparisons for neuronal models on SST stimulus

The results of this experiment indicate that the Hodgkin Huxley model is best suited to finding the closest results to the target trace, after which the LIF model surpasses AdEx. But, as MSE results alone are not the best indication of accurate traces, we should take a look at the voltage traces:

Figure 3.39: Comparison between neuronal models on SST stimulus

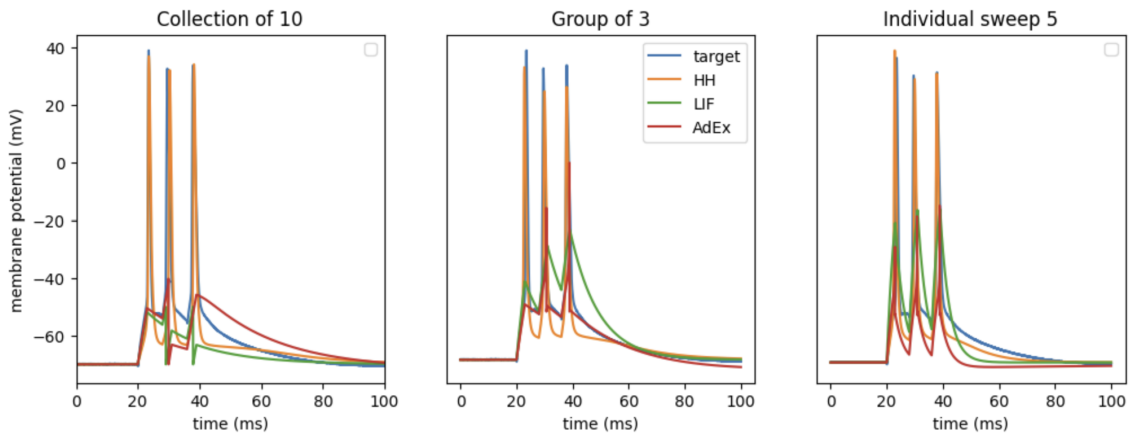

We can see that although all models improve as the volume of input data is reduced, the Hodgkin Huxley model appears to be the most accurate in terms of voltage trace.

3.2 Long Square

The required data was collected for sweeps 40-47 and organised into a collection of 8 arrays.

From this point onwards, sweeps will be referred to by the index number of the dataset. See Table 3.21 for the conversions.

Original Sweep Number	becomes	Index of Data Collection (new sweep number)
40	$\Longrightarrow$	0
41	$\Longrightarrow$	1
42	$\Longrightarrow$	2
43	$\Longrightarrow$	3
44	$\Longrightarrow$	4
45	$\Longrightarrow$	5
46	$\Longrightarrow$	6
47	$\Longrightarrow$	7

Table 3.20: Conversion for sweep numbers for 'Long Square' stimulus

The dataset was sliced to make code execution more efficient.

Figure 3.41 shows a visual representation of the input current and output response for these sweeps.

Figure 3.40: Initial input current and output response on sliced Long Square stimulus for 8 sweeps

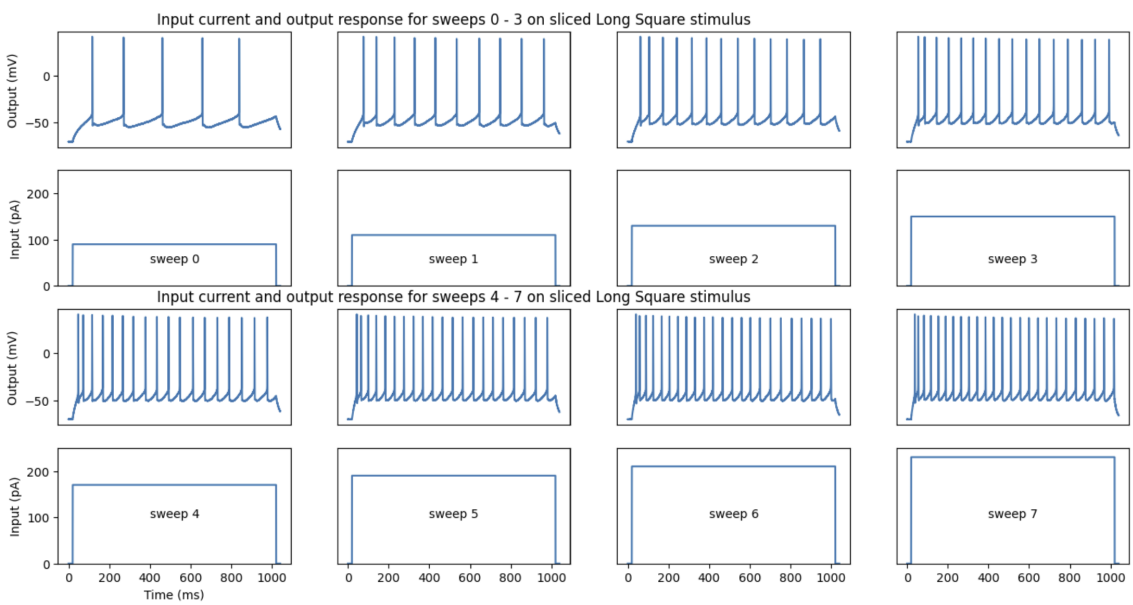

We can see that the input current for sweep 0 is approximately 90 pA, and that this

is raised for each subsequent sweep. Mostly the output seems to respond with tonic spiking but there is slight adaptation.

An initial run for all models using previously found best fit initial parameters was not successful in producing desired results.

Figure 3.42 shows the voltage traces produced by the three neuronal models for sweeps 0, 4 and 7:

Figure 3.41: Voltage traces for sweeps 0, 4, and 7

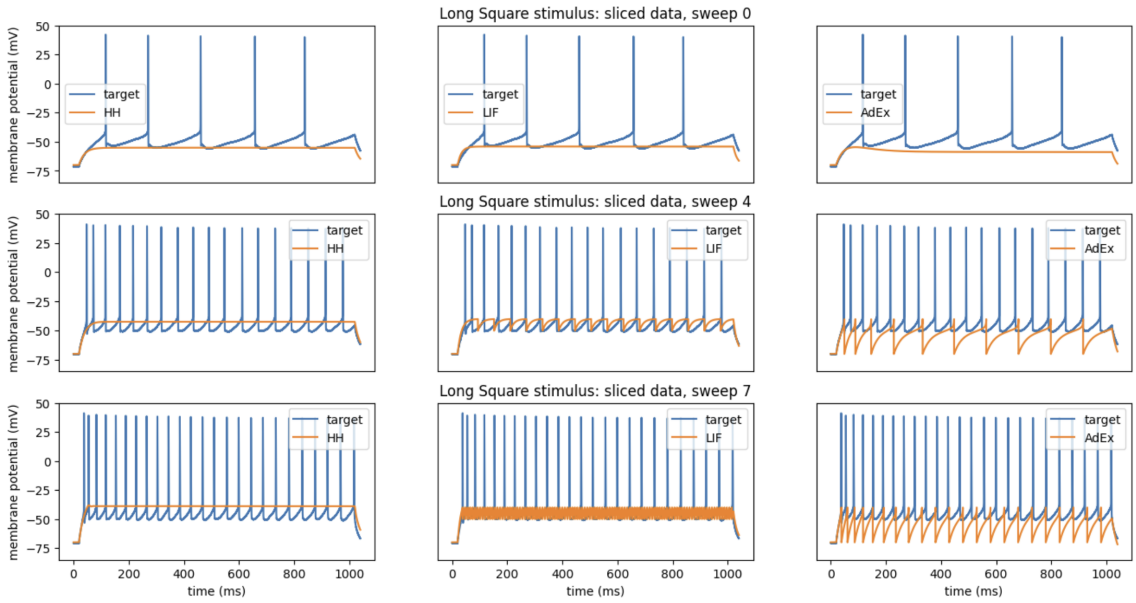

Despite the increasing strength of the input currents, the Hodgkin Huxley model did not respond at all.

Neither the LIF nor the AdEx model responded to the input current for sweep 0 but by sweep 7, they responded, the LIF model with great sensitivity.

This suggests that these sweeps may have to be separated, as adjusting parameters in order for sweep 0 to respond would compromise the effects in sweep 7.

Therefore, sweeps 5, 6, and 7 were extracted from the collection.

3.2.1 Group of 3 arrays

The dataset was reduced to sweeps 5 to 7.

An initial run of the three neuronal models on the same parameters, but with the reduced number of sweeps, produced the traces seen in Figure 3.42.

Figure 3.42: Voltage traces for sweeps 5 to 7 on reduced data

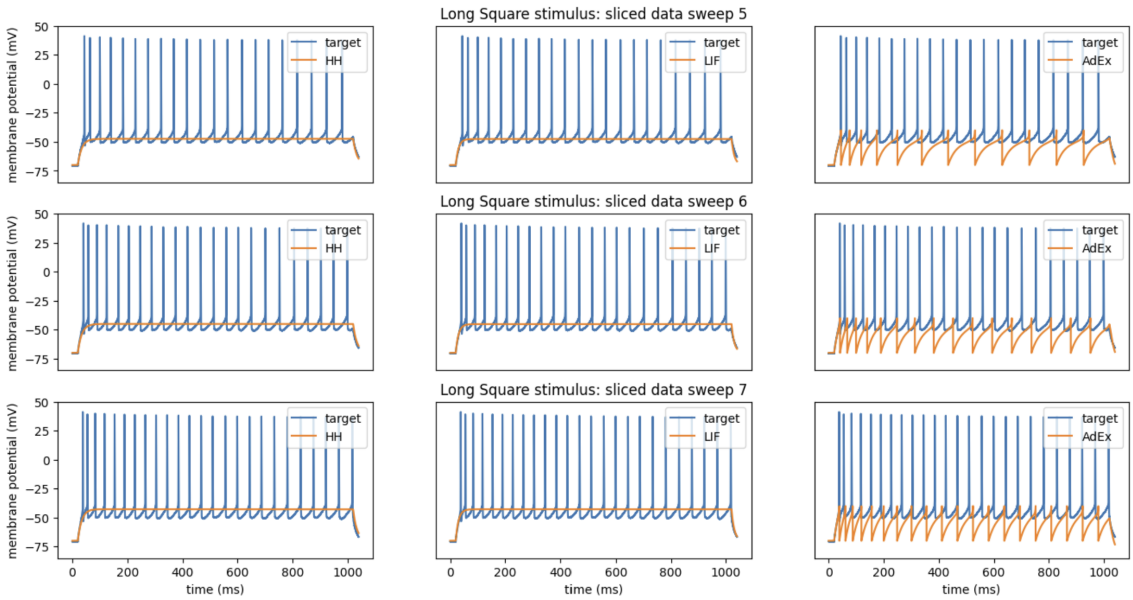

Although the Hodgkin Huxley model remained unaffected, we can see that the Leaky Integrate-and-Fire model no longer responded to the input current, and that the AdEx model became more accurate in its response.

Adaptive Exponential Integrate-and-Fire

As the AdEx model was the only one to respond to the input current, the experiment started here.

Increasing the range for the optimised parameters did not produce more accurate results. Given ranges of τ_w between 120-250 ms, a between 1-10 nS, and b between 0-5 nA, the program was run ten times with the number of rounds set to 10. Only one run produced a response.

Figure 3.43: Spikes produced on wider parameters

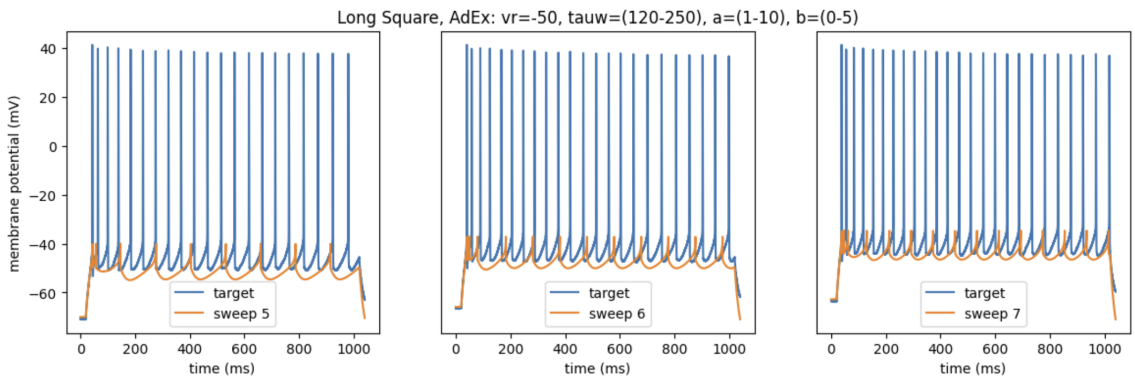

It is possible that increasing the number of rounds may have produced a better fit. However, the results for the runs in which no response was produced, the model seemed to have found best fit parameters so it is unlikely that any further rounds would have improved the results.

Optimised parameter ranges were reduced to:

τ_w = 120-160 ms, a = 1-5 nS, b = 0-2 nA, and the number of rounds increased to 30.

The program was run ten times. The best fit parameters are given in in Table 3.22.

Run Number	a (nS)	b (pA)	τ_w (ms)	error (mV^2)
0	1.07	3.39	120.38	126.22
1	1.48	28.51	144.35	134.85
2	1.94	19.73	125.52	131.76
3	1.24	5.61	122.33	126.55
4	1.63	2.98	129.15	126.47
5	1.16	3.14	154.45	126.85
6	1.45	30.21	135.04	136.11
7	1.43	39.39	123.39	141.13
8	1.19	8.67	129.83	128.75
9	1.06	3.41	120.81	126.80

Table 3.21: Best parameters tested for 30 rounds

Run number 7, highlighted in blue, resulted in the highest value for b, a mid-range value for a and a value in the lower range for τ_w. The voltage trace produced an ISI that was too wide to match that of the target trace. Towards the end of sweep 7, it became more accurate in matching the target trace.

The run numbers highlighted in orange produced values in the higher range for all fields. The voltage traces produced an ISI that was too wide at the beginning of the trace, matching some spike times to the target trace in the latter parts of the trace.

Run number 2, highlighted in green, resulted in the highest value for a, a mid-range value for b and a low-mid-range value for τ_w. This produced a voltage trace with an ISI that was narrow in comparison to the target trace.

The run numbers highlighted in red resulted in the lowest errors. However, the voltage traces they produced caused excessive spiking. They produced lower values for all fields, particularly noticeable for the values of b, which are in single digits, compared to the much higher values found for the other rows.

Results usually converged by the end of the rounds.

Table 3.22 shows six rows of red results which cover the errors that are at the lower end of the MSE range.

A calculation of $\frac{\tau_w}{a+b}$ can be seen in Table 3.23:

Run Number	$\frac{tauw}{a+b}$	Error (mV^2)
0	26.99	126.22
1	4.81	134.85
2	5.79	131.76
3	17.86	126.55
4	28.02	126.47
5	35.92	126.85
6	4.27	136.11
7	3.02	141.13
8	13.17	128.75
9	27.03	126.80

Table 3.22: Correlation between $\frac{\tau_w}{a+b}$ and MSE

These results suggests that when the ratio between τ_w and $(a + b)$ is high (in double digits), the MSE error is lower, but this causes extremely fast spiking.

Figure 3.45 shows the increasingly narrow ISI as $\frac{tauw}{a+b}$ increases. The colour of the title of the row corresponds with the colour of the row in tables 3.22 and 3.23.

Figure 3.44: Differing voltage trace results on 30 rounds of the same parameters

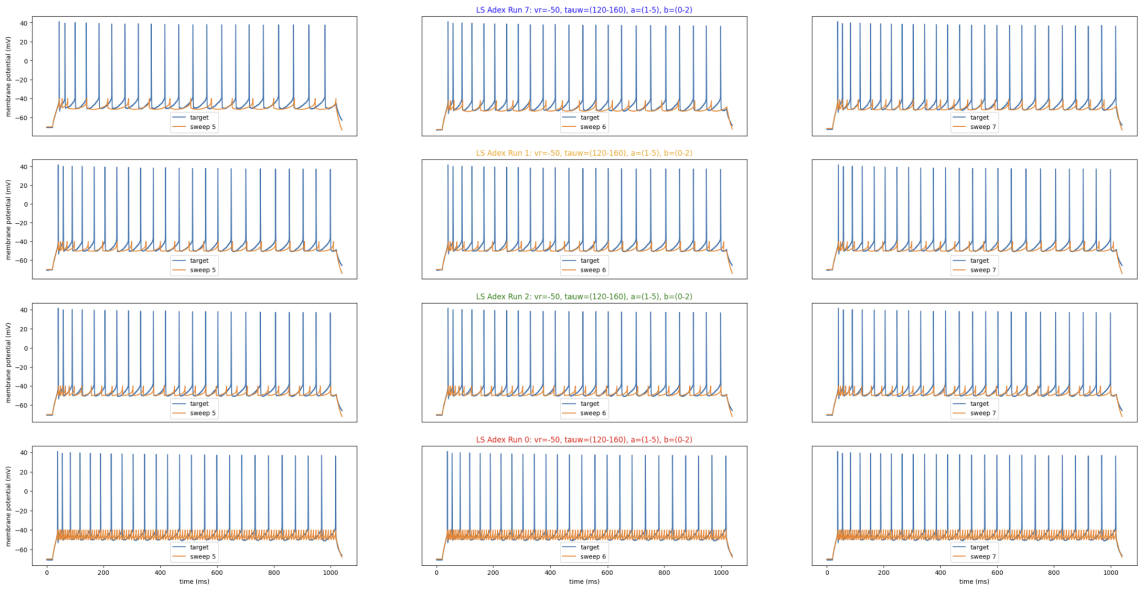

The variability of the results suggests that the model is unable to easily find best fit parameters given these ranges. An experiment reducing the range, taking the best fit suggestions so far was attempted. However, as results also depended on the

relationship between a, b, and τ_w, and not just their independent values, it was not certain results would improve.

The optimised parameter ranges were set at τ_w between 120-160 ms, a between 1.4-1.5 nS, and b between 0.01-2 nA. The program was run ten times with the number of rounds set to 30. The results can be seen in Table 3.24.

Run Number	a (nS)	b (pA)	τ_w (ms)	Error (mV^2)
0	1.48	26.56	124.32	133.34
1	1.49	13.81	124.49	129.80
2	1.41	22.48	126.22	131.93
3	1.50	12.43	124.11	129.29
4	1.40	14.03	120.93	129.93
5	1.40	22.05	129.67	131.83
6	1.49	21.93	126.98	131.58
7	1.40	13.97	121.49	129.89
8	1.50	21.82	127.66	131.66
9	1.50	21.83	127.62	131.63

Table 3.23: Reduced ranges for optimised parameters tested for 30 rounds

Results have narrowed down and become binary. An error of under 130 mV^2 causes fast spiking for all three sweeps (highlighted in red in Table 3.24), whereas those that converge towards an error of 131 mV^2 or higher, lean towards better spike times across the three sweeps.

As MSE accuracy has shown to be lower for those that voltage traces suggest are actually closer to the target trace, we should investigate the voltage traces.

Figure 3.45: Example of run with more accurate spike times

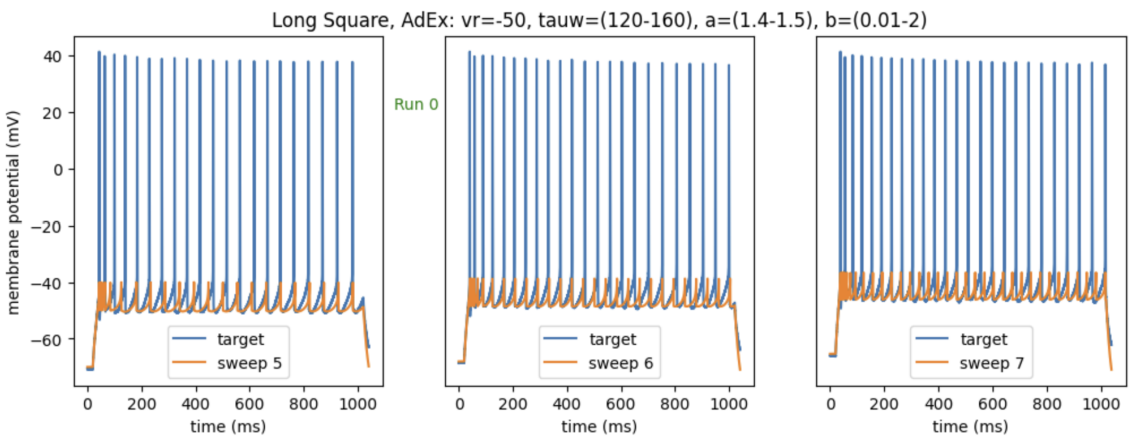

Figure 3.46: Example of run with fast spiking

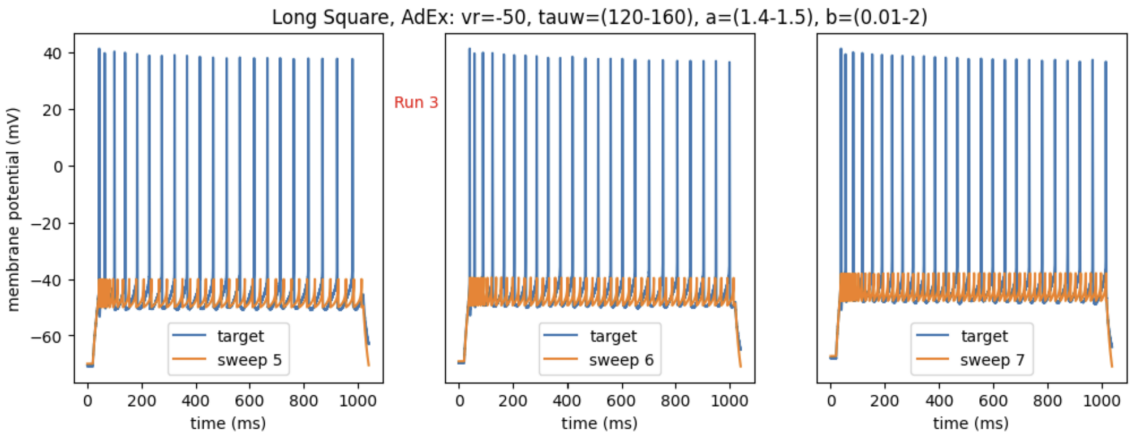

As we can see in Figure 3.46, for Run 0, spike times became more accurate towards the end of sweep 5, with an ISI too wide in the first half of the trace, whereas spike times were more accurate near the beginning for traces 6 and 7 with an ISI too narrow in comparison to the target trace. This suggested that further adjustments may enhance accuracy for some traces, whilst simultaneously causing further inaccuracy in other traces.

Therefore, it was decided to move straight onto individual arrays.

3.2.2 Individual array

Adaptive Exponential Integrate-and-Fire

An initial run on the previously found best fit range for the optimised parameters produced a more accurate voltage trace, illustrated by Figure 3.47.

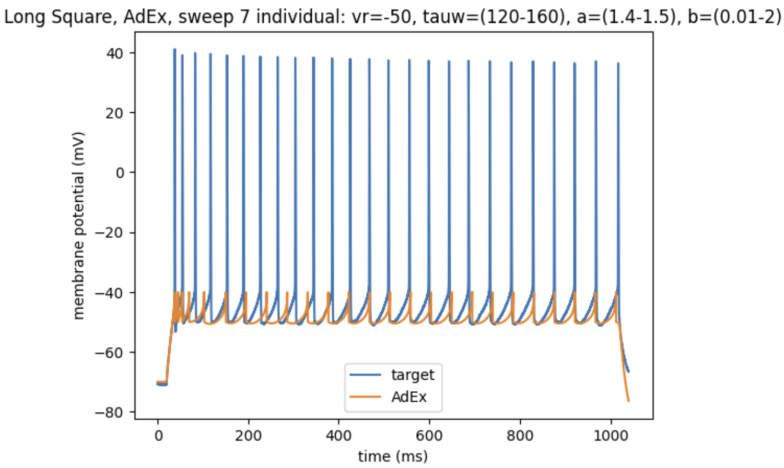

Figure 3.47: Initial run for individual sweep 7

Spike times started matching shortly after the 400 ms mark.

To check whether there would be any variability in the best parameters found, the same ranges were tried ten times with the number of rounds set to 10.

Run Number	a (nS)	b (pA)	τ_w (ms)	$\frac{tauw}{a+b}$	Error (mV^2)
0	1.41	37.95	120.85	3.07	147.72
1	1.41	36.06	128.51	3.43	147.11
2	1.41	31.62	151.90	4.60	147.12
3	1.48	31.73	148.01	4.46	145.57
4	1.47	36.15	126.37	3.36	146.30
5	1.49	24.48	155.20	5.98	145.56
6	1.44	21.88	136.89	5.87	146.00
7	1.41	24.87	151.63	5.77	144.98
8	1.48	36.31	125.65	3.32	145.81
9	1.45	22.48	121.44	5.07	146.83

Table 3.24: Initial parameter ranges for AdEx on individual sweep 7

We can see that variability has been reduced in the numerical values produced, but there are variations in the traces.

The rows highlighted in green in Table 3.25 produced traces similar to that seen in Figure 3.48.

Those highlighted in orange, produced some accurate spike times in the first half of the trace with a narrower ISI than the target trace in the second half of the trace.

Those highlighted in red produced very fast spiking. A lower ratio between τ_w and a and b created more accurate trace outputs (but higher MSE results.) There are very small margins between the orange and red rows, but values for b and for τ_w are higher for the orange rows.

Figure 3.48: Examples of different trace outputs

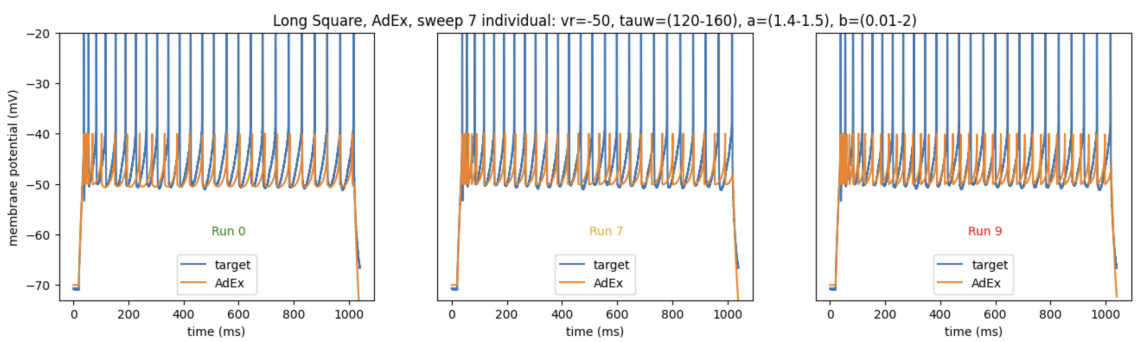

Leaky Integrate-and-Fire

An initial run on standard parameters did not produce a response, as seen in Figure 3.43.

The range for τ was increased from 0.01-0.03 ms to 0.01-5 ms.

This produced a reasonable voltage trace and was subsequently tried on the same parameters ten times with the number of rounds set to 20.

Run Number	R (MΩ)	τ (ms)	Error (mV^2)
0	275.56	45.11	136.72
1	229.83	122.83	145.72
2	286.66	93.15	141.53
3	276.45	87.80	141.25
4	276.46	150.47	146.94
5	288.51	48.62	137.68
6	280.11	46.36	136.90
7	274.46	86.80	141.28
8	271.62	58.68	140.57
9	277.41	59.67	139.33

Table 3.25: Parameters tested for LIF

Table 3.26 shows us that larger differences between R and τ cause fast spiking (highlighted in red), although (as with AdEx) lower MSE scores.

Figure 3.49: Examples of different trace outputs for LIF

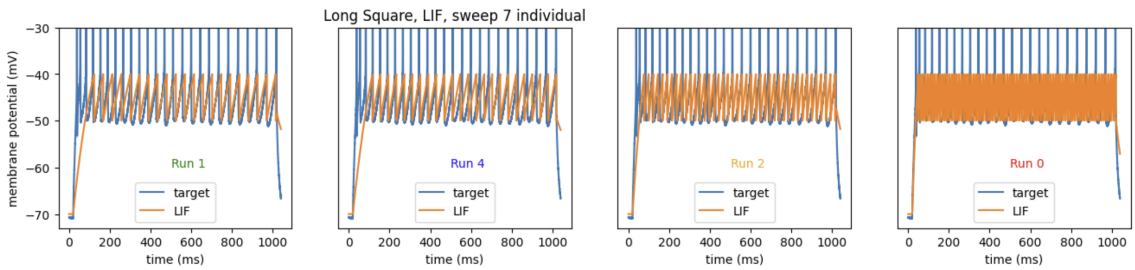

If we look at Figure 3.49, we can see that the voltage trace from run 1 of Table 3.26 (highlighted in green in the table) starts responding upon the fourth spike of the target voltage trace. The ISI of the AdEx trace is slightly too wide to begin with, but spike times then begin to match.

Run 4 (highlighted in blue in Table 3.26) also starts responding upon the fourth spike of the target voltage trace. Spike times match to begin with, and then the ISI becomes too narrow to match spike times of the target trace.

Run 2 has been taken as an example of the traces corresponding to the rows highlighted in orange in Table 3.26. These traces start responding before the third spike of the target trace, followed by very fast spiking.

Run 0 has been taken as an example of the traces corresponding to the rows highlighted in red in Table 3.26. These produced excessive spiking but started responding upon the first spike of the target trace.

In order for spike times to match at all, the AdEx trace begins to respond upon the fourth spike of the target trace. It appears that a response any earlier and the ISI becomes too narrow. As technically there would still be more matches in the rows highlighed in red, this results in a lower MSE score. However, in this case, a higher MSE score with less, but more precise spikes is more desirable.

Hodgkin Huxley

An intial run for sweep 7 on previously found best parameters:

Cm = 120 pF, E_L = -70 mV, E_K = -78 mV, E_{Na} = 40 mV, V_T = -50 mV, g_L = 0-10 nS, g_{Na} = 1-20 μS, g_{Kd} = 0.01-4 μS,

did not respond, as in Figure 3.41.

Parameters were adjusted to E_K = -60 mV, g_L = 1-10 nS, g_{Na} = 5-20 μS, g_{Kd} = 0-2, and μS.

The program was executed ten times with the number of rounds set to 20.

Run Number	g_{Kd} (μS)	g_{Na} (μS)	g_L (nS)	Error (mV^2)
0	1.80	5.17	9.93	157.63
1	1.83	5.82	9.43	182.38
2	1.84	5.37	9.93	163.04
3	1.89	5.96	9.45	181.31
4	1.89	5.29	9.95	158.65
5	1.75	5.36	9.87	163.55
6	1.68	5.50	9.40	178.13
7	1.83	5.88	9.44	181.46
8	1.82	6.01	9.47	183.43
9	1.62	5.34	9.87	164.63

Table 3.26: Variability on same parameters for LIF on sweep 5, for 20 rounds

Most results had converged by the end of the rounds. Run 8 found its best parameters by round 4.

As with previous results, a lower MSE score did not correlate with a more accurate trace output.

For simplicity, these results have been separated into two categories. Those with an ISI too wide (highlighted in purple) in comparison to the target trace, and those that match spike times from approximately the 600 ms mark (highlighted in green.)

An example of the output traces with the lowest and highest MSE scores can be seen in Figure 3.50.

Figure 3.50: Run 0 and run 8

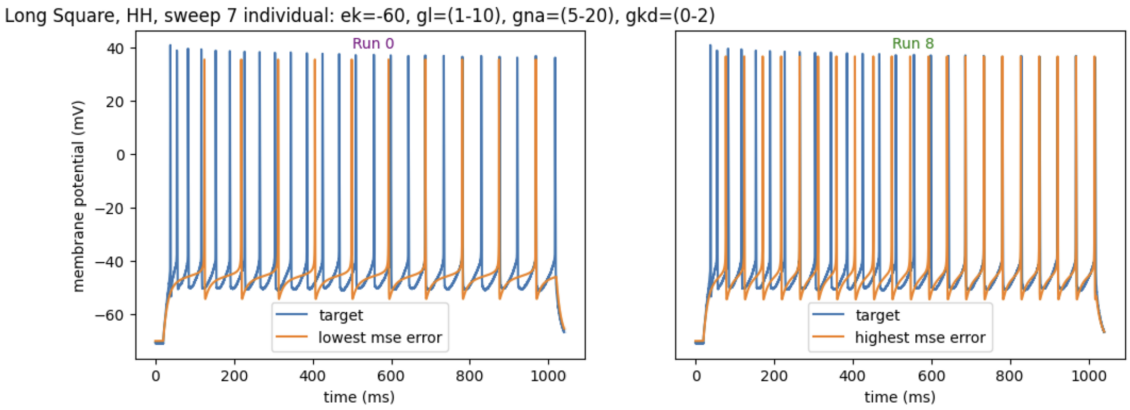

Optimised parameter ranges were increased to:

g_L = 0-15 nS, g_{Na} = 5-20 μS, g_{Kd} = 0-8 μS.

The program was run ten times with the number of rounds set to 20. Each run produced at maximum three spikes with great variability between the traces.

3.2.3 Evaluation

The MSE scores for all three neuronal models can be found in Table 3.28.

Model	Error (mV^2)
HH	156.95
LIF	145.72
AdEx	147.72

Table 3.27: Best fit MSE comparison for LS: sweep 7

We might assume from this that the LIF model produced the most accurate results. However, if we compare the voltage traces...

Figure 3.51: Comparison for best results on sweep 7

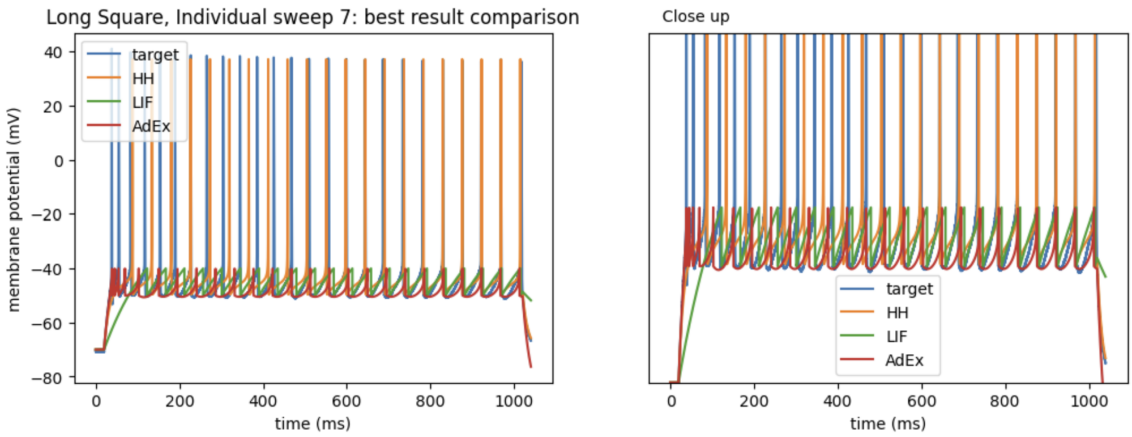

Figure 3.51 illustrates that all models become more accurate at the 500 ms mark. We can take a look at the output traces of the models against the target trace separately for more clarity.

Figure 3.52: Separate comparisons for best results on sweep 7

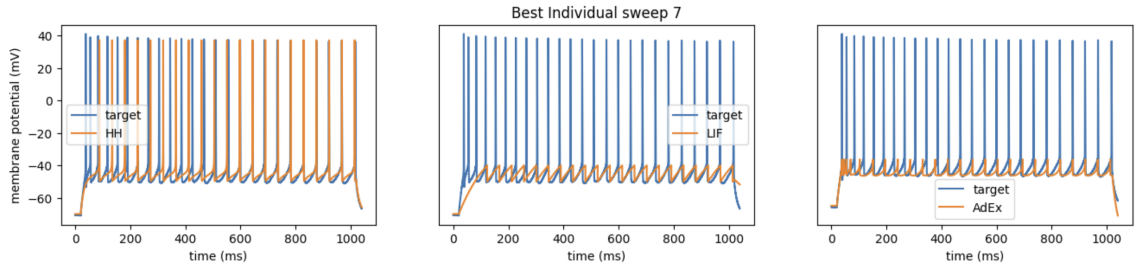

Figure 3.52 shows that the AdEx model is the only model that starts and ends spikes in line with the target trace. It spikes 24 times compared to the target output's 25. The LIF model manages 21, starting on the 4th spike of the target trace, and the Hodgkin Huxley model manages 21, starting on the third spike of the target trace. Of the spikes that do occur, AdEx manages to match spike times more consistently.

So we can say that the AdEx model here is the most accurate.

3.3 Ramp Stimulus

3.3.1 Collection of 3 arrays

The required data was collected for sweeps 4-6 and organised into a collection of 3 arrays.

The lengths of these sweeps were:

sweep 4: 229,960

sweep 5: 248,955

sweep 6: 285,972

The input current was identical for all three sweeps for the length of sweep 4. Then input current was increased and the additional data was identical for sweeps 5 and 6 until the end of sweep 5. At this point, the input current was increased for sweep 6 until the end of the array.

In order for the length of arrays to match, initially the sweeps were reduced, but ultimately additional null data was added to sweeps 4 and 5.

From here onwards, the sweeps will be referred to by their index number according to the dataset. See Table 3.29 for the conversions.

Original Sweep Number	becomes	Index of Data Collection (new sweep number)
4	$\Longrightarrow$	0
5	$\Longrightarrow$	1
6	$\Longrightarrow$	2

Table 3.28: Conversion for sweep numbers

A look at the initial input current and how it affects the output response shows us that the neuron begins to respond at 80 pA with delayed accelerating:

Figure 3.53: Visualisation for neuronal response on Ramp stimulus

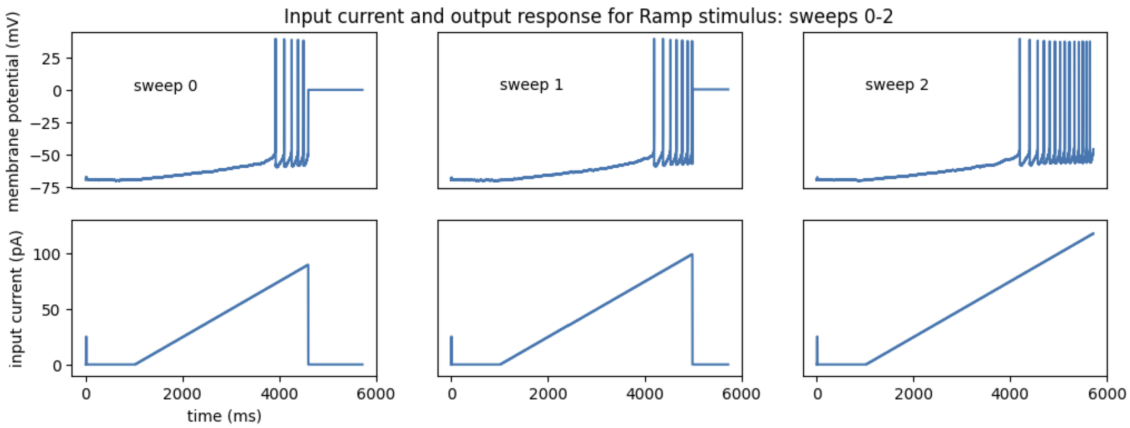

Leaky Integrate-and-Fire

Initial parameters were set to:

Cm = 120 pF, E_L = -70 mV, reset: v = -50 mV, threshold: v > -40 mV, R = 100 - 300 MΩ, and τ = 10 - 30 ms.

Regardless of adjustments, only sweep 2 responded to input current:

Figure 3.54: Initial LIF trial on Ramp stimulus

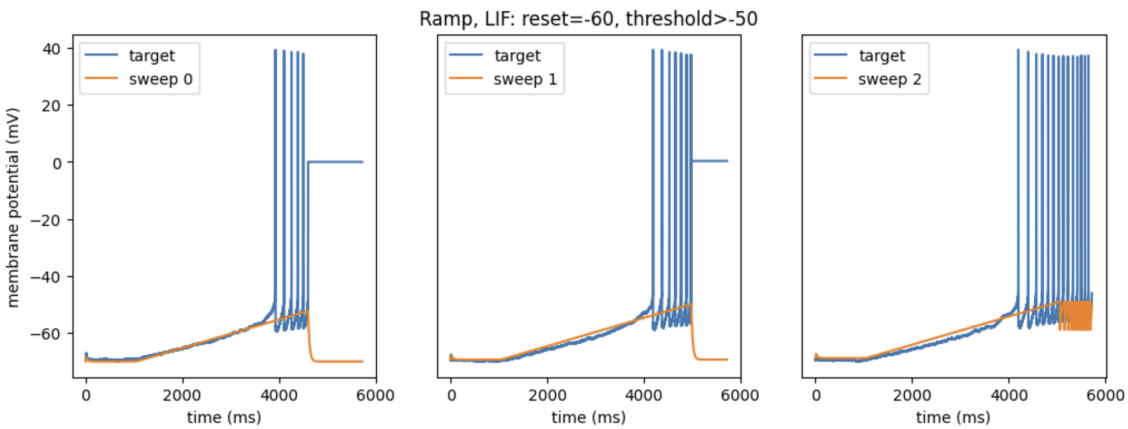

A closer look at sweep 2 indicates that the threshold should be set to -45 mV, and reset should be set to -53 mV.

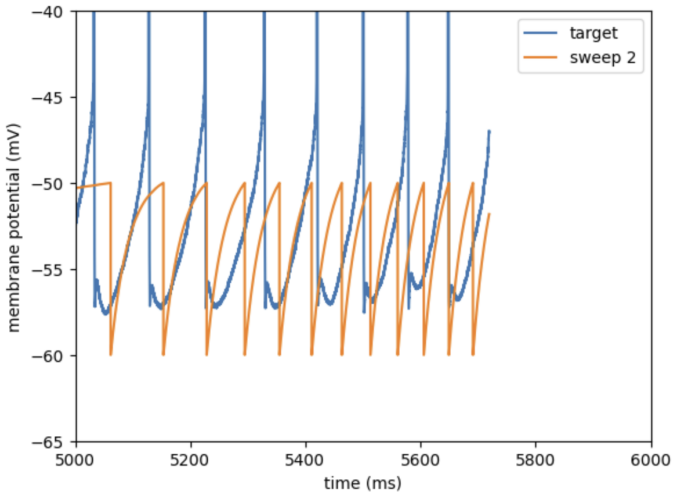

Figure 3.55: Close up of sweep 2

It is also apparent that adjustments to the parameters will not produce more accurate voltage traces as the LIF model does not reach -45 mV at the point of the first spike of the target trace.

Therefore further attempts were concentrated on matching spike times as closely as possible.

The following parameters produced the closest result:

reset: v = -72 mV, threshold: $v >$ -62 mV, R = 100-110 MΩ, τ = 10-50 ms

The resulting voltage traces can be seen in Figure 3.56.

Figure 3.56: Best fit for LIF on Ramp stimulus

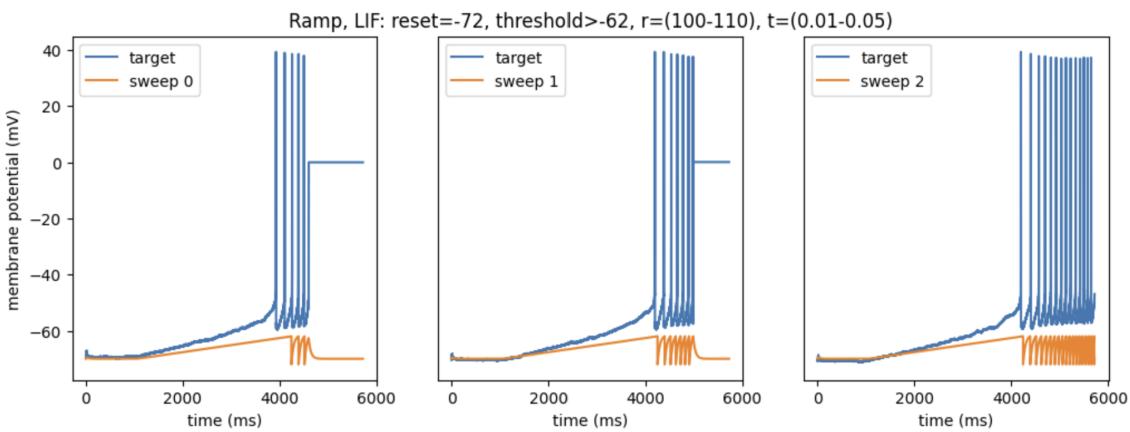

Figure 3.57: Close up for LIF on Ramp stimulus

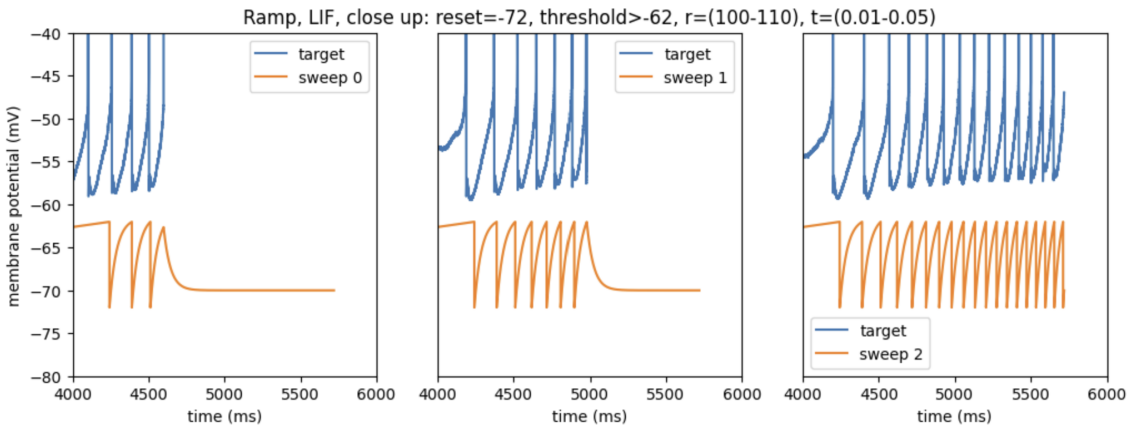

Upon closer examination, it is evident that although spike times are accurate for spikes that hit the threshold for sweep 0, they do not start in time to match the target trace. By sweep 2, the start time and duration of spikes improves, but the interspike interval becomes too narrow in comparison to the target output.

This suggests that for more accurate results, it may be necessary to separate the sweeps.

Adaptive Exponential Integrate-and-Fire

As with the Leaky Integrate-and-Fire model, the threshold was difficult to reach whilst matching the voltage trace of the target trace.

Using initial parameters:

Cm = 120 pF, g_L = 5 nS, V_T = -50 mV, Δ_T = 2 mV, vc = 5, V_r = -70 mV, τ_w = 120-160 ms, a = 1-4 nS, and b = 0-0.5 nA,

we can see in Figure 3.58 that only sweep 2 reaches the threshold at the very end of the trace:

Figure 3.58: AdEx on Ramp stimulus

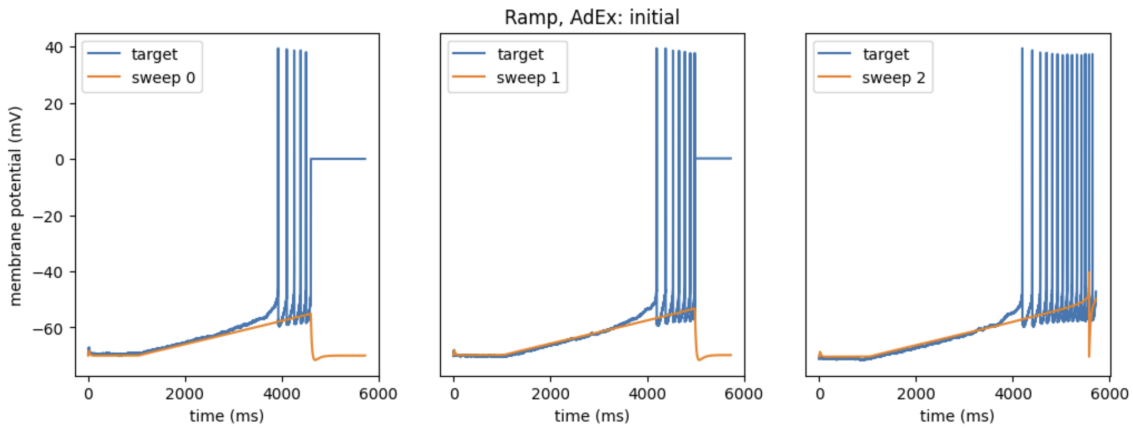

Therefore, as with the LIF model, the threshold and reset values were set lower than that for the target trace, and focus was concentrated on matching spike times.

As with the LIF model, it was difficult to find parameters that would optimise to suit all three sweeps. See Figure 3.59 for an example.

Figure 3.59: Best fit for AdEx on Ramp stimulus

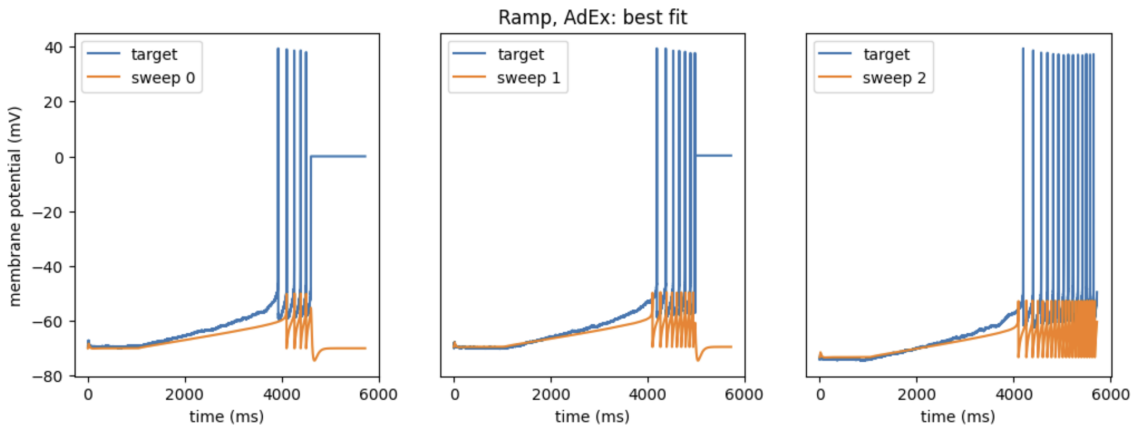

Figure 3.60: Close up for best collection AdEx parameters on Ramp stimulus

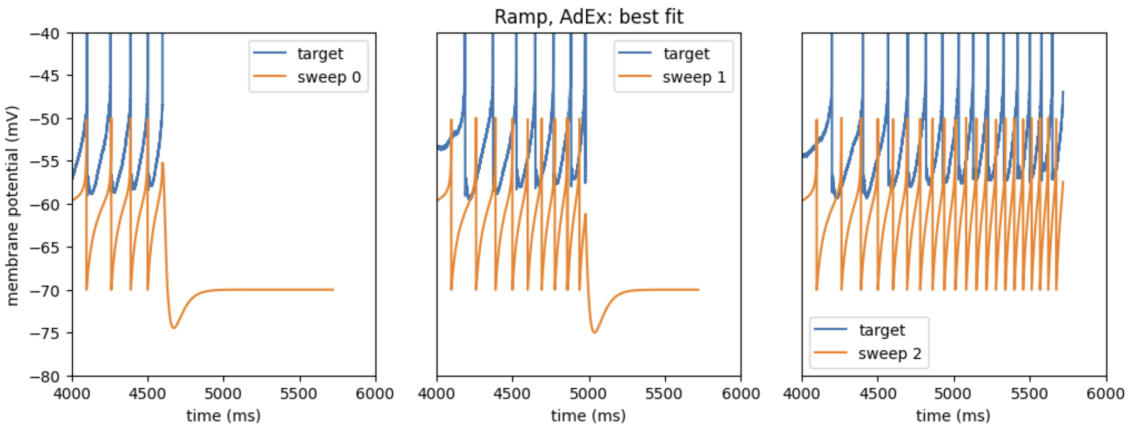

Figure 3.60 shows us that although spike times match very closely for sweep 0, the ISI increasingly narrows for each sweep. There are 9 spikes for the AdEx trace to the target trace's 7 spikes in sweep 1; there are 22 spikes for the AdEx trace in place of the target trace's 15. The spike times do not match here. This suggests that accuracy for one sweep may have to be sacrified for accuracy in another sweep when executing the code for the model in a collection dataset.

Therefore, for refined results, the sweeps may have to be separated.

Hodgkin Huxley

Initial parameters were set to those found from the best fit results of the 'Short Square: Triple' experiment. This did not enable the threshold to be reached. E_K was adjusted from -78 mV to -60 mV, and V_T from -50 mV to -55 mV. This caused damped oscillations as illustrated by Figure 3.61.

Figure 3.61: Damped oscillations for the Hodgkin Huxley model on Ramp stimulus input

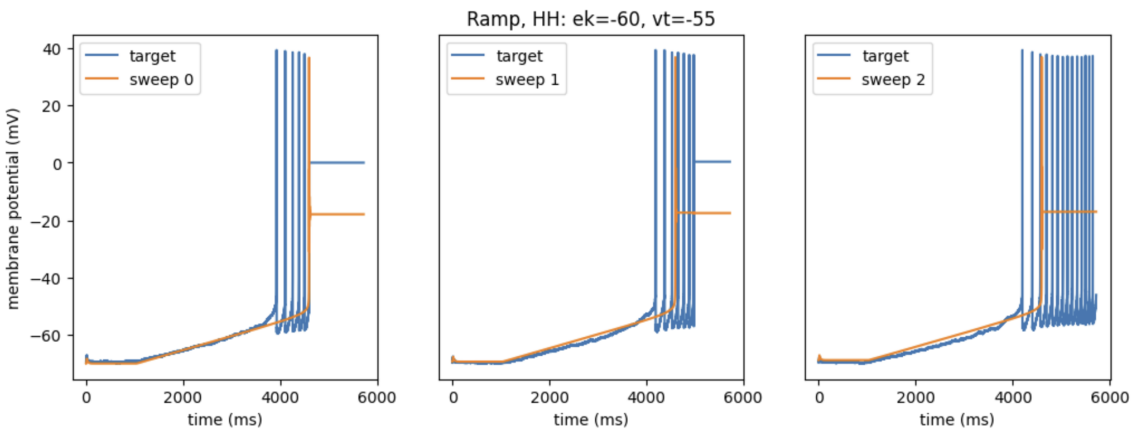

Figure 3.62: Traces for all three sweeps are exactly the same

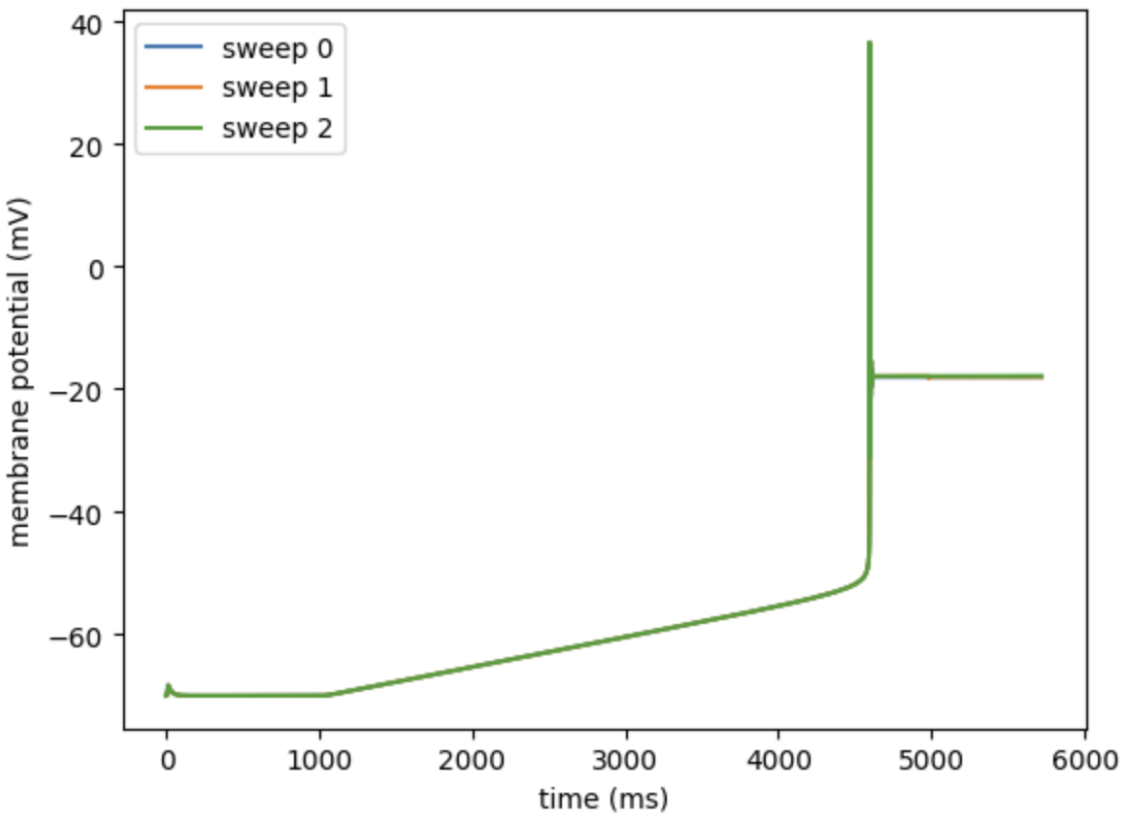

A closer look confirms this, illustrated by Figure 3.63.

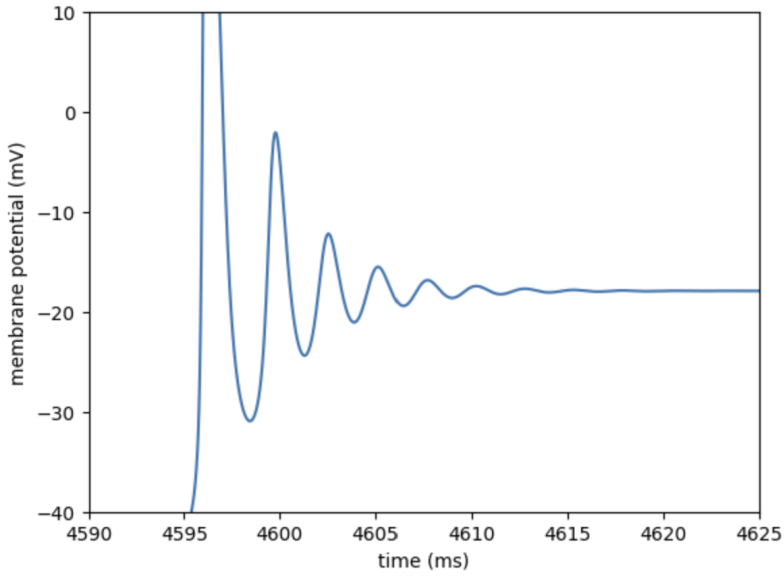

Figure 3.63: Close up of damped oscillation from Ramp stimulus

Table 3.30 gives us the results of running the Hodgkin Huxley model multiple times with the following parameters:

Cm = 120 pF, E_L = -70 mV, E_K = -60 mV, E_{Na} = 40 mV, V_T = -55 mV, g_L = 0-6 nS, g_{Na} = 1-20 μS, and g_{Kd} = 0.01-4 μS

g_{Kd} (μS)	g_{Na} (μS)	g_L (nS)	Effect
3.6	1.28	5.19	0
7.83	5.83	5.99	0
3.95	1.03	5.59	0
3.24	1.49	6.06	0
3.67	1.7	5.55	0
0.31	6.38	5.36	d/o
0.28	2.58	4.9	d/o
0.45	6.91	5.41	d/o
0.40	6.51	5.39	d/o
0.45	9.29	5.58	d/o
0.55	11.3	5.70	d/o
0.21	2.49	4.90	d/o
0.30	3.26	5.01	d/o
0.32	4.61	5.19	d/o
3.78	1.48	5.81	0/0/1
3.68	1.39	5.90	0/0/3
3.89	5.44	5.88	0/2/n
3.77	10.53	5.87	0/3/n
1.91	10.44	5.93	0/3/n
1.90	10.76	5.9	0/3/n
2.99	1.59	5.36	0/0/n

Table 3.29: Results for HH on Ramp stimulus and the differing effects caused on same parameters

Effect column key:

0 = no response for any of the sweeps

d/o = damped oscillations (at -20 mV)

0/3/n = here numbers refer to the number of spikes produced by that sweep, in the order of sweep number. Where there were numerous spikes, this is represented by 'n'. E.g., 0/3/n would signify, 0 spikes for the first sweep, 3 spikes for the second sweep, numerous spikes for the third sweep.

We can see that usually when g_{Kd} is higher than g_{Na}, there is no effect. When g_{Kd} is very low (below 1), damped oscillations are the effect. Finally, in most cases, g_{Na} is significantly higher than g_{Kd} for there to result in a response, especially in more than one sweep. Sweep 0 remains unaffected, which suggests that the combination of the strength of input and time given for an affect to be produced do not result in the threshold being reached.

In order to pass the bifurication point, E_{Na} was raised to 80 mV and optimised parameters had to be forcibly reduced so that g_{Na} was at minimum 5 μS , and g_{Kd} at a minimum of 1 μS.

This allowed for a response once the threshold had been reached, although only for sweep 2.

Figure 3.64: Voltage trace for best parameters found for HH

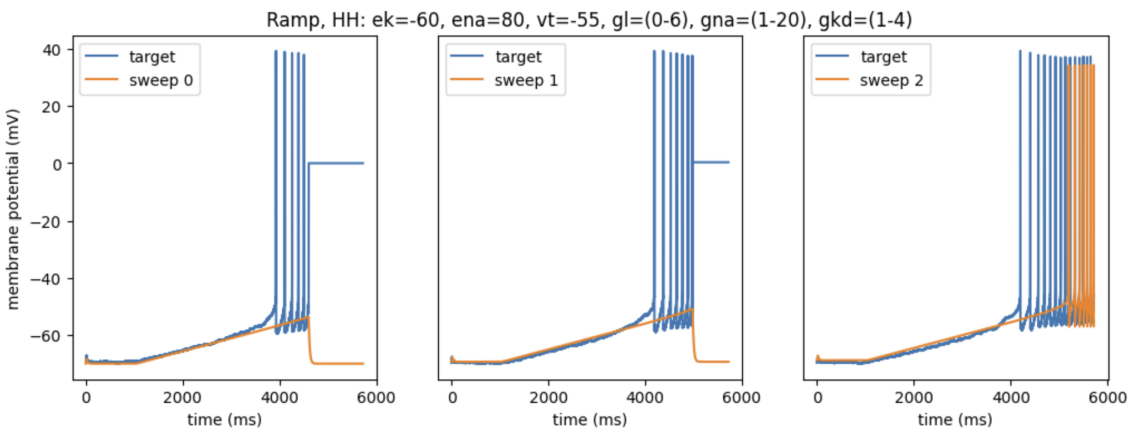

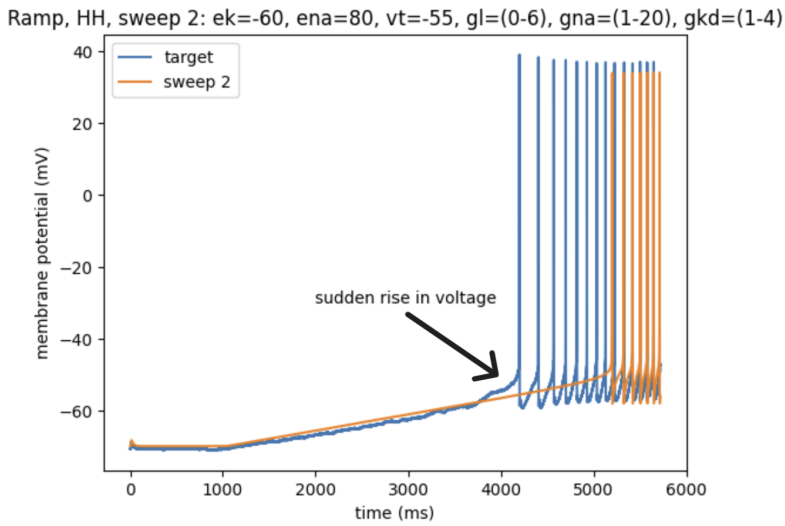

Figure 3.65: Only sweep 2 spikes

All models struggled with the sudden rise in voltage at 4000 ms (marked by a black arrow in Figure 3.65.) Unfortunately, it is not as simple to manually adjust threshold and reset variables for the Hodgkin Huxley model as it is with the Leaky Integrate-and-Fire and Adaptive Integrate-and-Fire models, so it was difficult to initiate a response with accurate spike times before the 5000 ms mark.

Enforcing g_{Na} to a minimum of 5 caused three spikes for sweep 2, and very fast spiking for sweep 3. This caused both sweeps to overshoot and start spiking late. Sweep 0 remained unaffected. This suggested that Figure 3.64 may be the closest result possible within a collection of sweeps.

3.3.2 Individual array

Leaky Integrate-and-Fire

Starting parameters were taken from previously found best fit when run as a 'Collection of 3' arrays. This produced far too many spikes, although the duration of spikes was accurate.

Adjustments were subsequently made to the minimum and maximum ranges for R and τ in order to replicate accurate spike times, but attempts to match voltage accuracy with reset and threshold were omitted.

Complete accuracy was difficult with the LIF model. Making slight adjustments affected the spike times which either started later with a more accurate ISI, or started on time but with very fast spiking and not aligned with the target trace.

Widening optimised parameters did not produce better results. For example widening the optimised parameters for R, such that min = 80 MΩ and max = 300 MΩ, and ranges for τ such that min = 10 ms, and max = 90 ms, had the model converge at round 6 with the following results:

R = 85.48 MΩ, τ = 39.46 ms, error = 57.03 mV^2,

which remained the same until the end of the run. This produced a voltage trace that started spikes later than the target trace, although with a closer ISI.

Running the following parameters mutliple times:

Cm = 120 pF, E_L = -70 mV, reset: v = -72 mV, threshold: v > -62 mV, R = 80-300 MΩ, and τ = 10 - 90 ms

produced the results shown in Table 3.31.

R (MΩ)	τ (ms)	Error (mV^2)	start/ spikes
85.48	39.46	57.03	4750/ 10
84.56	19.54	57.10	4750/ 18
82.40	34.25	56.01	4900/ 9
83.21	38.01	56.86	4850/ 9
83.27	37.60	56.26	4850/ 9
85.93	40.79	56.86	4750/ 10

Table 3.30: LIF run on same parameters for Ramp stimulus

We can see that the much lower τ in the second line (highlighted in red) is the outlier and causes excessive spiking.

Despite arguably better parameters found in previous runs of: R = 100.48 MΩ, τ = 40.21 ms, which produced an error of 62.63 mV^2, this was not explored by the model.

Either spike times started in time with the target trace but caused excessively fast spiking, or the LIF spikes began later but the ISI matched more accurately.

The best results found can be seen in Figure 3.66.

Figure 3.66: Best result found for LIF on Ramp stimulus, individual sweep 2

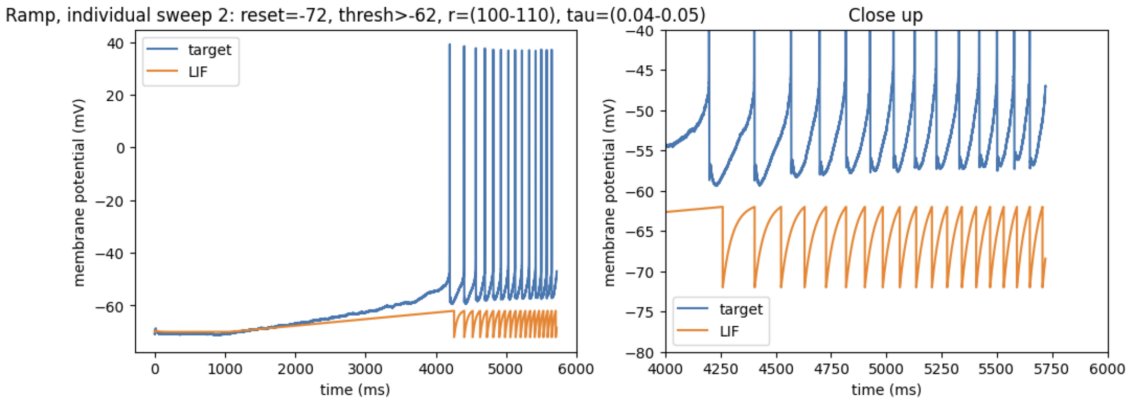

Adaptive Exponential Integrate-and-Fire

Taking previously found best parameters from the 'Collection of 3' sweeps, the response from the AdEx model was immediately quite accurate. It was still not possible to replicate the voltage trace in terms of threshold and reset variables while also managing to match spike times.

See Figure 3.67 for the best result found.

Figure 3.67: Best result found for AdEx on Ramp stimulus, individual sweep 2

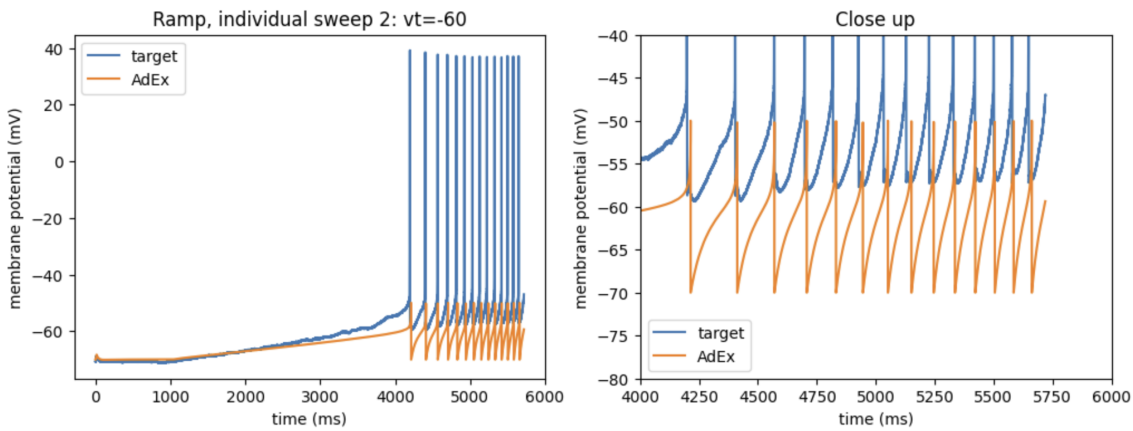

Hodgkin Huxley

Experiments began with best fit parameters found from the 'Collection of 3' arrays result.

The model immediately began with an error of 43.85 mV^2 (compared to around 500 mV^2 for the 'Collection of 3' sweeps) and by round 2 it seemed that all parameters had converged. However, adjustments were made in round 7, although these were

minimal.

There was a compromise between starting spikes earlier and more accurate interspike intervals.

This is to say that it was difficult to initiate a response any earlier with the individual array than from that with the collection of arrays. The earliest spike recorded remained just before 5250 ms for the recorded spikes to match spike times with the target trace. Raising E_{Na} and/ or g_{Na} started an earlier response, but at the cost of extremely fast spiking.

.

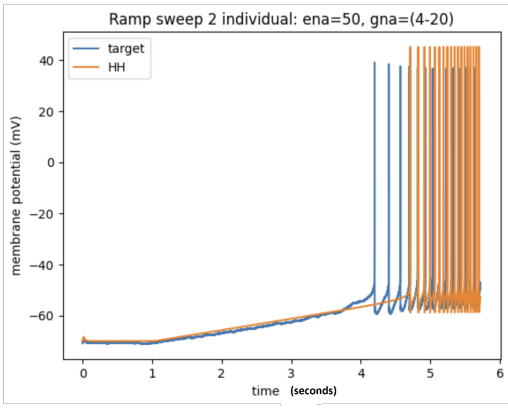

Figure 3.68: An example of an earlier initial spike followed by excessive spiking

Figure 3.69: Best result found for the Hodgkin Huxley model on Ramp stimulus, individual sweep 2

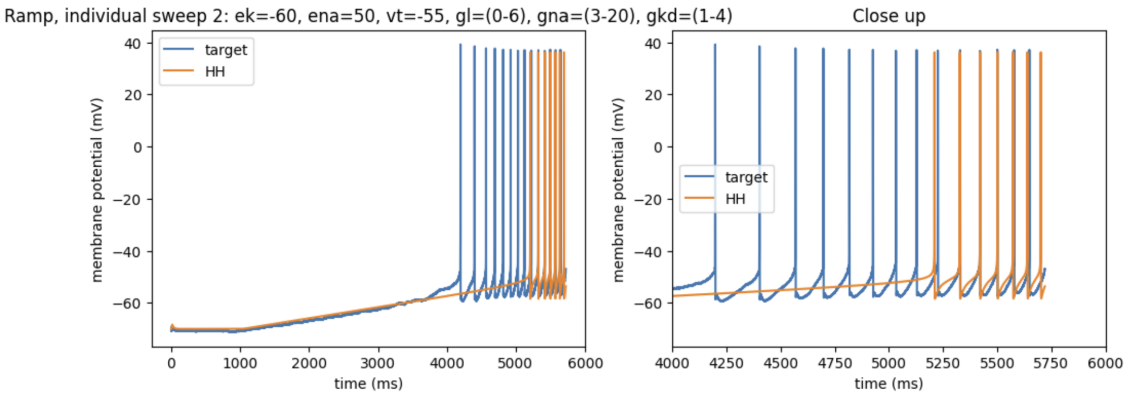

The above results were all tested for several runs in the same range of parameters for each neuronal model to check whether better results could be found. The variability was minimal.

3.3.3 Evaluation

In the following, we will compare the results for each neuronal model in the collection dataset and on the individual sweep to see how much the voltage traces improved. Then we will compare the models to each other.

Figure 3.70: Comparison for best LIF result on Ramp stimulus between the collection dataset and the individual array

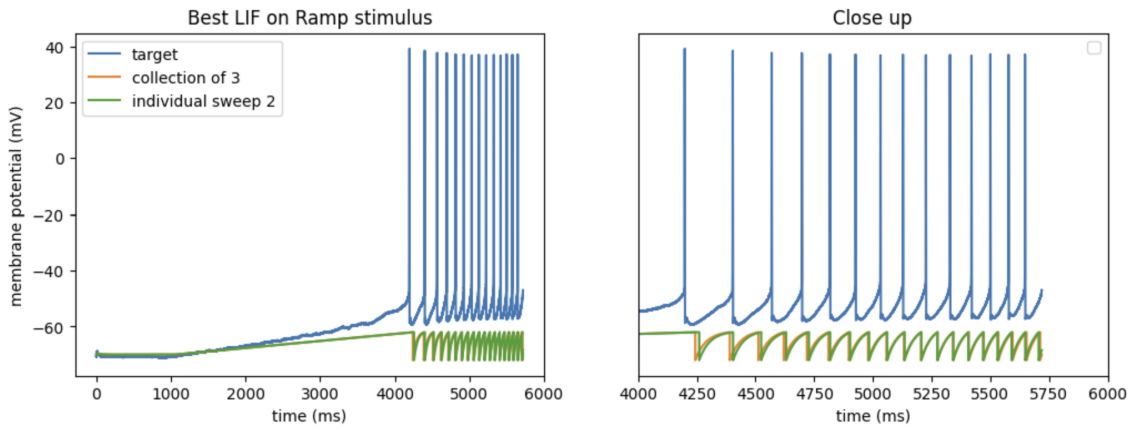

Figure 3.71: Comparison for best AdEx result on Ramp stimulus between the collection dataset and the individual array

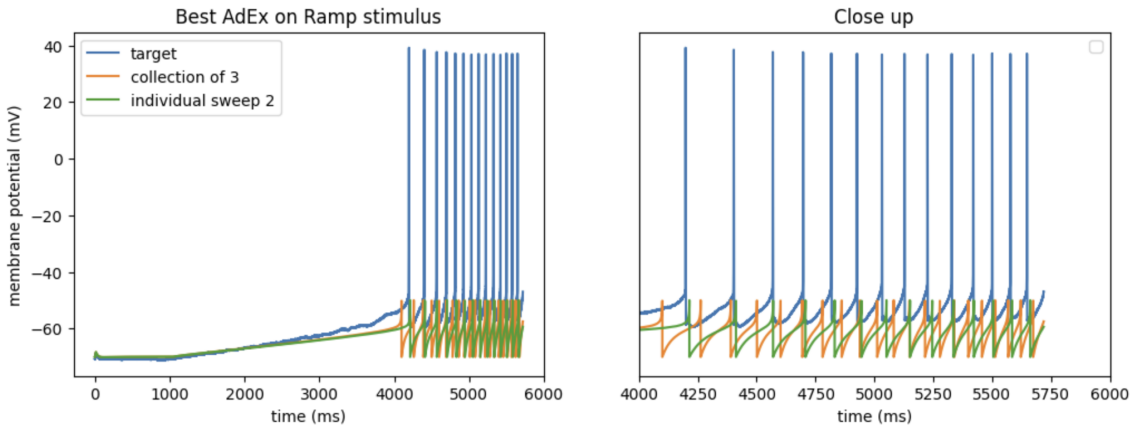

Figure 3.72: Comparison for best HH result on Ramp stimulus between the collection dataset and the individual array

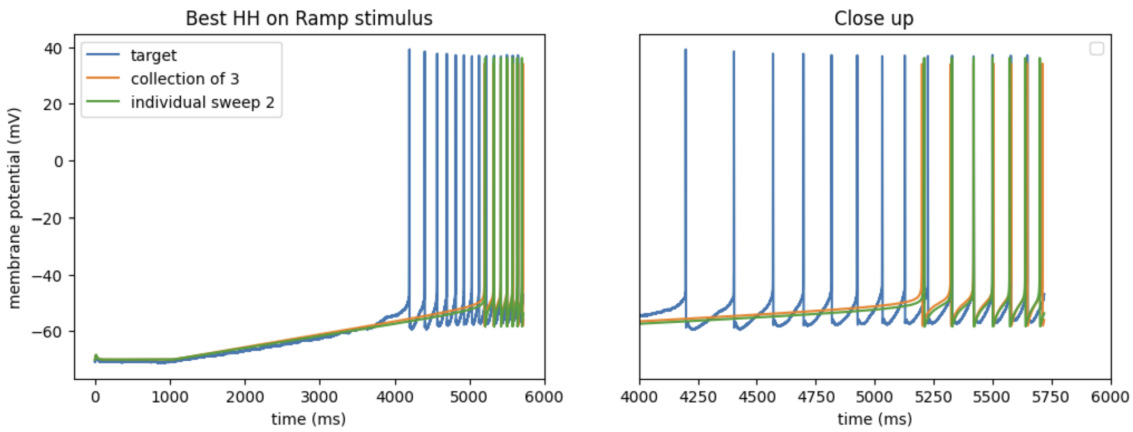

It is apparent from this data that differences are minimal between the voltage traces for the LIF and Hodgkin Huxley models between the Collection of 3 Sweeps and that tested for the Individual Array for Sweep 2. However, there is a marked improvement for the AdEx model.

Table 3.32 gives us the MSE scores for these experiments.

Model	Type of dataset	Error (mV^2)
HH	Collection of 3 sweeps	536.85
LIF	Collection of 3 sweeps	567.49
AdEx	Collection of 3 sweeps	565.99
HH	Individual sweep 2	18.23
LIF	Individual sweep 2	62.37
AdEx	Individual sweep 2	38.13

Table 3.31: MSE comparisons for neuronal models on Ramp stimulus

These numbers suggest that the Hodgkin Huxley model produces the closest results, but as we have discovered, lower MSE scores do not always indicate a closer voltage trace. Therefore, we will examine the voltage traces for all models.

Figure 3.73: Comparison for best results on Ramp stimulus from the Collection of 3 arrays

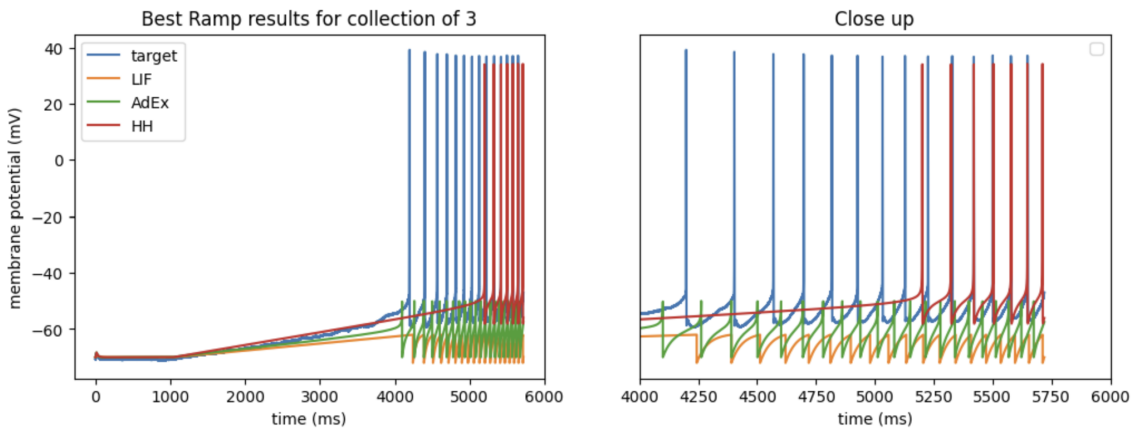

Figure 3.74: Comparison for best results on Ramp stimulus for Individual sweep 2

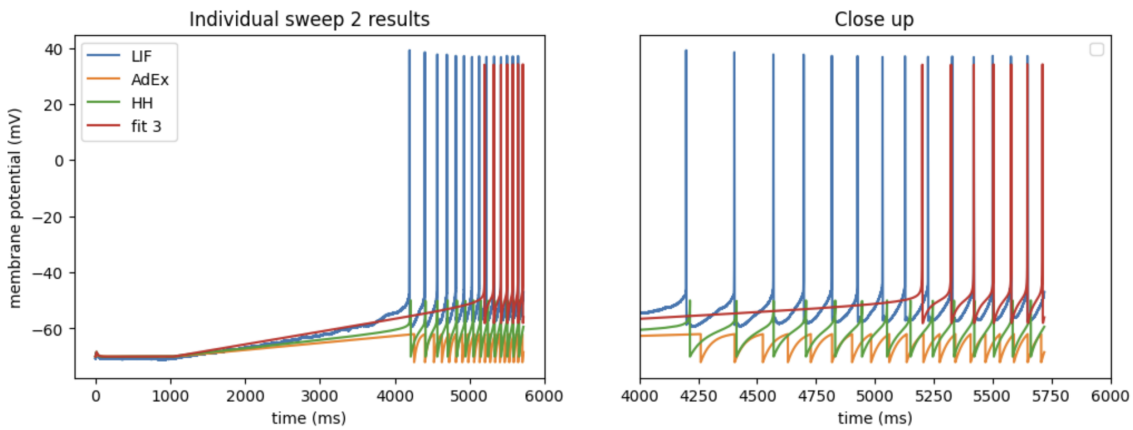

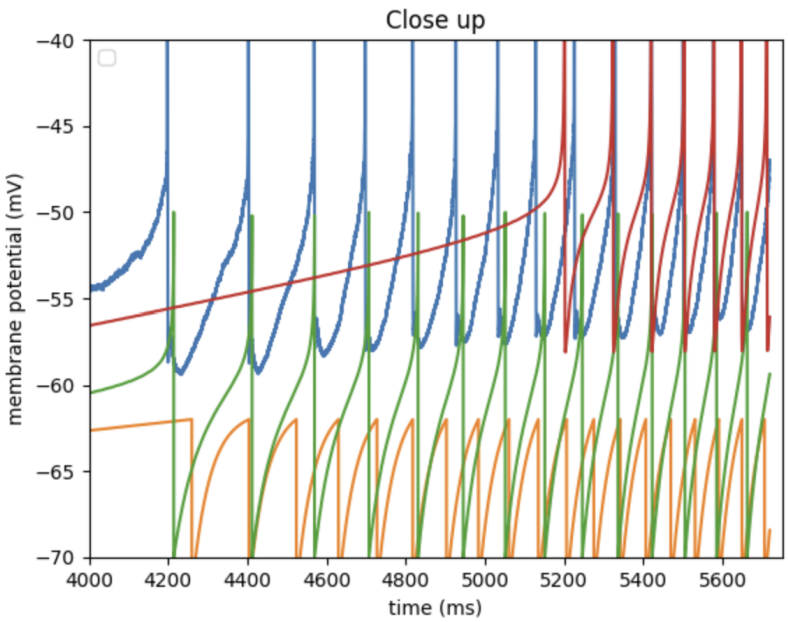

Figure 3.75: Close up for best results for individual sweep 2 on Ramp stimulus

As accurate voltage traces were not possible for any of the models, we will need to use further measures to differentiate between the models.

We will take into account the time of the first and last spikes, the number of spikes, and how closely the spikes that do occur match with spike times for the original output.

We can see that the Hodgkin Huxley model spikes 7 times to the target trace's 14. It does not respond until the target trace's 9th spike, and adds an additional spike at the end.

At this point, we can discount the Hodgkin Huxley model.

Comparing the LIF model with the AdEx model, we can see that although both models start and end spike times aligned with that of the target trace, the close up shows that AdEx has the correct number of spikes and the closest matches to the spike times of the target trace. Therefore, we can say that the AdEx model is the most accurate for this experiment.

Chapter 4

Summary

1. For stimulus types that result in uncomplicated response patterns, such as the 'Short Square: Triple' stimulus in this study, all models are able to replicate the target trace.

2. For stimulus types that result in some adaptation in their response and delayed accelerating, such as 'Long Square' or 'Ramp' in this study, the AdEx model returns the most accurate results for number of spikes and spike times.

3. For stimulus types that result in unexpected sensitivity in repsonse to increased input current, such as the 'Ramp' stimulus in this study, all models fail to respond aligned with the target trace. As the threshold and reset variables are able to be adjusted in the LIF and AdEx models, it is possible to match spikes and spike times, although not voltage traces. AdEx returns the most accurate results in this form.

4. Sweeps with a narrow ISI should be separated for more accurate results.

5. MSE scores alone cannot be relied upon as an accurate measure for comparison, in the sense that one cannot assume a lower score results in a more accurate voltage trace. However, they can be considered an important evaluation tool once the point at which more (or less) accuracy has been noted.

6. The program may need to be run several times to check that best fit parameters have been found for the optimised parameters.

7. Set parameters (i.e., capacitance, etc...) to find best fit voltage traces may vary for the neuronal models.

4.1 Limitations and Future Iterations

The time taken to run simulations was not fully taken into account for these experiments. However, the Hodgkin Huxley model takes approximately three times longer than the LIF and AdEx models to run.

If this is taken into account, it would be reasonable to state that the LIF model would be the most suitable for the 'Short Square: Triple' stimulus since it is marginally faster to run than the AdEx model.

It was also not possible to account for the time taken for variable adjustments. In other words, the number of iterations before the best model trace was found. Again, the LIF model has the least number of variables to adjust so in cases where all models return similar results, this would be the most time-efficient choice.

For more accurate comparisons, these variables could be taken into account.

It would also be interesting to compare spikes and spike times rather than voltage traces for future comparisons. This could be done using Brian2modelfitting's SpikeFitter.

Appendix A

Secondary Data Analysis Compliance Form

School of Engineering and Informatics SECONDARY DATA ANALYSIS COMPLIANCE FORM FOR UG AND PGT PROJECTS This form must be completed before any analysis of secondary data may begin. Introduction This form should be read in conjunction with the document entitled "Research Ethics Guidance for UG and PGT Projects (V4.0)". This form is for project that will use secondary data, that is pre-existing data. For projects that will collect new data, either the User-testing Compliance Form must be completed, or a full Low-risk or High-risk ethics application made to the Science and Technology Research Ethics Committee. There are four types of secondary data: • 1A: Meta-analysis – data obtained directly from published peer-reviewed articles • 1B: Publicly available anonymised data sets uploaded to open access repositories or databases • 1C: Secondary datasets available from previous School or Sussex University (ethics approved) projects • 1D: Secondary datasets not publicly available but which may be accessed under certain conditions/agreements Figure 1 is a decision flow chart of when this form can be used. The four types of secondary data listed at the top of the flow chart: boxes 1A-1D. Both meta-analyses (1A) and publicly available anonymized datasets (1B) do not require a University ethics review. Instead, you should complete the Secondary Data Analysis Compliance Form (Box 3A). Figure 1. Secondary Data Analysis Flow Chart For secondary datasets available from previous School or Sussex (ethics approved) projects (1C), you need to determine whether the data is anonymized and if the original consent form permits its re-use (Box 2). • If the answer to both in Box 2 is 'Yes', then a University ethics review is not required, and you should complete the Secondary Data Analysis Compliance Form (Box 3A). • If the answer to both

in Box 2 is 'No', then you must complete an online ethics review application form on Sussex Direct (Box 3B). For secondary datasets not publicly available but which may be accessed under certain conditions/agreements, you will need to make an online ethics review application (Box 3B). Part 1: Determining whether you can use this Secondary Data Analysis Compliance form or whether you need to submit a full ethics application via Sussex Direct.

You can use this form if your project involves (1) AND/OR (2) below (double click the check box to tick):

1. A meta-analysis.

2. Using publicly available anonymized datasets (e.g., data obtained from open access repositories or databases).

URL of dataset: Cell Features :: Allen Brain Atlas: Cell Types

Error! Bookmark not defined.

You can use this form if your project involves research described in (3), and meets BOTH criteria A and B below:

3. Analysing datasets that were originally collected by researchers at the University of Sussex, according to a previously approved ethics application.

The data to be analysed also meets both of the following criteria:

A. The data is fully anonymised. Yes / No (delete the inapplicable)

B. The original ethics application permits the re-use of data collected. Yes / No

Sussex Ethics Application Number (e.g., ER/XYZ99/1): Add Number

Sussex Ethics Application Project Title: Add Title

If the dataset does not meet BOTH criteria A and B, then you will need to apply for an ethics review on Sussex Direct.

You CANNOT use this form if your project involves the following (4):

4. Analysing datasets that are not publicly available and not originally collected by Sussex researchers. The datasets can only be accessed according to conditions/agreements arranged by your supervisor or the University.

In this scenario, you will need to apply for ethics approvals on Sussex Direct, regardless of how the data is anonymised. The ethics review will also consider whether the

re-use of the data is permitted according to the original ethics application.

Based on your answers above, please either complete Parts 2-4 of this form or discuss with your supervisor about submitting an ethics application via Sussex Direct.

Part 2: Project information

Project Title: A Comparative Study Between Three Neuronal Models on Ex Vivo, Intracellular, Electrophysiological Datasets

Student: Yoon-ji Kim

Supervisor: Dr. Benjamin Evans

Start End Dates: Start: 14th May 2025 End: 19th Aug 2025

Part 3: Project description and ethical considerations

This project aims to use ex vivo, intracellular, electrophysiological datasets to simulate voltage traces, and explore comparisons between the neuronal models of Hodgkin Huxley, Leaky Integrate and Fire, and Adaptive Exponential Integrate and Fire.

Reflection on ethics of data collection (up to 2000 characters) Consider the procedures performed by the individuals who originally collected the data you'll analyse. We recommend discussing how the researchers ensured participant wellbeing, consent, confidentiality. Reflect on the four ethical principles for psychologists that are outlined in the BPS Code of Ethics: (1) Respect, (2) Competence, (3) Responsibility, and (4) Integrity. You can also refer to specific BPS guidelines and policies, including the Code of Human Research Ethics.

The Allen Cell Types Database contains data from de-identified patients who underwent a surgical procedure, for (in the case of the data used in this project) treatment of temporal lobe epilepsy. As stated in the Allen Cell Types Database Technical Whitepaper, 'Only tissue specimens deemed not essential for diagnostic purposes and that would otherwise be discarded were collected for research purposes. It was an essential requirement that tissue collection did not interfere in any way with clinical evaluation of the core pathology, or with the health and well-being of the patient beyond the normal risk associated with brain surgery.' All donors had voluntarily signed an Internal Review Board approved Informed Consent Form.

Part 4: Approvals

Role	Name	Signature	Date
Student	Yoon-ji Kim	YKim	7/8/25

Supervisor Dr. Benjamin Evans BDEvans 7/8/25

EngInf SREO, V1.0, Oct 2023. Adapted from the School of Psychology "Ethics form for UG/PGT projects involving secondary data analysis (not NHS-related)"

Bibliography

[1] A. Shapson-Coe, M. Januszewski, D. R. Berger, A. Pope, Y. Wu, T. Blakely, R. L. Schalek, P. H. Li, S. Wang, J. Maitin-Shepherd, N. Karlupia, S. Dorkenwald, E. Sjostedt, L. Leavitt, D. Lee, L. Bailey, A. Fitzmaurice, R. Kar, B. Field, H. Wu, J. Wagner-Carena, D. Aley, J. Lau, Z. Lin, D. Wei, H. Pfister, A Peleg, V. Jain, and J. W. Lichtman. A connectomic study of a petascale fragment of human cerebral cortex. *bioRxiv*, 2021.

[2] D. Hendricks, A Pagliaro, F. Andreatta, Z. Ma, J. van Giessen, S. Massalini, C. Lopez-Iglesias, G. J. F. van Son, J. DeMartino, J. M. A. Damen, I. Zoutendijk, N. Staliarova, A. L. Bredenoord, F. C. P. Holstege, P. J. Peters, T. Margaritis, S. C. de Sousa Lopes, W. Wu, H. Clevers, and B. Artegiani and. Human fetal brain self-organizes into long-term expanding organoids. *Cell*, 187:712–732, 2024.

[3] Y. Shou, F. Liang, S. Xu, and X. Li. The application of brain organoids: From neuronal development to neurological diseases. *Frontiers in Cell and Development Biology*, 8, 2020.

[4] O. L. Eichmuller and J. A. Knoblich. Human cerebral organoids — a new tool for clinical neurology research. *Nature Reviews Neurology*, 18, 2022.

[5] M. Birtele, M. Lancaster, and G. Quadrato. Modelling human brain development and disease with organoids. *Nature Reviews Molecular Cell Biology*, 26:389–415, 2025.

[6] J. Croxford and T. Bayne. The case against organoid consciousness. *Neuroethics*, 17, 2024.

[7] M. Binz, E. Akata, M. Bethge, F. Brandle, F. Callaway, J. Coda-Forno, P.Dayan, C. Demircan, M. K. Eckstein, N. Elteto, T. L. Griffiths, S. Haridi, A. K. Jagadish, L. Ji-An, A. Kipnis, S. Kumar, T. Ludwig, M. Mathony, M. Mattar, A. Modirshanechi, S. S. Nath, J. C. Peterson, M. Rmus, E. M. Russek, T. Saanum,

J. A. Schubert, L. M. Schulze Buschoff, N. Singhi, X. Sui, M. Thalmann, F. J. Theis, V. Truong, V. Udandarao, K. Voudouris, R. Wilson, K. Witte, S. Wu, D. U. Wulff, H. Xiong, and E. Schulz. A foundation model to predict and capture human cognition. *Nature*, 2025.

[8] X. Tu, Z. He, Y. Huang, Z. Zhang, M. Yang, and J. Zhao. An overview of large ai models and their applications. *Visual Intelligence*, 2, 2024.

[9] B. Goncalves. Passed the turing test: Living in turing futures. *Intelligent Computing*, 3, 2024.

[10] M. Mitchell. The turing test and our shifting conceptions of intelligence. *Science*, 385, 2024.

[11] M. Gams and S. Kramar. Evaluating chatgpt's consciousness and its capability to pass the turing test: A comprehensive analysis. *Journal of Computer and Communications*, 12, 2024.

[12] R. Long, J. Sebo, P. Butlin, K. Finlinson, K. Fish, J. Harding, J. Pfau, T. Sims, J. Birch, and D. Chalmers. Taking ai welfare seriously. *Arxiv*, 2024.

[13] Z. Liu, Y. Chen, and P. Ao. Entangled biphoton generation in the myelin sheath. *Physical Review*, 110, 2024.

[14] E. Carmeliet. From bernstein's rheotome to neher–sakmann's patchelectrode. the action potentia. *Physiological Reports*, 7:164–168, 2018.

[15] S. M. Schuetze. The discovery of the action potential. *Perspectives*, 6:164–168, 1983.

[16] W. Gerstner, M Kistler, R. Naud, and L. Paninski. Chapter: Integrate-and-fire models. *Neuronal Dynamics*, 2014.

[17] A. L. Hodgkin, A. F. Huxley, and B. Katz. Measurement of current-voltage relations in the membrane of the giant axon of loligo. *J Physiol*, 116:424–448, 1951.

[18] A. L. Hodgkin and A. F. Huxley. Currents carried by sodium and potassium ions through the membrane of the giant axon of loligo. *J Physiol*, 116:449–472, 1951.

[19] A. L. Hodgkin and A. F. Huxley. The components of membrane conductance in the giant axon of loligo. *J Physiol*, 116:473–496, 1951.

[20] A. L. Hodgkin and A. F. Huxley. The dual effect of membrane potential on sodium conductance in the giant axon of loligo. *J Physiol*, 116:497–506, 1951.

[21] A. L. Hodgkin and A. F. Huxley. A quantitative description of membrane current and its application to conduction and excitation in nerve. *J Physiol*, 117:500–544, 1952.

[22] C. J. Schwiening. A brief historical perspective: Hodgkin and huxley. *J. Physiol*, 590.11:2571–2575, 2012.

[23] M. Hausser. The hodgkin-huxley theory of the action potential. *Nature Neuroscience*, 3, 2000.

[24] R. Brette and W. Gerstner. Adaptive exponential integrate-and-fire model as an effective description of neuronal activity. *Journal of Neurophysiology*, 94:3637–3642, 2005.

[25] R. Naud, N. Marcille, C. Clopath, and W. Gerstner. Firing patterns in the apdaptive exponential integrate-and-fire model. *Biological Cybernetics*, 99:335–347, 2008.

[26] D. Goodman and R. Brette. Brian: a simulator for spiking neural networks in python. *Frontiers in Neuroinformatics*, 2008.

[27] M. Stimberg, R. Brette, and D. Goodman. Brian2, an intuitive and efficient neural simulator. *eLife*, 2019.